

**Aus dem Max von Pettenkofer-Institut für Hygiene und  
Medizinische Mikrobiologie der Ludwig-Maximilians-Universität  
München**

Vorstand: Prof. Dr. Dr. Jürgen Heesemann

**Effects of *Helicobacter pylori* Vacuolating Cytotoxin A  
on intracellular calcium signalling in T-lymphocytes**

**Dissertation**

**zum Erwerb des Doktorgrades der Humanbiologie  
an der Medizinischen Fakultät der  
Ludwig-Maximilians-Universität zu München**

vorgelegt von

**Utkarsh Jain**

aus Pune / Indien

2014

Mit Genehmigung der Medizinischen Fakultät  
der Universität München

Berichterstatter: Prof. Dr. Rainer Haas

Mitberichterstatter: Prof. Dr. med. Martin Storr  
Prof. Dr. med. Hermann Fießl

Mitbetreuung durch den  
promovierten Mitarbeiter: Dr. Luisa F. Jiménez-Soto

Dekan: Prof. Dr. med. Dr. h.c. M. Reiser, FACR, FRCR

Tag der mündlichen Prüfung: 27.02.2014

Part of the research work presented here is published under the title:

Luisa F. Jiménez-Soto, Stefanie Rohrer, **Utkarsh Jain**, Claudia Ertl, Xaver Sewald, and Rainer Haas (2012). Effects of cholesterol on *Helicobacter pylori* growth and virulence properties *in vitro*. *Helicobacter*, **17**, 133-139.

# Contents

<b>Contents.....</b>	<b>i</b>
<b>List of Figures .....</b>	<b>vi</b>
<b>List of Tables.....</b>	<b>viii</b>
<b>Summary .....</b>	<b>ix</b>
<b>Zusammenfassung .....</b>	<b>xi</b>
<b>1. Introduction .....</b>	<b>1</b>
<b>1.1 <i>Helicobacter pylori</i> .....</b>	<b>1</b>
1.1.1 History and discovery .....	1
1.1.2 Microbiology.....	1
1.1.3 Epidemiology and infection .....	2
1.1.4 Pathogenesis and virulence determinants.....	4
1.1.5 The versatility of Vacuolating Cytotoxin A.....	6
<b>1.2 The host .....</b>	<b>9</b>
1.2.1 <i>H. pylori</i> survival in the human host.....	11
<b>1.3 Calcium signalling .....</b>	<b>12</b>
1.3.1 Calcium signalling in general.....	12
1.3.1.1 Calcium ion channels .....	12
1.3.1.1.1 Voltage-dependent calcium channels .....	13
1.3.1.1.2 Ligand gated ion channels (LGICs) .....	14
1.3.1.1.3 Transient receptor potential (TRP) channels .....	14
1.3.1.1.4 Calcium release-activated calcium (CRAC) channels.....	14
1.3.2 Calcium signalling in T-cells .....	14
1.3.2.1 T-cell receptor signalling .....	15
1.3.2.2 Store-operated calcium channels.....	15
<b>1.4 Aim of this study.....</b>	<b>19</b>
<b>2. Materials and Methods .....</b>	<b>20</b>

---

<b>2.1</b>	<b>Materials .....</b>	<b>20</b>
2.1.1	Bacterial strains.....	20
2.1.1.1	<i>Helicobacter pylori</i> strains.....	20
2.1.1.2	<i>Escherichia coli</i> strains.....	20
2.1.1.3	Yeast strains ( <i>Saccharomyces cerevisiae</i> ).....	21
2.1.1.3.1	<i>Saccharomyces cerevisiae</i> strains.....	21
2.1.2	Cell lines .....	23
2.1.3	Plasmids and vectors.....	23
2.1.4	Oligonucleotides .....	25
2.1.5	Broth or culture media .....	28
2.1.5.1	Broth or culture media for bacteria .....	28
2.1.6	Inhibitors and media supplements.....	28
2.1.7	Cell culture medium and buffers.....	29
2.1.8	Enzymes and proteins .....	29
2.1.9	Molecular markers .....	30
2.1.10	Chemicals and reagents.....	30
2.1.11	Cosumables and equipments.....	31
2.1.11.1	Consumables.....	31
2.1.11.2	Equipments.....	31
2.1.12	Computer programmes.....	32
<b>2.2</b>	<b>Methods.....</b>	<b>32</b>
2.2.1	Work with Bacteria .....	32
2.2.1.1	Growth and cultivation of <i>E. coli</i> .....	32
2.2.1.2	Freezing of <i>E.coli</i> .....	32
2.2.1.3	Growth and cultivation of <i>H. pylori</i> .....	32
2.2.1.4	Freezing of <i>H. pylori</i> .....	33
2.2.1.5	Determination of optical density of bacteria.....	33
2.2.1.6	Production of chemical competent <i>E. coli</i> cells.....	33
2.2.1.7	Transformation of chemical competent cells .....	33
2.2.2	Work with yeast .....	34
2.2.2.1	Growth and cultivation of <i>Saccharomyces cerevisiae</i> .....	34
2.2.2.2	Determination of the optical density of yeasts.....	34
2.2.2.3	Preparation of yeast competent cells.....	34
2.2.2.4	Transformation of yeast competent cells (Geitz protocol).....	34
2.2.2.5	Production of diploid yeast strains (Uetz <i>et al.</i> , 2006).....	35
2.2.2.6	Test for protein-protein interaction in <i>Saccharomyces cerevisiae</i> (Busler <i>et al.</i> , 2006) .....	35

---

2.2.3	Work with DNA.....	36
2.2.3.1	Primer design for yeast plasmid cloning.....	36
2.2.3.2	Polymerase Chain Reaction .....	36
2.2.3.3	Purification and quantitative estimation of DNA concentration.....	37
2.2.3.4	DNA gel electrophoresis.....	38
2.2.3.5	Extraction and isolation of DNA from agarose gel.....	38
2.2.3.5.1	Isolation of plasmid DNA of <i>E. coli</i> by QIAGEN Miniprep.....	38
2.2.3.6	DNA restriction.....	39
2.2.3.7	Ligation.....	39
2.2.3.8	Colony PCR .....	39
2.2.3.9	Gateway cloning .....	39
2.2.3.9.1	“nested”-PCR .....	40
2.2.3.9.2	BP Clonase™-Reaction.....	42
2.2.3.9.4	LR Clonase™-Reaction.....	43
2.2.3.10	DNA sequencing.....	43
2.2.4	Work with cell culture.....	44
2.2.4.1	Cell counting with Neubauer counting chamber.....	44
2.2.4.2	Cultivation of adherent cells .....	44
2.2.4.2.1	Cultivation of HEK-293 cells.....	44
2.2.4.2.2	Cultivation of HEK-293 cells expressing mCherry-STIM1 .....	44
2.2.4.2.3	Cultivation of HEK-293 cells expressing eGFP-myc-ORAI1 .....	45
2.2.4.3	Cultivation of suspension cells.....	45
2.2.4.3.1	Cultivation of Jurkat E6.1 cells .....	45
2.2.4.4	Transfection of adherent cells .....	45
2.2.4.4.1	Generation of Flp-In™ T-REx designed HEK-293 cells stably expressing eGFP-myc-ORAI1 .....	45
2.2.4.4.2	Generation of HEK-293 cell stably expressing mCherry-STIM1 .....	46
2.2.4.5	Isolation of human CD <sup>4+</sup> T-lymphocytes .....	46
2.2.4.6	Lymphocyte purification from normal human peripheral blood.....	46
2.2.4.7	Calcium assay .....	47
2.2.4.8	Cryopreservation of cells .....	47
2.2.4.9	Cell thawing .....	47
2.2.4.10	Microscopy.....	47
2.2.4.10.1	Live cell imaging.....	47
2.2.5	Work with Protein.....	48
2.2.5.1	Protein estimation by Bradford assay .....	48

2.2.5.2	Ammonium sulphate precipitation and concentration of VacA from culture supernatant....	48
2.2.5.3	Acid activation of VacA .....	48
2.2.5.4	Cell vacuolating activity induced by VacA.....	49
2.2.5.5	Detection of protein in SDS polyacrylamide gel electrophoresis .....	49
2.2.5.6	Staining of proteins by Coomassie Blue .....	49
2.2.5.7	Fluorescent staining of VacA.....	50
2.2.6	Statistical analysis .....	50
<b>3.</b>	<b>Results .....</b>	<b>51</b>
<b>3.1</b>	<b>Growth of <i>H. pylori</i> and purification of VacA .....</b>	<b>51</b>
3.1.1	Growth of <i>H. pylori</i> in solid and liquid culture.....	51
3.1.2	<i>H. pylori</i> 60190 VacA protein precipitation and purification through Gel filtration .....	51
<b>3.2</b>	<b>Quantification of VacA induced cell vacuolation in human Jurkat E6.1 T-cell line.....</b>	<b>52</b>
<b>3.3</b>	<b>VacA inhibits the increase of cytosolic free Ca<sup>2+</sup> in response to stimulation by ionomycin and thapsigargin in T-lymphocytes .....</b>	<b>54</b>
3.3.1	Effect of VacA on increase of cytosolic free Ca <sup>2+</sup> concentration in human Jurkat E6.1 T-cell line .....	54
3.3.1.1	<i>H. pylori</i> VacA inhibits calcium influx in human Jurkat E6.1 T-cell line after stimulation by ionomycin .....	54
3.3.1.2	<i>H. pylori</i> VacA inhibits the increase of cytosolic free Ca <sup>2+</sup> in human Jurkat E6.1 T-cell line after stimulation by thapsigargin.....	61
3.3.2	Effect of VacA on increase of cytosolic free Ca <sup>2+</sup> concentration in human CD <sup>4+</sup> T-cells .....	68
3.3.2.1	<i>H. pylori</i> VacA inhibits calcium influx in human CD <sup>4+</sup> T-cells after stimulation by ionomycin .....	68
3.3.2.2	<i>H. pylori</i> VacA inhibits the increase of cytosolic free Ca <sup>2+</sup> in CD <sup>4+</sup> T-cells after stimulation by thapsigargin.....	70
<b>3.4</b>	<b>Cellular processes that are essential for store operated calcium entry .....</b>	<b>74</b>
3.4.1	Stromal interaction molecule-1 (STIM1) clusters in response to thapsigargin treatment in T-cells.....	75
3.4.2	STIM1/ORAI1 coupling and store operated calcium entry .....	77
3.4.3	<i>H. pylori</i> VacA co-localizes with STIM1 before and after thapsigargin stimulation .....	79
3.4.4	VacA substantially reduces movement of STIM1 towards the plasma membrane protein ORAI1 .....	81
3.4.5	Co-localization of VacA with STIM1 substantially increases after stimulation by two times thapsigargin .....	84

---

3.4.6	VacA co-localizes with STIM1 in vicinity of ER membrane protein translocator Sec61 before and after stimulation with thapsigargin .....	86
<b>3.5</b>	<b>Yeast two-hybrid assay to study the interaction between <i>H. pylori</i> VacA and different domains of STIM1 and ORAI1 .....</b>	<b>89</b>
3.5.1	Amplification of STIM1, ORAI1 and VacA domain DNA sequences by nested-PCR.....	90
3.5.2	Cloning of the Gateway® compatible nested-PCR amplified products in pDonr207 vector ...	91
3.5.3	Sequence analysis of the genes cloned in pDONR207 vector .....	91
3.5.4	Recombination cloning of entry clones into yeast two-hybrid prey and bait vectors .....	92
3.5.5	Transformation of prey/bait vectors into <i>Saccharomyces cerevisiae</i> .....	93
3.5.6	Generation of diploid yeast by mating .....	93
3.5.7	Yeast two-hybrid growth assay to study the interaction of STIM1 with VacA .....	94
3.5.7.1	cEF-hand of STIM1 shows positive interaction with VacA .....	94
<b>4.</b>	<b>Discussion .....</b>	<b>96</b>
<b>4.1</b>	<b>Effects of <i>H. pylori</i> VacA in epithelial and immune cells.....</b>	<b>96</b>
<b>4.2</b>	<b><i>H. pylori</i> VacA effects on calcium influx in T-cells.....</b>	<b>99</b>
<b>4.3</b>	<b><i>H. pylori</i> VacA inhibits calcium influx induced by ionomycin and thapsigargin .....</b>	<b>99</b>
<b>4.4</b>	<b>VacA targets SOCE to inhibit calcium influx induced by thapsigargin.....</b>	<b>100</b>
<b>4.5</b>	<b>VacA binds to STIM1 and not to ORAI1 in order to prevent their conformational coupling .....</b>	<b>100</b>
<b>4.6</b>	<b>cEF-hand domain of STIM1 is target of VacA .....</b>	<b>102</b>
<b>4.7</b>	<b>Effects of inhibition of calcium influx by VacA on T-cell activation and proliferation .</b>	<b>103</b>
<b>4.8</b>	<b>Effects of VacA on localized calcium uptake in mitochondria .....</b>	<b>106</b>
<b>4.9</b>	<b>Role of cytoplasmic free Ca<sup>2+</sup> in regulating the effects of bacterial toxins.....</b>	<b>106</b>
	<b>References .....</b>	<b>108</b>
	<b>Abbreviations.....</b>	<b>122</b>
	<b>Acknowledgements.....</b>	<b>125</b>
	<b>Declaration .....</b>	<b>126</b>
	<b>Curriculum Vitae .....</b>	<b>127</b>

## List of Figures

Figure 1-1 Worldwide prevalence of <i>H. pylori</i> infection. ....	3
Figure 1-2 <i>H. pylori vacA</i> gene structure. ....	7
Figure 1-3 <i>H. pylori VacA</i> protein structure. ....	7
Figure 1-4 Anatomy of the stomach and histology of the gastric mucosa. ....	10
Figure 1-5 $Ca^{2+}$ signalling network: the ON/OFF mechanisms. ....	12
Figure 1-6 Calcium ion channels at cell membrane and the intracellular compartments. ....	13
Figure 1-7 Calcium signalling in T-cells. ....	17
Figure 2-1 BP Clonase™-Reaction. ....	42
Figure 2-2 LR Clonase™-Reaction. ....	43
Figure 3-1 Growth curve of <i>H. pylori</i> 60190 in liquid culture. ....	51
Figure 3-2 Purified VacA protein after Gel filtration and comparison of the sizes of VacA proteins purified from culture supernatant of <i>H. pylori</i> 60190 VacA WT and VacA M strain. ....	52
Figure 3-3 Neutral red uptake assay of Jurkat E6.1 cells. ....	53
Figure 3-4 Mechanism of action of $Ca^{2+}$ ionophores and inhibitors. ....	55
Figure 3-5 Measurement of $Ca^{2+}$ influx stimulated by ionomycin and the effect of VacA on the increase of the cytosolic free $Ca^{2+}$ concentration in Jurkat E6.1 cells. ....	57
Figure 3-6 Measurement of $Ca^{2+}$ influx evoked by ionomycin and the effect of VacA on the increase of the cytosolic free calcium concentration in Jurkat E6.1 cells. ....	59
Figure 3-7 Measurement of $Ca^{2+}$ influx evoked by ionomycin and the effect of VacA on the increase of the cytosolic free calcium concentration in Jurkat E6.1 cells. ....	60
Figure 3-8 Measurement of $Ca^{2+}$ influx evoked by thapsigargin and the effect of VacA on the increase of the cytosolic free calcium concentration in Jurkat E6.1 cells. ....	62
Figure 3-9 Fluorescence measurement of $Ca^{2+}$ influx evoked by thapsigargin and the effect of VacA on the increase of the cytosolic free calcium concentration in Jurkat E6.1 cells treated with EDTA-EGTA and thapsigargin. ....	63
Figure 3-10 Fluorescence measurement evoked by thapsigargin and the effect of VacA on the increase of the cytosolic free calcium concentration in Jurkat E6.1 cells treated with BAPTA AM and thapsigargin. ....	64
Figure 3-11 Fluorescence measurement evoked by thapsigargin and the effect of VacA on the increase of the cytosolic free calcium concentration in Jurkat E6.1 cells treated with EDTA-EGTA, BAPTA AM and thapsigargin. ....	65
Figure 3-12 Fluorescence measurement evoked by thapsigargin and the effect of VacA on the increase of the cytosolic free calcium concentration in Jurkat E6.1 cells treated with BAPTA AM. ....	66
Figure 3-13 Fluorescence measurement of $Ca^{2+}$ influx in the effect of VacA on the increase of the cytosolic free calcium concentration in Jurkat E6.1 cells treated with two times thapsigargin. ....	67

Figure 3-14 Measurement of Ca <sup>2+</sup> influx evoked by ionomycin and the effect of VacA on Ca <sup>2+</sup> influx in CD <sup>4+</sup> T-cells. .....	69
Figure 3-15 Measurement of the increase of the cytosolic free calcium concentration in CD <sup>4+</sup> T-cells pre-incubated with VacA and then stimulated by thapsigargin. ....	71
Figure 3-16 Measurement of the increase of the cytosolic free calcium concentration in CD <sup>4+</sup> T-cells pre-incubated with VacA and then stimulated by two times thapsigargin. ....	72
Figure 3-17 Fluorescence measurement of CD <sup>4+</sup> T-cells pre-incubated with VacA and treated with EDTA-EGTA, BAPTA AM and thapsigargin. ....	73
Figure 3-18 mCherry-STIM1 oligomerization upon thapsigargin treatment in HEK-293 cells.....	76
Figure 3-19 Co-localization study of eGFP-myc-ORAI1 and mCherry-STIM1 before and after thapsigargin stimulation. ....	78
Figure 3-20 Co-localization of mCherry-STIM1 and VacA <sup>Alexa 647</sup> before and after thapsigargin stimulation. ....	80
Figure 3-21 Co-localization of eGFP-myc-ORAI1, mCherry-STIM1 and VacA <sup>Alexa 647</sup> at 120 s after stimulation by thapsigargin. ....	82
Figure 3-22 Co-localization of eGFP-myc-ORAI1, m-Cherry STIM1 and VacA <sup>Alexa 647</sup> at 30 min after stimulation by thapsigargin. ....	83
Figure 3-23 Co-localization of eGFP-myc-ORAI1, mCherry-STIM1 and VacA <sup>Alexa 647</sup> after two times thapsigargin stimulation. ....	85
Figure 3-24 Co-localization of GFP-Sec61, mCherry-STIM1 and VacA <sup>Alexa 647</sup> before thapsigargin stimulation. ....	87
Figure 3-25 Co-localization of GFP-Sec61, mCherry-STIM1 and VacA <sup>Alexa 647</sup> after thapsigargin stimulation. .	88
Figure 3-26 Different domains of STIM1 and ORAI1. ....	90
Figure 3-27 Recombination cloning of domains of STIM1, ORAI1 and VacA into prey (pGADT7) and bait (pGBKT7) vectors. ....	92
Figure 3-28 Generation of diploid yeast strains and selction on double selective dropout SD medium. ....	93
Figure 3-29 Determination of interaction between STIM1 and ORAI1 with VacA by yeast two-hybrid growth test. .....	95
Figure 3-30 Determination of interaction between the cEF-hand motif and VacA.....	95
Figure 4-1 Schematic diagram of <i>H. pylori</i> VacA effects on epithelial and immune cells. ....	98
Figure 4-2 cEF-hand domain of STIM1 is target of VacA.....	103
Figure 4-3 Possible <i>H. pylori</i> VacA effects on calcium signalling in T-cells. ....	105

---

## List of Tables

Table 2-1 <i>Helicobacter pylori</i> strains.....	20
Table 2-2 <i>Escherichia coli</i> strains.....	20
Table 2-3 <i>Saccharomyces cerevisiae</i> strains.....	21
Table 2-4 Eukaryotic cell lines.....	23
Table 2-5 Plasmids and vectors.....	23
Table 2-6 Oligonucleotides sequence (5' to 3') and their description.....	25
Table 2-7 Culture media and nutrients for bacteria.....	28
Table 2-8 Inhibitors and media supplements.....	28
Table 2-9 Cell culture media.....	29
Table 2-10 Enzymes and proteins with their respective sources.....	29
Table 2-11 Molecular markers and their sources.....	30
Table 2-12 PCR protocol.....	37
Table 2-13 Protocol for "nested"-PCR step-I.....	41
Table 2-14 Protocol for "nested"-PCR step-II.....	41
Table 3-1 The domains of STIM1, ORAI1 and VacA and their amino acid positions.....	91

## Summary

More than 50% of the world's population harbor *Helicobacter pylori* in their stomach mucosa. The chronic gastric infection is associated with several diseases including peptic ulcer disease and gastric carcinoma.

One of the most thoroughly studied virulence factors produced by *H. pylori* is the Vacuolating Cytotoxin A (VacA). All isolated *H. pylori* strains possess the *vacA* gene, although significant sequence diversity was noticed in *vacA* genes across *H. pylori* isolates. VacA protein is produced and secreted as an 88 kD mature toxin. The protein binds to the host cells and is internalized. Inside the host cells, it causes “vacuole”-like membrane vesicles in the cytoplasm of gastric epithelial cells. Besides vacuolation, VacA exerts various other effects on target cells. VacA also forms membrane-embedded pores at the inner-mitochondrial membrane, resulting in mitochondrial dysfunction by cytochrome c release and apoptosis induction. VacA suppresses nuclear translocation of nuclear factor of activated T-cells (NFAT) resulting in down regulation of interleukin-2 (IL2) gene transcription to efficiently block proliferation of T-cells.

The aim of this work was to understand the effects of VacA on intracellular calcium signalling in T-lymphocytes by considering the fact that VacA inhibits the  $\text{Ca}^{2+}$ -calmodulin-dependent phosphatase calcineurin and induces cell cycle arrest. However, the exact mechanism how VacA exerts this response in T-cells is not known.

Therefore, in this thesis various cell lines were used to study the effects of VacA on calcium influx. Calcium influx was found to be affected in the presence of VacA protein in the human Jurkat E6.1 T-cell line and primary human  $\text{CD}^{4+}$  T-cells activated by phorbol myristate acetate (PMA). Once inside T-cells, it could be shown that VacA suppresses the increase of the cytosolic free calcium concentration after stimulation by the calcium ionophore ionomycin and thapsigargin. Ionomycin forms pores in the cytoplasmic membrane, whereas thapsigargin blocks the sarcoplasmic/endoplasmic reticulum calcium ATPase (SERCA) and thereby causes depletion of the endoplasmic reticulum (ER) calcium store. In contrast, a VacA mutant, which was constructed by deletion of the hydrophobic region (amino acids 6-27), was unable to induce vacuolation activity and to block  $\text{Ca}^{2+}$  influx.

A major result of this work was to demonstrate that one of the main components of store operated calcium entry (SOCE), the ER localized calcium sensor protein STIM1, is a target of VacA. Using co-localization studies and yeast two-hybrid (YTH) assays, it was found that VacA localizes to the lumen of the ER where it binds to the cEF-hand domain of STIM1. Furthermore, these data show that VacA strongly reduced the movements of the STIM1 towards the plasma membrane localized calcium channel ORAI1 after  $\text{Ca}^{2+}$  store depletion by thapsigargin. A YTH screen identified cEF-hand domain of STIM1 as the target of VacA to inhibit calcium influx.

The results obtained in this work showing involvement of VacA in the modulation of intracellular calcium signalling will provide new insights that are required to understand how VacA inhibits T-cell proliferation and signalling.

## Zusammenfassung

Mehr als 50% der Weltbevölkerung tragen *Helicobacter pylori* in ihrem Magenepithel. *H. pylori* kolonisiert dauerhaft die Magenschleimhaut und ist mit verschiedenen Erkrankungen wie Magen- oder Zwölffingerdarmgeschwüren sowie Magenkrebs assoziiert.

Einer der am besten untersuchten Virulenzfaktoren von *H. pylori* ist das vakuolisierende Cytotoxin VacA. Alle *H. pylori*-Isolate haben ein *vacA*-Gen, wobei allerdings deutliche Sequenzvariationen zwischen verschiedenen Stämmen auftreten. Das VacA-Protein wird als Vorläuferprotein produziert und als reifes Toxin von 88 kDa sekretiert. Das reife Protein bindet an Wirtszellen und wird von diesen internalisiert. In der Zielzelle verursacht es die Bildung vakuolenartiger Membranvesikel im Zytoplasma. Unabhängig von dieser Vakuolisierung hat VacA verschiedene weitere Effekte auf Zielzellen. So bildet es Poren in der inneren Mitochondrienmembran, die zu einer Mitochondrien-Fehlfunktion mit Cytochrom c-Freisetzung und Apoptose-Induktion führen. VacA unterdrückt auch die Translokation des Transkriptionsfaktors NFAT (*Nuclear Factor of Activated T-cells*) in den Zellkern und damit die Transkription des Interleukin-2 (IL-2)-Gens, was zu einer effizienten Hemmung der T-Zell-Proliferation führt.

Ziel dieser Arbeit war die Untersuchung des Einflusses von VacA auf die intrazelluläre Calcium-Signalübertragung in T-Zellen vor dem Hintergrund, dass VacA die Calcium/Calmodulin-abhängige Phosphatase Calcineurin inhibiert und einen Stopp des Zellzyklus induziert. Der genaue Mechanismus dieser Antwort in T-Zellen ist allerdings nicht bekannt.

In dieser Arbeit wurden verschiedene Zelllinien zur Untersuchung des Effekts von VacA auf den Calciumeinstrom verwendet. Es konnte nachgewiesen werden, dass der Calciumeinstrom in der humanen T-Zelllinie Jurkat E6.1 und in primären humanen CD<sup>4+</sup> T-Zellen nach Aktivierung mit Phorbol-Myristat-Acetat (PMA) durch VacA beeinträchtigt wird. VacA supprimiert auch den Anstieg der freien Calcium-Konzentration im Cytosol nach Stimulierung mit den Calcium-Ionophoren Ionomycin und Thapsigargin. Ionomycin bildet Poren in der Cytoplasmamembran, während Thapsigargin die ATPase SERCA (*sarcoplasmic/endoplasmic reticulum calcium ATPase*) blockiert und dadurch eine Calcium-Depletion im endoplasmatischen Reticulum (ER) verursacht. Im Gegensatz zu VacA war eine rekombinante VacA-Variante, die durch Deletion

einer hydrophoben Region (Aminosäuren 6-27) hergestellt wurde, nicht in der Lage, eine Vakuolisierung zu induzieren und den Calciumeinstrom zu blockieren.

Ein wichtiges Ergebnis dieser Arbeit war es zu zeigen dass eine der Hauptkomponenten der Calciumaufnahme (*Store-Operated Calcium Entry*, SOCE), das ER-lokalisierte Calcium-Sensorprotein STIM1, als Zielmolekül für VacA dient. Mittels Kollokalisationsstudien und einem *Yeast Two-Hybrid*-Verfahren (YTH) konnte gezeigt werden, dass VacA im ER-Lumen lokalisiert ist und mit der calciumbindenden (*EF-hand*)–Domäne von STIM1 interagiert. Der Transport von STIM1 zur Plasmamembran und zu dem dort lokalisierten Calciumkanal ORAI1 ist nach Calciumdepletion mit Thapsigargin in Gegenwart von VacA deutlich reduziert. Mittels eines YTH Screens konnte die *EF-hand*-Domäne von STIM1 als Interaktionspartner von VacA identifiziert werden.

Die im Rahmen dieser Arbeit beobachtete Aktivität von VacA bei der Modulation der intrazellulären Calcium-Signaltransduktion liefert damit neue Erkenntnisse, die für ein genaueres Verständnis der durch VacA hervorgerufenen Inhibition der T-Zell-Proliferation und Signaltransduktion notwendig sind.

*Dedicated to all my true friends and well wishers.*

# 1. Introduction

The human gastric pathogen *Helicobacter pylori* causes chronic gastritis, and plays an important role in peptic ulcer diseases, gastric carcinoma, and gastric lymphoma in the human stomach. Therefore, *H. pylori* was classified as a type 1 carcinogen by the World Health Organization (WHO) in 1994. The relationship between *H. pylori* and the human host has developed already about 60.000–80.000 years ago. This very intimate relationship did not primarily evolve in order to damage the host, but rather to coexist and establish a persistent infection of the bacterium over many years.

The deleterious effects caused by *H. pylori* infections are mainly due to the host's response to the bacterium, which can mediate significant harm to the host. Thus, persistence and colonization of the microorganism in a particular site within the host may induce harmful effects on the host.

## 1.1 *Helicobacter pylori*

### 1.1.1 History and discovery

In 1982, *Helicobacter pylori* was first discovered by Dr. Barry Marshall and Dr. Robin Warren of Royal Perth Hospital in Perth, Australia. They noted the appearance of spiral shaped bacteria overlaying the mucus of inflamed gastric mucosa. Dr. Marshall and Dr. Warren were able to culture *H. pylori* from 11 patients with gastritis.

However, already about 100 years ago, a Polish clinical researcher, Walery Jaworski described the presence of spiral-shaped microorganisms in the stomach mucosa of humans. These microorganisms were placed in the *Campylobacter* species, which share so many characteristics to *H. pylori*. Thus, *H. pylori* was previously named *Campylobacter pyloridis*, which was then changed to *Campylobacter pylori*. Based on specific morphologic, structural and genetic features, *H. pylori* is now placed in a new genus. The genus *Helicobacter* consists of over 20 recognised species (Fox, 2002).

### 1.1.2 Microbiology

*H. pylori* is a Gram-negative, motile, spiral shaped, curved rod with 2-6 unipolar sheathed flagella, a microaerophilic and fastidious microorganism, which expresses enzymes such as oxidase, catalase, and urease (Konturek, Gillessen, Konturek, & Domschke, 1995; Konturek *et*

*al.*, 2001; Mendz, Shepley, Hazell, & Smith, 1997; O'Toole, Lane, & Porwollik, 2000). The enzyme urease is important for survival and colonization of *H. pylori* in the human stomach. *H. pylori* can transform from its normal helical bacillary morphology to a coccoid form, which allows *H. pylori* to adapt to the hostile environment of the human stomach. However, the coccoid form can not be cultured *in vitro* (Kusters, Gerrits, Van Strijp, & Vandenbroucke-Grauls, 1997). The genome sequence analysis of *H. pylori* from unrelated strains shows that the size of the *H. pylori* genome is approximately 1.7 Mbp (Alm & Trust, 1999). *H. pylori* is genetically heterogeneous, which is possibly an adaptation of the bacterium to the gastric conditions of its host and a distinct pattern of host-mediated immune response to *H. pylori* infections (Kuipers *et al.*, 2000). *H. pylori* shows a wide range of genetic diversity at the nucleotide level by several mechanisms, which includes mutation and transcriptional and translational phase variation (Achtman & Suerbaum, 2000; Falush *et al.*, 2001). The phase variation leads to phenotypic diversity in several *H. pylori* virulence genes, including outer membrane protein encoding genes and lipopolysaccharide biosynthetic enzymes (Appelmek *et al.*, 1999; de Jonge *et al.*, 2004; Mahdavi *et al.*, 2002).

### 1.1.3 Epidemiology and infection

More than half of the world's population is infected with *H. pylori*. However the prevalence of *H. pylori* shows a varying geographical distribution. The infection rates in emerging countries and developing countries are much higher (more than 80%) and infections appear to be more rapidly spread than in developed countries (Mitchell *et al.*, 1992; Pounder & Ng, 1995) (Figure 1-1). *H. pylori* infection is usually acquired at a young age (al-Moagel *et al.*, 1990; Malaty, 2007). In contrast, the prevalence of *H. pylori* in developed countries is normally much lower (40%), and is also considerably lower in children than in adults (Crew & Neugut, 2006). *H. pylori* acquisition seems to be more frequent in children than in adults (Feldman, Eccersley, & Hardie, 1998), which suggests that the increase in prevalence of *H. pylori* with age is mainly due to a birth cohort effect rather than a new infection. Interestingly, prevalence of *H. pylori* is related with socioeconomic status. Individuals having high family income levels, hygienic housing conditions and widespread use of antimicrobials for treatment are less infected with *H. pylori*. Therefore, these may be the reasons for the significantly lower prevalence of *H. pylori* in developed regions.

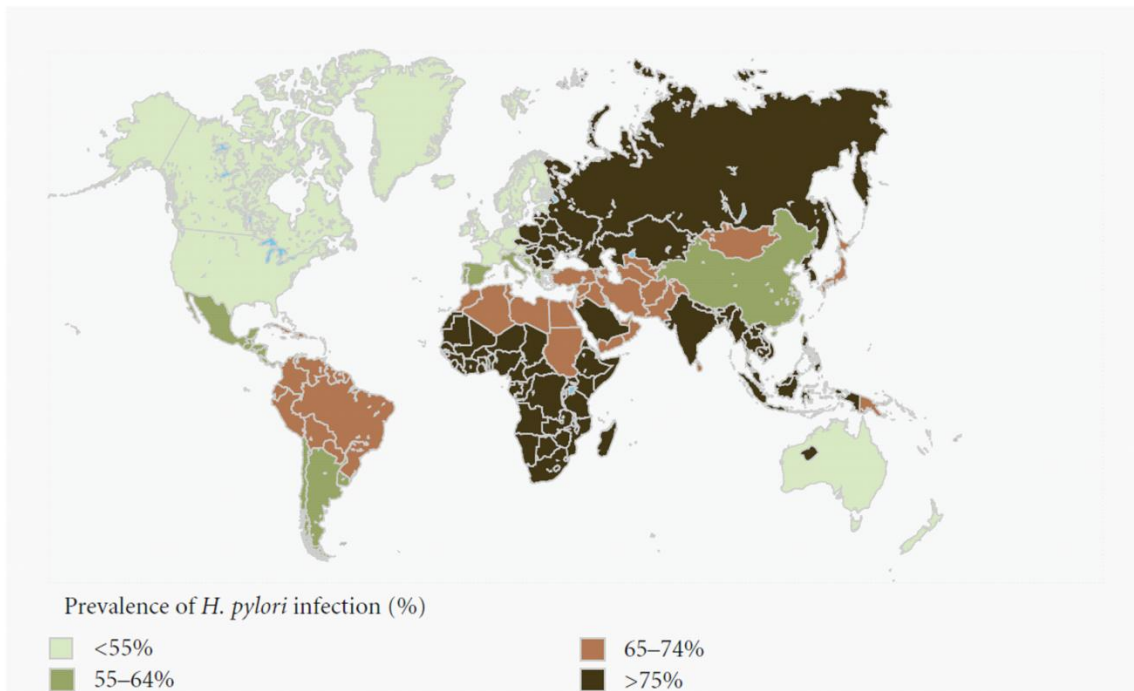


**Figure 1-1 Worldwide prevalence of *H. pylori* infection.**

Infection rates in percent. *H. pylori* infection is highly prevalent in Africa, Asia, and South America.

Besides geographical distribution, also racial differences contribute to the diversity in the prevalence of *H. pylori* (Graham *et al.*, 1991; Hyams *et al.*, 1995; Malaty, Evans, Evans, & Graham, 1992; Replogle, Glaser, Hiatt, & Parsonnet, 1995; Smoak, Kelley, & Taylor, 1994). This variability in the prevalence of *H. pylori* may also be explained by differences in ethnicity or genetic predisposition to infections (Brown, 2000).

Infection by *H. pylori* may cause digestive tract diseases including peptic ulcer, gastric cancer, and gastric MALT lymphoma. Spontaneous clearance of the infection is rare. Only one out of 5-6 infected individuals develop peptic ulcer disease in their lifetime, while < 1% develops gastric cancer. The prevalence of *H. pylori* infection and its associated diseases is declining in developed countries, but remains very common in developing countries, which includes most of the world's population. The majority of severe gastric illnesses are linked to *H. pylori* infection (Go, 2002).

The epidemiology and transmission pathways of *H. pylori* infection are important for the understanding of this common worldwide infection (Taylor & Blaser, 1991). The transmission of *H. pylori* remains unclear, but two different pathways have been suggested: faecal-oral and oral-oral (Feldman, Eccersley, & Hardie, 1998). Different transmission routes may be predominant in different geographical areas. In developed countries, in which sanitary procedures such as water treatment are well managed, transmission is rare. The clustering of *H. pylori* infection occurs

within families supporting an oral-oral transmission pathway (Brenner, Rothenbacher, Bode, Dieudonne, & Adler, 1999). The source of *H. pylori* could be saliva and dental plaques, since *H. pylori* organisms have been isolated from these locations (Ferguson *et al.*, 1993). Studies from developing countries with low socio-economic status and poor management of drinking water suggest that environmental factors are more important than the oral-oral transmission route in *H. pylori* spread (Hopkins *et al.*, 1993).

The most commonly recommended treatment in international guidelines for the eradication of *H. pylori* is the standard triple therapy consisting of two antibiotics and a proton pump inhibitor to prevent acid production in the stomach mucosa (Chan, Zhou, Ng, & Tam, 2001).

#### 1.1.4 Pathogenesis and virulence determinants

*H. pylori* has developed various strategies which allows it to perfectly adopt to the human host. (Bik *et al.*, 2006). *H. pylori* possesses the enzyme urease, which hydrolyses urea into NH<sub>3</sub> and CO<sub>2</sub>. This breakdown of urea is catalyzed by urease facilitating *H. pylori* to maintain a neutral pH in the microenvironment of the gastric lumen.

Most *H. pylori* reside within the apical surface of the mucus layer of the gastric mucosa although some *H. pylori* bind to the gastric epithelial cells. *H. pylori* expresses several putative outer membrane proteins (OMPs) consisting of two major families called the *hop* and *hor* gene families. The major OMPs of these families are AlpA, AlpB, BabA, SabA and OipA. AlpA and AlpB are associated with adhesion and cytokine induction (Lu *et al.*, 2007). BabA is another adhesion molecule. BabA is encoded by highly conserved strain specific genes *babA1* and *babA2*. Only *babA2* is functionally active. *BabB* is one homologous allele of BabA, which differs from *babA2* mainly in the central region. This central region determines the binding specificity of *H. pylori*. The functional BabA2 adhesin binds the Lewis histo-blood-group antigen Le<sup>b</sup> on gastric epithelial cells. *H. pylori* strains which encode *babA2* have an increased risk of gastric cancer induction (Gerhard *et al.*, 1999; Solnick, Hansen, Salama, Boonjakuakul, & Syvanen, 2004). In addition to BabA, *H. pylori* also encodes adhesion molecules SabA and OipA. SabA binds the sialyl-Lewis<sup>x</sup> (FUT4) antigen, which is a tumor antigen and a marker for gastric dysplasia in chronic gastric inflammation (Mahdavi *et al.*, 2002). OipA is a differentially expressed OMP. The expression of OipA is linked to the induction of chronic inflammation and injury, which is coregulated by the expression of proinflammatory cytokines IL-8, IL-6, RANTES (CCL5) and effector proteins such as metalloproteinase1 (MMP1) or intestinal

collagenase (Yamaoka *et al.*, 2002). OipA interacts directly with epithelial cells to trigger  $\beta$ -catenin expression (Dossumbekova *et al.*, 2006). Thus, the presence of these OMPs facilitates the attachment of *H. pylori* to the gastric epithelial cell surface and allows the bacteria to colonize the gastric mucosa effectively and to deliver the major virulence factors such as CagA and VacA.

*H. pylori* CagA (cytotoxin-associated gene A) is an effector protein encoded by the *cag* pathogenicity island (*cagPAI*). The size of the CagA protein is 121-145 kDa. It has been shown that *cagPAI* positive strains are predominantly associated with peptic ulceration, gastric adenocarcinoma or distal gastric cancer as compared to *cagPAI* negative strains (Peek & Blaser, 2002). The *cagPAI*, which contains 30 genes on a 40 kb segment of DNA, encodes proteins that form a type IV secretion system (T4SS) to act as a “molecular syringe”. When *H. pylori* attaches to the epithelial cell, CagA is translocated into the cell through the T4SS and phosphorylated (Odenbreit *et al.*, 2000). The CagA protein leads to gastric epithelial cell proliferation and carcinoma development and attenuates apoptosis *in vivo*. Therefore, the CagA molecule is considered a bacteria-derived oncoprotein (Mimuro *et al.*, 2007).

Various putative cell surface receptors have been identified for CagA translocation. Studies suggest that CagA is translocated through integrin  $\alpha_5\beta_1$  as a cell surface receptor to gastric epithelial cells. CagL, which is a T4SS-pilus-localized protein, facilitates CagA translocation by utilizing integrin  $\alpha_5\beta_1$  and subsequently activating host cell kinases, such as focal adhesion kinase (FAK) and SRC kinases (Kwok *et al.*, 2007). Additional Cag proteins (CagI and CagY) bind integrin  $\beta_1$  and induce conformational changes, which leads to CagA translocation (Jimenez-Soto *et al.*, 2009). Once injected into the epithelial cell, CagA undergoes tyrosine phosphorylation by SRC and ABL kinases at repeating Glu-Pro-Ile-Tyr-Ala sequences, called EPIYA motifs (Selbach, Moese, Hauck, Meyer, & Backert, 2002; Stein *et al.*, 2002).

The EPIYA motif shows genetic variations, which occur in four distinct segments, the EPIYA -A, -B, -C, and -D segments (Backert, Moese, Selbach, Brinkmann, & Meyer, 2001). Intracellular phosphorylated CagA then interacts with SH2 domain containing proteins, such as the tyrosine phosphatase SHP-2, SRC tyrosine kinase (SCK) and the adaptor protein Crk. This leads to cytoskeleton reorganization and cell elongation (Higashi *et al.*, 2002). Besides cell elongation, phosphorylated CagA induces MAP kinase signalling causing abnormal cell cycle progression, cell proliferation and movement of the gastric epithelial cells. On the other hand, the nonphosphorylated CagA interacts with the epithelial tight junction scaffolding protein zonulin (ZO-1) (Amieva *et al.*, 2003), cadherin\beta-catenin and the kinase PAR1 (Murata-Kamiya *et*

*al.*, 2007), causing disruption of tight and adherent junctions leading to the induction of proinflammatory cytokines and loss of cell polarity. Altogether, these effects may support the formation of gastric carcinogenesis.

Besides CagA, another major virulence determinant and a key toxin produced by *H. pylori* is the Vacuolating Cytotoxin A (VacA). In addition to CagA, VacA is important for initial colonization and subsequent persistence in the gastric environment. Interestingly, VacA shows various deleterious effects on epithelial as well as immune cells. Therefore, VacA is considered a multifunctional toxin.

### 1.1.5 The versatility of Vacuolating Cytotoxin A

*H. pylori* VacA was first described as an effective toxin in broth culture supernatant, which led to the formation of massive vacuoles in diverse cultured epithelial cell lines (Leunk, Johnson, David, Kraft, & Morgan, 1988). After the discovery of its natural toxic activity, it was purified and named the Vacuolating Cytotoxin A (Cover & Blaser, 1992). Following the purification and characterization of VacA and its gene (Cover, Tummuru, Cao, Thompson, & Blaser, 1994; Phadnis, Ilver, Janzon, Normark, & Westblom, 1994; Schmitt & Haas, 1994), the role of *H. pylori* VacA has been intensively studied.

The *vacA* gene seems to be present in all *H. pylori* strains with a high level of allelic diversity. The *vacA* gene shows diversity in vacuolating activity of the bacterial culture filtrate among different strains (Cover & Blaser, 1992; Leunk *et al.*, 1988). Mutations of VacA resulting in the diversity in the vacuolating activity among *H. pylori* strains were identified. These mutations include internal duplication, large deletions, 1-bp insertions, and non-sense mutations (Ito *et al.*, 1998).

This high level of sequence diversity is found in the three variable regions: the signal sequence region (*s*-region), the intermediate region (*i*-region) and the mid region (*m*-region) (Figure 1-2).

There are two types of alleles of the *s*-region and *m*-region, which are classified as *s1* or *s2* and *m1* or *m2* (Atherton *et al.*, 1995). The *s2* type contains an additional *N*-terminal hydrophobic amino acid region. The VacA proteins of *s2* type do not cause cell vacuolation (McClain *et al.*, 2001). The specificity for cellular receptors is based on the difference of 140 amino acids between the *m1* and *m2 vacA* genotypes (Ji *et al.*, 2000). It has been observed that the *s1m1* allele combination has the highest level of virulence, resulting in the highest risk of developing gastric cancer (Atherton *et al.*, 1995; Gerhard *et al.*, 1999; Louw *et al.*, 2001). The newly identified *i1*

allele has a strong correlation with the production of CagA. This suggests that the *i-region* plays a vital role in more severe outcomes of chronic *H. pylori* infections (Chung *et al.*, 2010).

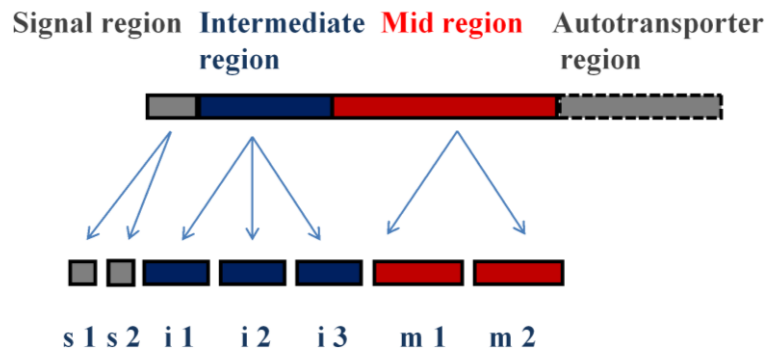


**Figure 1-2** *H. pylori vacA* gene structure.

*VacA* is a polymorphic gene, which shows allelic variation through homologous recombination. The *vacA* gene shows sequence diversity at three regions, which are the signal sequence region (*s1* and *s2*), the intermediate region (*i1*, *i2* and *i3*) and the mid region (*m1* and *m2*).

Depending on the strain, the *vacA* gene encodes a protoxin of about 145 kDa. This protoxin consists of a signal sequence, a passenger domain and an autotransporter domain (Figure 1-3).

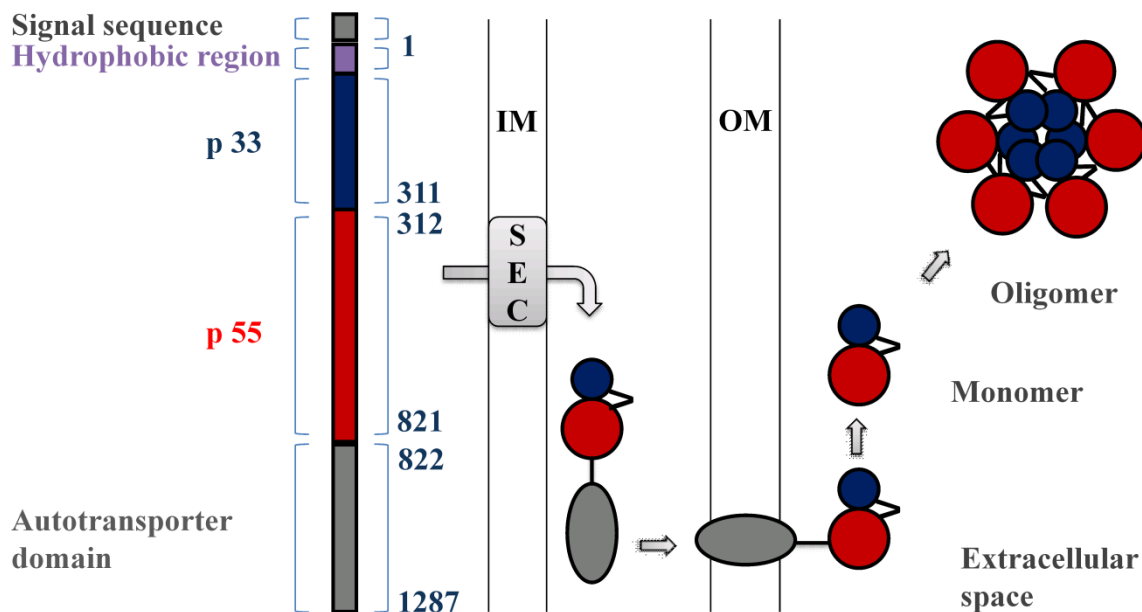


**Figure 1-3** *H. pylori VacA* protein structure.

The amino-terminal signal sequence region is cleaved from protoxin across the inner bacterial membrane. The *VacA* protein secretes about 88 kDa mature toxin, is then transported to the extracellular space via the autotransporter mechanism. The secreted toxin spontaneously forms flower-shaped dodecameric oligomers of 900 kDa.

The VacA autotransporter acts as a type V secretion system. The passenger domain contains p33 and p55 subunits, which are processed and cleaved from the autotransporter domain during secretion into the extracellular space. This results in the formation of the mature VacA toxin of 88 kDa. The two subunits of the mature toxin represent functional domains of VacA. The cleavage between p33 and p55 subunits has been shown *in vitro* (Lupetti *et al.*, 1996), but there has been no cleavage detected *in vivo* (Ricci *et al.*, 1997). The p33 subunit contains a hydrophobic region (amino acids 6-27), which is involved in membrane insertion and pore formation (McClain *et al.*, 2003; Vinion-Dubiel *et al.*, 1999). The crystal structure of p55 domain shows a right handed parallel beta-helix (Gangwer *et al.*, 2007). The p55 subunit mediates VacA binding to the host cells. The two putative domains are able to interact with each other to form complexes. It has been observed that the mixture of p33 and p55 proteins exhibits enhanced binding as compared to the p55 subunit alone to the plasma membrane of mammalian cells. In addition to the binding, the two domains together play an important role in internalization and cytotoxic activity. Therefore, it has been suggested that both the p33 and p55 domains are required for binding and internalization of VacA and both domains together contribute to the functionality of the mature toxin including vacuolating cytotoxic activity. The mature toxin of VacA can assemble into water soluble oligomeric forms, which resemble a flower-like configuration (Cover, Hanson, & Heuser, 1997). This oligomeric form of VacA is able to insert into planar lipid bilayers to form anion-selective membrane channels (Tombola *et al.*, 1999). VacA undergoes structural changes in response to acidic pH. These changes increase cellular activity and resistance to proteolysis by pepsin (de Bernard *et al.*, 1995). *In vivo* studies on *H. pylori* VacA suggest that VacA, which is secreted by *H. pylori* in the stomach, is fully active independent of mild acidic pH of gastric lumen. However, highly purified VacA is poorly active and needs to be acid activated.

## 1.2 The host

*H. pylori* colonizes in the human stomach. The stomach is located between the esophagus and the duodenum. The human stomach consists of four main sections, each of which consists of different cells and has different functions. These sections are called the cardia, the fundus, the body or the corpus and the pylorus (Figure 1-4A). The cardia is the part of the stomach where all the contents of the esophagus empty into the stomach. The fundus is formed by the upper curvature of the corpus. The main central region of the stomach consists of the body or corpus area, whereas the lower part of the stomach, the pylorus, facilitates emptying of the stomach contents into the duodenum.

The wall of the stomach is composed of four layers from inside to outside, the mucosa, the submucosa, the muscularis externa, and the serosa. The gastric glands are of three kinds: cardiac, fundic and pyloric. The shapes of the gastric glands are tubular and form a basement membrane, which consists of transparent endothelial cells lined by the epithelium.

The anatomically divided four regions have distinct histological features. The cardia predominantly contains mucus-secreting glands, called cardiac glands. They are fewer in number and occur close to the cardiac orifice (surrounding the entrance of the esophagus). The gastric pits in the cardiac region are shorter. The fundus and the body are two major histological regions. The fundus consists of straight and parallel tubular glands. These are known as chief cells and parietal cells. The chief cells are open, short columnar or polyhedral and form a very fine channel, which is altered by epithelium. Parietal cells are located between the chief cells and the basement membrane. They are oval and studded throughout the tube at intervals. The base of the gastric pit in the fundic region also contains gastrin producing enteroendocrine cells (Figure 1-4B).

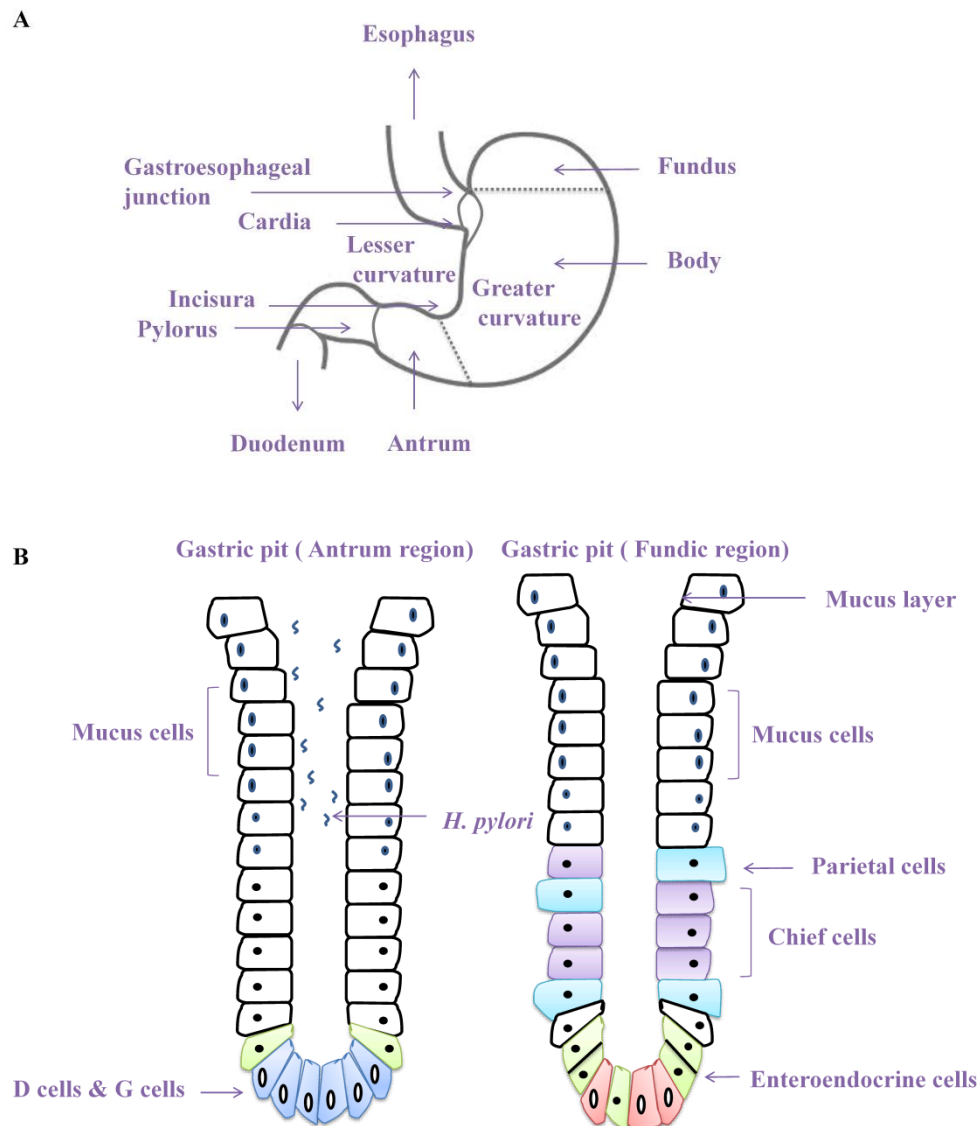


**Figure 1-4 Anatomy of the stomach and histology of the gastric mucosa.**

- A. Anatomically divided four regions of the human stomach: cardia, fundus, corpus and pylorus.
- B. Histology of the gastric pit in antrum and fundic region.

The pyloric region of the stomach consists of the pyloric glands, which are branched and open into deep irregular shaped pits. They are composed of mucus secreting cells. Mucus produced and secreted by pyloric glands lubricates and protects the entrance to the duodenum. The base of the gastric pit consists of scattered 'G' cells.

*H. pylori* resides in this gastric environment causing numerous changes and elicits various physiological and immunological responses.

### 1.2.1 *H. pylori* survival in the human host

The human stomach has to cope with many microorganisms everyday by ingestion, but most of them cannot colonize the stomach. To colonize the stomach, a microorganism has to survive in the acidic pH of the stomach lumen and requires flagella to dive into the mucus attached to the epithelial cell layer (Amieva & El-Omar, 2008). The mucus secreting cells continuously produce mucus and remove it towards the luminal side.

*H. pylori* is able to grow in this tough environment of the stomach. The colonization of *H. pylori* is achieved by a combination of specific pathogenicity factors. During the infection, *H. pylori* synthesizes the enzyme urease, which allows the bacterium to survive in the acidic environment by buffering the pH of its immediate surroundings. The shape of the bacterium (helical) and the motion of flagella facilitate crossing the thick layer of the mucus lining and allow it to reach the apical domain of gastric epithelial cells, where *H. pylori* binds with specific adhesins. *H. pylori* is able to inject the CagA protein (encoded by the Cytotoxin-associated gene A) into the host cells by a type IV secretion system (cag-T4SS). In addition, the bacteria produce and secrete a cytotoxin, the vacuolating cytotoxin (VacA).

The cag-T4SS triggers IL-8 secretion priming an inflammatory response with recruitment of neutrophil granulocytes and lymphocytes (Backert & Selbach, 2008). This promotes cell proliferation, scattering and migration and further induces the release of reactive oxygen intermediates (ROI). The released ROI together with the toxic activity of VacA leads to the tissue damage, which is deeply enhanced by loosening of the protective mucus layer and acid permeation.

## 1.3 Calcium signalling

### 1.3.1 Calcium signalling in general

$\text{Ca}^{2+}$  is a divalent cation, which is used by cells as an intracellular signal. Once inside the cell,  $\text{Ca}^{2+}$  controls many cellular processes including metabolism, cell proliferation, transcription, growth, secretion, muscle contraction, cell division and cell death. In the resting conditions of the cell, the  $\text{Ca}^{2+}$  concentration is tightly regulated in the range of 100 nM, however when the cell is activated the  $\text{Ca}^{2+}$  level rises to 1000 nM. Calcium signalling is divided into four basic functional processes. In the first process,  $\text{Ca}^{2+}$  is triggered by a stimulus, resulting in the activation of calcium mobilizing signals. Second, these signals activate various ON mechanisms that bring  $\text{Ca}^{2+}$  into the cytoplasm. Third, the ON mechanisms facilitate  $\text{Ca}^{2+}$  to act as a secondary messenger to stimulate various  $\text{Ca}^{2+}$  sensitive processes. Finally, the resting stage is restored by the OFF mechanisms, through pumps and exchangers (Figure 1-5).

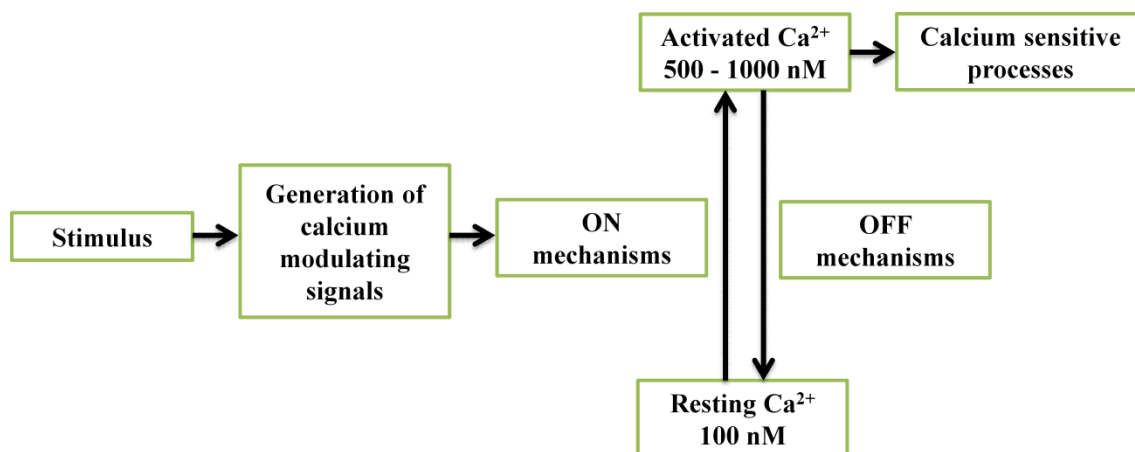


**Figure 1-5**  $\text{Ca}^{2+}$  signalling network: the ON/OFF mechanisms.

Stimuli generate  $\text{Ca}^{2+}$  mobilizing signals, which act on various ON mechanisms to trigger the increase of the intracellular  $\text{Ca}^{2+}$  concentration. The elevated  $\text{Ca}^{2+}$  concentration influences various  $\text{Ca}^{2+}$  sensitive processes. The response is terminated by OFF mechanisms, resulting in the resting  $\text{Ca}^{2+}$  level to be restored.

#### 1.3.1.1 Calcium ion channels

The  $\text{Ca}^{2+}$  entry into the cells occurs through numerous channels. These channels are located either on the plasma membrane or in intracellular compartments. These channels co-ordinate the operation of  $\text{Ca}^{2+}$  influx to maintain the cellular calcium homeostasis. Depending upon their mechanism of action, these channels are divided into voltage-dependent calcium channels

(VDCC), ligand gated ion channels (LGIC), transient receptor potential cation channels (TRPC) and calcium release activated channels (CRAC) (Figure 1-6).

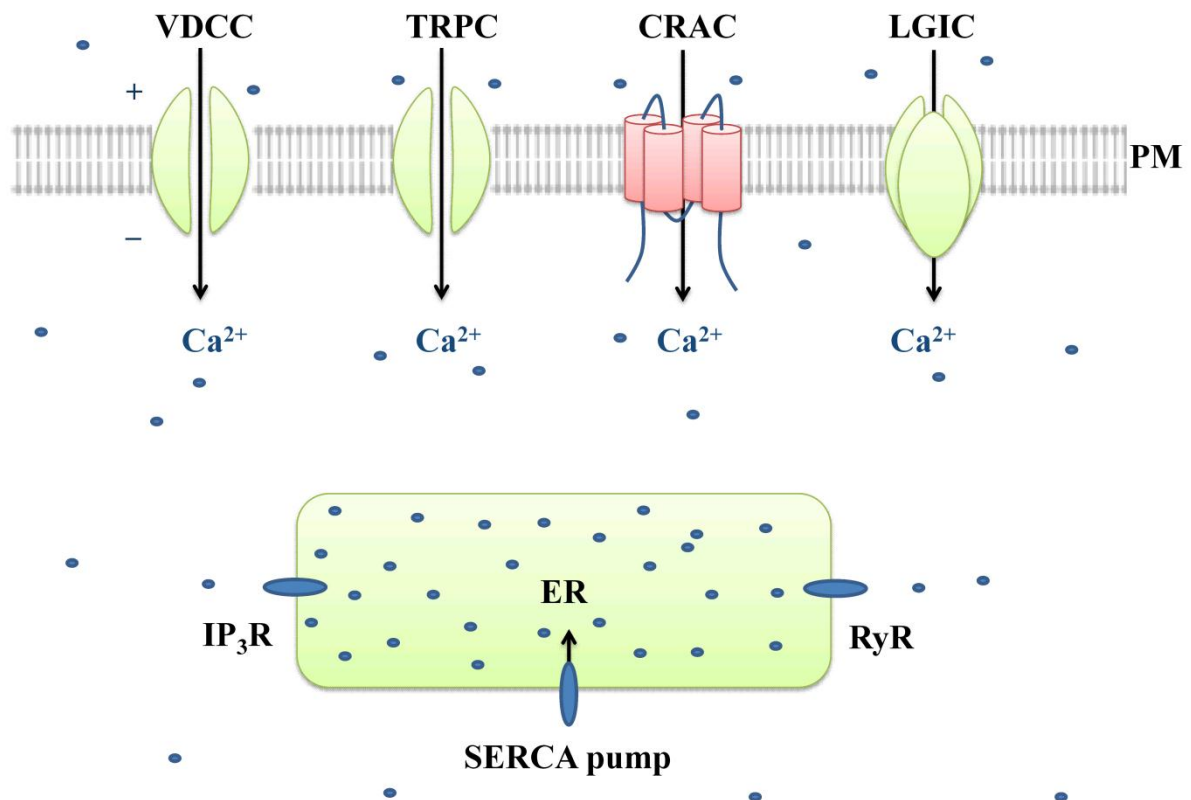


**Figure 1-6 Calcium ion channels at cell membrane and the intracellular compartments.**

The ion channels, which display selective permeability to  $\text{Ca}^{2+}$ , are located within the plasma membrane and many intracellular organelles such as the endoplasmic reticulum (ER). Many ions pass through the pore, which may be open or closed in response to various stimuli. On the plasma membrane, there are voltage-dependent calcium channels (VDCC), ligand gated ion channels (LGICs), transient receptor potential channels (TRPC) and calcium release-activated calcium (CRAC) channels.  $\text{Ca}^{2+}$  channels on the intracellular compartments are inositol trisphosphate receptor (InsP3R) and ryanodine receptors (RyRs).

#### 1.3.1.1.1 Voltage-dependent calcium channels

Voltage-dependent calcium channels (VDCC) are transmembrane ion channels located in the plasma membrane. During the resting membrane potential, VDCCs are normally closed. However, these channels are activated through changes in the electric potential difference by depolarization on the site of the channel. VDCCs function in muscle cells and neurons.

#### 1.3.1.1.2 Ligand gated ion channels (LGICs)

Ligand gated ion channels (LGICs) are also transmembrane ion channels. LGICs are a type of channel-linked receptor. LGICs are open and closed upon binding of a chemical messenger such as an endogenous ligand, which binds to a site distinct from the ion conduction pore. Ligands which can bind extracellularly are glutamate and GABA (gamma-aminobutyric acid). However, the intracellular ligands on  $\text{Ca}^{2+}$ -activated potassium channels are  $\text{Ca}^{2+}$ . It is very important to note that ligands itself do not transport across the membrane, but upon binding, cause drastic changes in the permeability of the channel, which is specific to ions. It is observed that upon activation, LGICs allow passing of  $10^7$  ions per second across the plasma membrane (Ackerman & Clapham, 1997).

#### 1.3.1.1.3 Transient receptor potential (TRP) channels

Transient receptor potential (TRP) channels are  $\text{Ca}^{2+}$  permeable cation channels, which have a polymodal activation property. TRPCs generate a transmembrane flux of cations along electrochemical gradients. TRPCs mediate downstream of cellular signal amplification processes through calcium permeation and membrane depolarization by multiple stimuli. The activation of TRPC occurs by direct activation or by receptor or ligand activation. TRPC have broadly defined roles as a cellular sensor (Clapham, 2003).

#### 1.3.1.1.4 Calcium release-activated calcium (CRAC) channels

$\text{Ca}^{2+}$  entry in immune cells occurs through highly selective channels, which are known as calcium release-activated calcium (CRAC) channels. CRAC channels are well defined examples of store-operated calcium channels (SOC). These channels open in response to the endoplasmic reticulum (ER)  $\text{Ca}^{2+}$  store depletion. The ER localized protein STIM1 senses the depletion of  $\text{Ca}^{2+}$  store, which leads to the opening of the pore subunit of the CRAC channel protein ORAI1, resulting in an increase of  $\text{Ca}^{2+}$  influx. Therefore, the intracellular  $\text{Ca}^{2+}$  level is elevated.

### 1.3.2 Calcium signalling in T-cells

$\text{Ca}^{2+}$  signalling is mandatory for many biological T-cell activities including cytokine secretion and cell proliferation, both of which are crucial to the immune response. In Th2 lymphocytes,  $\text{Ca}^{2+}$  mediates the production of interleukin 4 (IL-4), interleukin 5 (IL-5) and interleukin 13 (IL-13). Upon T-cell receptor induction, the production of inositol trisphosphate (IP3) is stimulated,

which binds to the IP<sub>3</sub> receptor on the ER, resulting in the release of Ca<sup>2+</sup> from intracellular Ca<sup>2+</sup> stores.

### 1.3.2.1 T-cell receptor signalling

T-cell receptor (TCR) activation induces the recruitment of adaptor molecules and tyrosine kinases, which form a signalling platform for the activation of downstream signalling pathways resulting in cell proliferation and cytokine production (Smith-Garvin, Koretzky, & Jordan, 2009; Yokosuka & Saito, 2010). In the key step, TCR activation ultimately leads to tyrosine phosphorylation of phospholipase C- $\gamma$  (PLC- $\gamma$ ) and leads to an increased intracellular Ca<sup>2+</sup> concentration (Weiss, Imboden, Shoback, & Stobo, 1984). PLC- $\gamma$  further hydrolyzes phosphatidylinositol 4, 5-bisphosphate (PtdIns (4, 5)P<sub>2</sub> or PIP<sub>2</sub>) to diacylglycerol (DAG) and inositol 1,4,5-trisphosphate (InsP<sub>3</sub> or IP<sub>3</sub>). IP<sub>3</sub> binds to IP<sub>3</sub> receptors (IP<sub>3</sub>R) on the ER and induces Ca<sup>2+</sup> release from the ER to the cytoplasm. (Figure 1-7 A).

### 1.3.2.2 Store-operated calcium channels

One of the most widespread and essential routes for Ca<sup>2+</sup> entry across the cell membrane in T-cells are store-operated calcium (SOC) channels (Spassova *et al.*, 2004). Ca<sup>2+</sup> entry in T-cells leads to secretion, gene expression and cell growth (Berridge, Bootman, & Roderick, 2003). Ca<sup>2+</sup> signals are a combination of Ca<sup>2+</sup> entry across the plasma membrane and Ca<sup>2+</sup> release from intracellular Ca<sup>2+</sup> stores, predominantly from the ER. It has been shown that Ca<sup>2+</sup> store depletion activates Ca<sup>2+</sup> entry into the cytosol (Muallem, Khademazad, & Sachs, 1990; Takemura & Putney, 1989), which is completely independent of TCR activation and does not require production of Ins(1,4,5)P<sub>3</sub> (Takemura, Hughes, Thastrup, & Putney, 1989), but an ionophore thapsigargin regulates Ca<sup>2+</sup> entry across membranes (Figure 1-7 B). Thus in 1990, J.W. Putney proposed a model explaining that the activation of Ca<sup>2+</sup> channels across the plasma membrane is a direct consequence of Ca<sup>2+</sup> store depletion. The process is referred as store-operated calcium entry (SOCE) (Putney, 1990). These channels, which are activated in response to the depletion of intracellular Ca<sup>2+</sup> are referred to calcium release-activated calcium (CRAC) channels or store-operated calcium channels

There are two essential components of SOCE, the ORAI calcium release-activated calcium modulator 1 (ORAI1) and the stromal interacting molecule 1 (STIM1). The ORAI1 protein was identified as a SOCE channel by three genome-wide-analyses in S2 cells (Vig *et al.*, 2006; Zhang

*et al.*, 2006). The gene encoding ORAI1 was identified by linkage analysis in which a mutation occurred in individuals with a rare immunodeficiency, resulting in T-cells displaying a defective SOCE (Feske *et al.*, 2006).

The role of STIM1 in SOCE was discovered by two studies performing RNA interference (RNAi) screening. In the first study, Ca<sup>2+</sup> responses in *Drosophila melanogaster* S2 cells were examined, and a single *D. melanogaster* STIM1 protein was identified (Roos *et al.*, 2005). In the other study, a pair of human STIM1 proteins in HeLa cells was identified (Liou *et al.*, 2005). The STIM1 protein is predominantly localized in the ER (Hewavitharana *et al.*, 2008; Manji *et al.*, 2000). Under resting conditions, STIM1 is distributed throughout the ER. STIM1 undergoes rapid redistribution and moves towards plasma membrane junctions within a few seconds following store depletion (Wu, Buchanan, Luik, & Lewis, 2006). These proteins sense Ca<sup>2+</sup> via the N-terminal domain, consisting of an EF-hand motif Ca<sup>2+</sup>-binding site, located in the lumen of the ER (Stathopoulos, Li, Plevin, Ames, & Ikura, 2006), which triggers this rapid oligomerization of STIM1. The C-terminal region consists of a CRAC activation domain (CAD) (Park *et al.*, 2009), which mediates coupling with ORAI1. The junction where STIM1 move towards the plasma membrane is called puncta, where STIM1 is localized towards ORAI1, that activates CRAC/SOC channels. Once the CRAC channels are activated and open, the Ca<sup>2+</sup> influx is increased, which leads to an increase in intracellular Ca<sup>2+</sup> concentration (Figure 1-7 B).

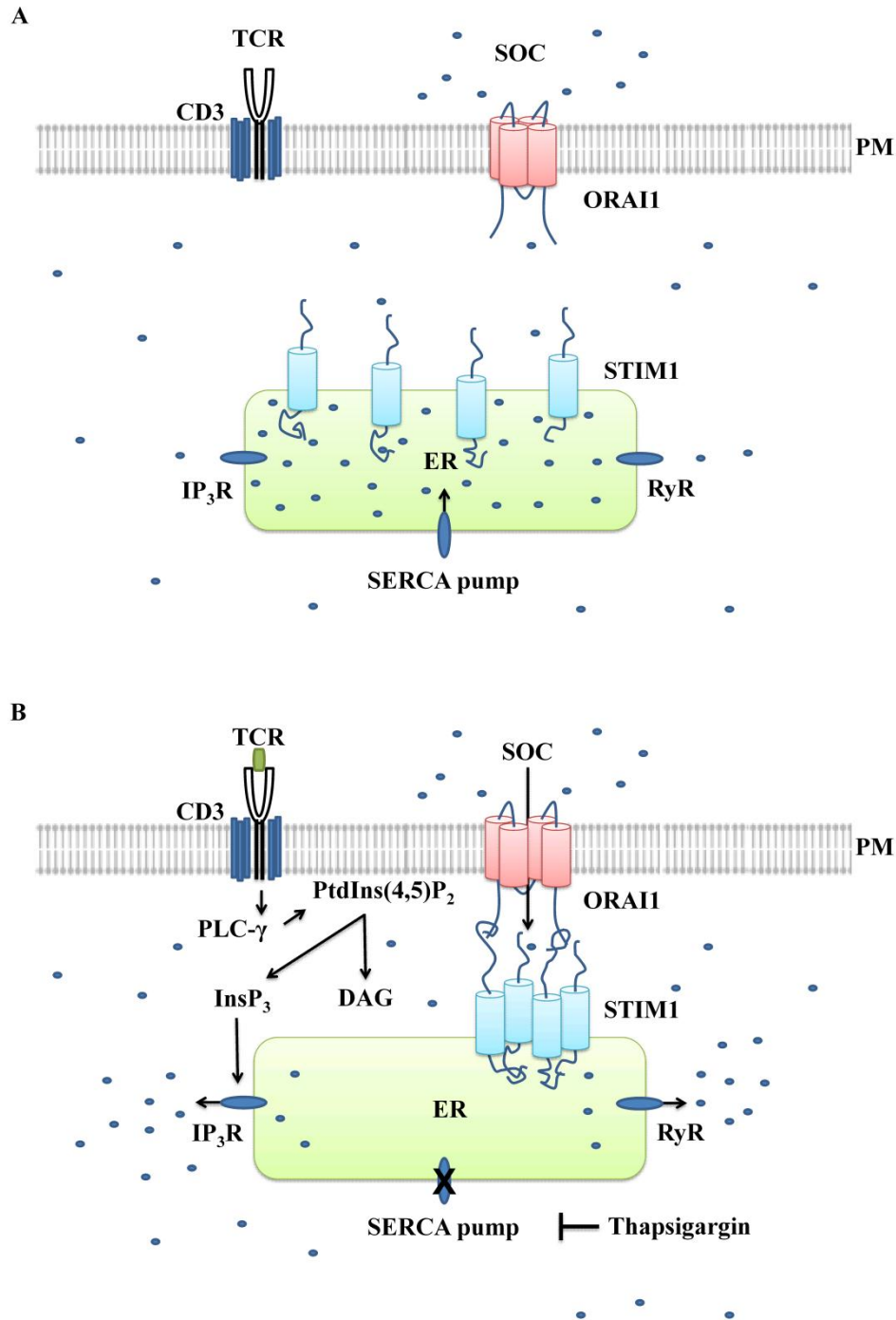


**Figure 1-7 Calcium signalling in T-cells.**

- A. Under normal resting conditions, the intracellular  $\text{Ca}^{2+}$  concentration is constant.
- B. Ligand binding to T-cell receptor (TCR) initiates the activation of tyrosine kinases, which activate phospholipase C- $\gamma$  (PLC- $\gamma$ ). The activated PLC- $\gamma$  cleaves phosphatidylinositol 4, 5-bisphosphate (PtdIns (4, 5)P) in inositol 1,4,5-trisphosphate (InsP<sub>3</sub>) and diacylglycerol (DAG). The InsP<sub>3</sub> binds to IP<sub>3</sub> receptor (IP<sub>3</sub> R) on the endoplasmic reticulum (ER). IP<sub>3</sub>R opens intracellular calcium channel. In another mechanism,  $\text{Ca}^{2+}$  depletion may also be induced by thapsigargin, which blocks the SERCA pump, resulting in inhibition of  $\text{Ca}^{2+}$  store refilling. In this process, when a T-cell releases  $\text{Ca}^{2+}$  from the ER,  $\text{Ca}^{2+}$  depletion is sensed by STIM1, which

induces clustering of STIM1. The clustering happens close to the plasma membrane, where it regulates calcium channels by activating the CRAC channel protein ORAI1.

## 1.4 Aim of this study

*H. pylori* colonization and persistence in the human stomach lead to the development of various gastroduodenal diseases. A lifelong infection by *H. pylori* modulates both the immune response and host cellular processes. One among many virulence factors of *H. pylori* important in this process is the Vacuolating Cytotoxin A (VacA).

VacA contributes to *H. pylori* colonization in the stomach and exhibits a high level of multifunctionality. VacA is able to intoxicate a wide range of cells in the host including gastric epithelial cells and various immune cells.

Despite the well-documented effect on epithelial cells, the effect of VacA on immune cells, particularly T-cells, has been demonstrated. VacA inhibits production of IL-2 and downregulates surface expression of the IL-2 receptor by inhibiting the activation of nuclear factor of activated T-cells (NFAT) in T-cells. The mechanism of inhibition of NFAT activation involves the blocking of  $\text{Ca}^{2+}$  influx into the cells from the extracellular environment, thereby inhibiting the activity of the  $\text{Ca}^{2+}$  calmodulin dependent phosphatase calcineurin. Moreover, VacA intoxication is reported to inhibit proliferation of activated T-cells and to induce mitochondrial depolarization, ATP depletion and cell cycle arrest.

However, the effect of VacA on T-cells involving the blocking of  $\text{Ca}^{2+}$  influx is poorly studied.

The specific aim of this study is to identify the mechanism by which VacA is able to block  $\text{Ca}^{2+}$  influx in T-cells. This will help to understand the biological effect of VacA on T-cells in detail and characterize further the modulatory properties of *H. pylori* VacA in the human host.

## 2. Materials and Methods

### 2.1 Materials

#### 2.1.1 Bacterial strains

##### 2.1.1.1 *Helicobacter pylori* strains

**Table 2-1 *Helicobacter pylori* strains**

Name/Strain	Genotype and Reference
60190	VacA wild type <i>sIm1</i> strain for production of VacA (Atherton <i>et al.</i> , 1995)
<i>H. pylori</i> AV452	60190 VacA $\Delta$ 6-27 mutant strain (Vinion-Dubiel <i>et al.</i> , 1999)
P12	Clinical isolate from the Department of Medicine Microbiology and Immunology, University of Hamburg (Schmitt & Haas, 1994)
P12 $\Delta$ VacA	P12 strain with deletion of VacA

##### 2.1.1.2 *Escherichia coli* strains

**Table 2-2 *Escherichia coli* strains**

Name/Strain	Genotype and Reference
DH5 $\alpha$	F-, $\phi$ 80lacZ $\Delta$ M15 $\Delta$ (lacZYA-argF)U169, deoR, recA 1, endA 1, hsdR 17(rK-, mK+), supE 44, thi -1, $\lambda$ - gyrA 96, relA 1 (Hanahan, 1983)
DB 3.1	F- gyrA462 endA1 glnV44 $\Delta$ (sr1-recA) mcrB mrr hsdS20 (r <sub>B</sub> <sup>-</sup> , m <sub>B</sub> <sup>-</sup> ) ara14 galK2 lacY1 proA2 rpsL20(Sm <sup>r</sup> ) xyl5 $\Delta$ leu mt11

### 2.1.1.3 Yeast strains (*Saccharomyces cerevisiae*)

#### 2.1.1.3.1 *Saccharomyces cerevisiae* strains

**Table 2-3** *Saccharomyces cerevisiae* strains

Name	Strain	Genotype and Reference
UJY 13	CG1945	Ade <sup>-</sup> , Leu <sup>-</sup> , His <sup>-</sup> , haploid, Mating Type a + pUJ 94
UJY 14	Y187	Ade <sup>-</sup> , Trp <sup>-</sup> , His <sup>-</sup> , haploid, Mating Type $\alpha$ + pUJ 95
UJY 15	CG1945	Ade <sup>-</sup> , Leu <sup>-</sup> , His <sup>-</sup> , haploid, Mating Type a + pUJ 77
UJY 16	CG1945	Ade <sup>-</sup> , Leu <sup>-</sup> , His <sup>-</sup> , haploid, Mating Type a + pUJ 81
UJY 17	CG1945	Ade <sup>-</sup> , Leu <sup>-</sup> , His <sup>-</sup> , haploid, Mating Type a + pUJ 78
UJY 18	CG1945	Ade <sup>-</sup> , Leu <sup>-</sup> , His <sup>-</sup> , haploid, Mating Type a + pUJ 79
UJY 19	CG1945	Ade <sup>-</sup> , Leu <sup>-</sup> , His <sup>-</sup> , haploid, Mating Type a + pUJ 82
UJY 20	Y187	Ade <sup>-</sup> , Trp <sup>-</sup> , His <sup>-</sup> , haploid, Mating Type $\alpha$ + pUJ 87
UJY 21	Y187	Ade <sup>-</sup> , Trp <sup>-</sup> , His <sup>-</sup> , haploid, Mating Type $\alpha$ + pUJ 88
UJY 22	Y187	Ade <sup>-</sup> , Trp <sup>-</sup> , His <sup>-</sup> , haploid, Mating Type $\alpha$ + pUJ 89
UJY 23	Y187	Ade <sup>-</sup> , Trp <sup>-</sup> , His <sup>-</sup> , haploid, Mating Type $\alpha$ + pUJ 92
UJY 24	Y187	Ade <sup>-</sup> , Trp <sup>-</sup> , His <sup>-</sup> , haploid, Mating Type $\alpha$ + pUJ 93
UJY 25	CG1945	Ade <sup>-</sup> , Leu <sup>-</sup> , His <sup>-</sup> , haploid, Mating Type a + pUJ 96
UJY 26	Y187	Ade <sup>-</sup> , Trp <sup>-</sup> , His <sup>-</sup> , haploid, Mating Type $\alpha$ + pUJ 98
UJY 27	CG1945	Ade <sup>-</sup> , Leu <sup>-</sup> , His <sup>-</sup> , haploid, Mating Type a + pUJ 97
UJY 28	Y187	Ade <sup>-</sup> , Trp <sup>-</sup> , His <sup>-</sup> , haploid, Mating Type $\alpha$ + pUJ 99
UJY 29	CG1945; Y187	Ade <sup>-</sup> , His <sup>-</sup> , diploid, Type $\alpha\alpha$ + pGADT7; pUJ 95
UJY 30	CG1945; Y187	Ade <sup>-</sup> , His <sup>-</sup> , diploid, Type $\alpha\alpha$ + pUJ 94; pGBKT7
UJY 31	CG1945; Y187	Ade <sup>-</sup> , His <sup>-</sup> , diploid, Type $\alpha\alpha$ + pUJ 77; pUJ 95
UJY 32	CG1945; Y187	Ade <sup>-</sup> , His <sup>-</sup> , diploid, Type $\alpha\alpha$ + pUJ 78; pUJ 95

UJY 33	CG1945; Y187	Ade <sup>-</sup> , His <sup>-</sup> , diploid, Type aa + pUJ 79; pUJ 95
UJY 34	CG1945; Y187	Ade <sup>-</sup> , His <sup>-</sup> , diploid, Type aa + pUJ 81; pUJ 95
UJY 35	CG1945; Y187	Ade <sup>-</sup> , His <sup>-</sup> , diploid, Type aa + pUJ 82; pUJ 95
UJY 36	CG1945; Y187	Ade <sup>-</sup> , His <sup>-</sup> , diploid, Type aa + pUJ 83; pUJ 95
UJY 37	CG1945; Y187	Ade <sup>-</sup> , His <sup>-</sup> , diploid, Type aa + pUJ 84; pUJ 95
UJY 38	CG1945; Y187	Ade <sup>-</sup> , His <sup>-</sup> , diploid, Type aa + pUJ 77; pGBKT7
UJY 39	CG1945; Y187	Ade <sup>-</sup> , His <sup>-</sup> , diploid, Type aa + pUJ 78; pGBKT7
UJY 40	CG1945; Y187	Ade <sup>-</sup> , His <sup>-</sup> , diploid, Type aa + pUJ 79; pGBKT7
UJY 41	CG1945; Y187	Ade <sup>-</sup> , His <sup>-</sup> , diploid, Type aa + pUJ 81; pGBKT7
UJY 42	CG1945; Y187	Ade <sup>-</sup> , His <sup>-</sup> , diploid, Type aa + pUJ 82; pGBKT7
UJY 43	CG1945; Y187	Ade <sup>-</sup> , His <sup>-</sup> , diploid, Type aa + pUJ 83; pGBKT7
UJY 44	CG1945; Y187	Ade <sup>-</sup> , His <sup>-</sup> , diploid, Type aa + pUJ 84; pGBKT7
UJY 45	CG1945; Y187	Ade <sup>-</sup> , His <sup>-</sup> , diploid, Type aa + pUJ 94; pUJ 87
UJY 46	CG1945; Y187	Ade <sup>-</sup> , His <sup>-</sup> , diploid, Type aa + pUJ 94; pUJ 88
UJY 47	CG1945; Y187	Ade <sup>-</sup> , His <sup>-</sup> , diploid, Type aa + pUJ 94; pUJ 89
UJY 48	CG1945; Y187	Ade <sup>-</sup> , His <sup>-</sup> , diploid, Type aa + pUJ 94; pUJ 92
UJY 49	CG1945; Y187	Ade <sup>-</sup> , His <sup>-</sup> , diploid, Type aa + pUJ 94; pUJ 93
UJY 50	CG1945; Y187	Ade <sup>-</sup> , His <sup>-</sup> , diploid, Type aa + pUJ 94; pUJ 85
UJY 51	CG1945; Y187	Ade <sup>-</sup> , His <sup>-</sup> , diploid, Type aa + pUJ 94; pUJ 86
UJY 52	CG1945; Y187	Ade <sup>-</sup> , His <sup>-</sup> , diploid, Type aa + pGADT7; pUJ 87
UJY 53	CG1945; Y187	Ade <sup>-</sup> , His <sup>-</sup> , diploid, Type aa + pGADT7; pUJ 88
UJY 54	CG1945; Y187	Ade <sup>-</sup> , His <sup>-</sup> , diploid, Type aa + pGADT7; pUJ 89
UJY 55	CG1945; Y187	Ade <sup>-</sup> , His <sup>-</sup> , diploid, Type aa + pGADT7; pUJ 92
UJY 56	CG1945; Y187	Ade <sup>-</sup> , His <sup>-</sup> , diploid, Type aa + pGADT7; pUJ 93
UJY 57	CG1945; Y187	Ade <sup>-</sup> , His <sup>-</sup> , diploid, Type aa + pGADT7; pUJ 85

UJY 58	CG1945; Y187	Ade <sup>-</sup> , His <sup>-</sup> , diploid, Type aa + pGADT7; pUJ 86
--------	--------------	---

### 2.1.2 Cell lines

**Table 2-4 Eukaryotic cell lines**

Name/cell line	Description
HEK-293	Human embryonic kidney cell line
HEK-293 eGFP-myc-ORAI1	HEK-293 cells stably expressing eGFP-myc-ORAI1
HEK-293 mCherry-STIM1	HEK-293 cells stably expressing mCherry-STIM1
HEK-293 mCherry-STIM1 His tag	HEK-293 cells stably expressing mCherry-STIM1
Jurkat E6.1	Human T-cell line (ATCC TIB-152)
Human Primary CD <sup>4+</sup> T-cells	Human T-cells

### 2.1.3 Plasmids and vectors

**Table 2-5 Plasmids and vectors**

Plasmid/Vector	Description
pEGFPN-1	Vector for fusion of EGFP to the C-terminus of a partner protein. The MCS is between the immediate early promoter of CMV and EGFP coding sequence.
pDONR <sup>TM</sup> 207	Recombination plasmid for gateway cloning containing <i>ccdB</i> cassette, <i>attP1</i> and <i>attP2</i> sequence for the recombination with <i>attB1</i> , and <i>attB2</i> sequence, pUC ori (Invitrogen, Karlsruhe).
pGADT7	$\mu$ ori2, pUC ori, PADH1, PT7, SV40 NLS, GAL4-AD, TADH1, LEU2, AmpR (Clontech, California, USA)
pGBKT7	$\mu$ ori2, pUC ori, orif1, PADH1, PT7, GAL4-BD, TADH1&T7, TRP1, KanR (Clontech, California, USA)
pUj 1	mCherry-STIM1
pUj 2	ORAI1 before 1 <sup>st</sup> transmembrane domain 1

pUj 3	ORAI1 before 1 <sup>st</sup> transmembrane domain 2
pUj 4	ORAI1 after 4 <sup>th</sup> transmembrane domain
pUj 5	mCherry-STIM1 $\Delta$ CAD
pUj 11	mCherry-STIM1 with His-tag
pSp 24	pDONR <sup>TM</sup> 207 with sequence for VacA having <i>attL1</i> and <i>attL2</i> sites for yeast two-hybrid assay
pUj 77	pGADT7 with sequence for EF-SAM domain of STIM1 having <i>attB1</i> and <i>attB2</i> sites for yeast two-hybrid assay
pUj 78	pGADT7 with sequence for SAM domain of STIM1 having <i>attB1</i> and <i>attB2</i> sites for yeast two-hybrid assay
pUj 79	pGADT7 with sequence for CAD domain of STIM1 having <i>attB1</i> and <i>attB2</i> sites for yeast two-hybrid assay
pUj 81	pGADT7 with sequence for ORAI1 aa 48-91 having <i>attB1</i> and <i>attB2</i> sites for yeast two-hybrid assay
pUj 82	pGADT7 with sequence for ORAI1 aa 255-301 having <i>attB1</i> and <i>attB2</i> sites for yeast two-hybrid assay
pUj 83	pGADT7 with sequence for cEF domain of STIM1 having <i>attB1</i> and <i>attB2</i> sites for yeast two-hybrid assay
pUj 84	pGADT7 with sequence for hEF domain of STIM1 having <i>attB1</i> and <i>attB2</i> sites for yeast two-hybrid assay
pUj 85	pGBKT7 with sequence for cEF domain of STIM1 having <i>attB1</i> and <i>attB2</i> sites for yeast two-hybrid assay
pUj 86	pGBKT7 with sequence for hEF domain of STIM1 having <i>attB1</i> and <i>attB2</i> sites for yeast two-hybrid assay
pUj 87	pGBKT7 with sequence for EF-SAM domain of STIM1 having <i>attB1</i> and <i>attB2</i> sites for yeast two-hybrid assay
pUj 88	pGBKT7 with sequence for SAM domain of STIM1 having <i>attB1</i> and

	<i>attB2</i> sites for yeast two-hybrid assay
pUj 89	pGBKT7 with sequence for CAD domain of STIM1 having <i>attB1</i> and <i>attB2</i> sites for yeast two-hybrid assay
pUj 92	pGBKT7 with sequence for ORAI1 aa 48-91 having <i>attB1</i> and <i>attB2</i> sites for yeast two-hybrid assay
pUj 93	pGBKT7 with sequence for ORAI1 aa 255-301 having <i>attB1</i> and <i>attB2</i> sites for yeast two-hybrid assay
pUj 94	pGADT7 with sequence for VacA having <i>attB1</i> and <i>attB2</i> sites for yeast two-hybrid assay
pUj 95	pGBKT7 with sequence for VacA having <i>attB1</i> and <i>attB2</i> sites for yeast two-hybrid assay
SPE 151	eGFP-myc-ORAI1

#### 2.1.4 Oligonucleotides

The oligonucleotides were purchased from Biomers (Ulm, Germany). Table 2-6 shows the sequences (from 5' to 3'), the intended use, as well as interfaces or any other modifications of the oligonucleotides.

**Table 2-6 Oligonucleotides sequence (5' to 3') and their description**

Name	Sequence 5' - 3'	Description
Uj 5	gat <b>cag atc tgc</b> gcg gaa ccc cta ttt	Sense primer with the sequence of <b>BglIII</b> -Kanamycin/neomycin resistance gene for pEGFP-N1 vector
Uj 6	gat <b>cag atc tgg</b> tct cgg tgg ggt at	Antisense primer with the sequence of <b>BglIII</b> -Kanamycin/neomycin resistance gene for pEGFP-N1 vector
Uj 7	ggc <b>cgg tac cca tca tca</b> <b>tca tca cca</b> tat ggt gag caa ggg cga	Sense primer with the sequence of <b>Kpn1-His tag</b> for mCherry-STIM1 vector
Uj 8	gat <b>cgg tac cct</b> tgt aca	Sense primer with the sequence of <b>Kpn1</b> for

	gct cgt cca tgc c	mCherry-STIM1 vector
Uj 9	atg ggc cgg tac cca tca tca tca tca cca tat ggt gag caa ggg cga	Sense primer with the sequence of atg-kpn1- His tag for mCherry-STIM1 vector
Uj 21	aaa aag cag gct ccg cca tga gtg agg atg aga aac tca gc	Sense primer with the sequence of attB1 recombination sites for the amplification of EF hand-SAM domain at aa 58 of STIM1
Uj 22	aga aag ctg ggt cta aaa gag cac tgt atc cag agc	Antisense primer with the sequence of attB2 recombination sites for the amplification of EF hand-SAM domain at aa 200 of STIM1
Uj 23	acg cct cga gca tat ggt gga tgc cag ggt tgt tg	Antisense primer with the sequence of Xho1- Nde1 for the amplification of CAD domain of STIM1
Uj 24	atg cgt gga tgc cag ggt tgt tg	Sense primer for amplification of CAD domain of STIM1
Uj 25	cga tgc tga gct ctt aag cgt agc tag cga aac g	Antisense primer with the sequence of Sac1 for for amplification of p58 domain of VacA 60190
Uj 26	aaa aag cag gct ccg cca tga att gga ccg tgg atg agg tg	Sense primer with the sequence of attB1 recombination sites for the amplification of SAM domain at aa 131 of STIM1
Uj 27	aga aag ctg ggt cta ttc tga tga ctt cca tgc ctt	Antisense primer with the sequence of attB2 recombination sites for the amplification of cEF hand and hEF hand domain at aa 128 of STIM1
Uj 28	aga aag ctg ggt cta gag gtc ttc cct cag gaa ctc	Antisense primer with the sequence of attB2 recombination sites for the amplification of cEF hand domain at aa 96 of STIM1
Uj 29	aaa aag cag gct ccg cc atg aat tac cat gac cca aca gtg	Sense primer with the sequence of attB1 recombination sites for the amplification of hEF hand domain at aa 97 of STIM1
Sp 183	aaa aag cag gct ccg	Sense primer with the sequence of attB1

	cca tgt ccg ccg tca cct acc c	recombination sites for the amplification of N-terminal region at aa 48 of ORAI1
SP 184	aga aag ctg ggt cta ccg gct gga ggc ttt aag c	Antisense primer with the sequence of <i>attB2</i> recombination sites for the amplification of N-terminal region at aa 91 of ORAI1
Sp 185	aaa aag cag gct ccg cc atg gtc cac ttc tac cgc tca ctg	Sense primer with the sequence of <i>attB1</i> recombination sites for the amplification of C-terminal region at aa 255 of ORAI1
Sp 186	aga aag ctg ggt cta ggc ata gtg gct gcc g	Antisense primer with the sequence of <i>attB2</i> recombination sites for the amplification of C-terminal region at aa 301 of ORAI1
Sp 187	ggg gac aag ttt gta caa aaa agc agg ct	Sense primer with the sequence of <i>attB-external</i>
Sp 188	ggg gac cac ttt gta caa gaa agc tgg gt	Antisense primer with the sequence of <i>attB-external</i>

## 2.1.5 Broth or culture media

### 2.1.5.1 Broth or culture media for bacteria

**Table 2-7 Culture media and nutrients for bacteria**

Culture media/nutrients	Production and source
LB liquid medium	20 g/l Lennox medium (Gibco/Invitrogen, Carlsbad, USA), autoclaved
LB-plates	32 g/l Lennox-L-Agar (Gibco/Invitrogen, Carlsbad, USA), autoclaved
Brucella-Broth (BB)	28 g/l Brucella Broth (Falcon BD, Franklin Lakes, USA), autoclaved
Serum plates	36 g/l GC-Agar-Base (Oxoid, Darmstadt, Germany), autoclaved and subsequently added 10 ml/l Vitamin-Mix, 80 ml/l Horse serum, 10 mg/l Vancomycin, 5 mg/l Trimethoprim, 1 mg/l Nystatin
Vitamin mix	100 g/l $\alpha$ -D-Glucose, 10 g/l L-Glutamin, 26 g/l L-Cystein, 0.1 g/l Cocarboxylase, 20 mg/l Fe(III)-Nitrate, 333 mg/l Thiamine, 13 mg/l p- aminobenzoic acid, 0.25 g/l Nicotinamadeninindinucleotid (NAD), 10 mg/l Vitamin B12, 1.1 g/l L-Cystine, 1 g/l Adenine, 30 mg/l Guanine, 0.15 g/l L-Arginine, 0.5 g/l Uracil

## 2.1.6 Inhibitors and media supplements

**Table 2-8 Inhibitors and media supplements**

Media supplements	Solvents	Working concentrations
Ampicillin (Sigma-Aldrich, St. Louis, USA)	H <sub>2</sub> O	100 $\mu$ g/ml
Chloramphenicol (Merck, Darmstadt, Germany)	Ethanol	30 $\mu$ g/ml ( <i>E. coli</i> ) 6 $\mu$ g/ml ( <i>H. pylori</i> )

Gentamycin (Sigma-Aldrich, St. Louis, USA)	H <sub>2</sub> O	10 µg/ml ( <i>E. coli</i> )
Nystatin (Merck, Darmstadt, Germany)	H <sub>2</sub> O	440 µl/l ( <i>H. pylori</i> )
Trimethoprim (Sigma-Aldrich, St. Louis, USA)	H <sub>2</sub> O	5 µg/ml
Vancomycin (Sigma-Aldrich, St. Louis, USA)	H <sub>2</sub> O	10 µg/ml

### 2.1.7 Cell culture medium and buffers

A different medium is necessary for each cell line.

**Table 2-9 Cell culture media**

Name	Description
Cell Media	High Glucose DMEM, RPMI-1640 (Invitrogen/GIBCO BRL), 10X MEM
Antibiotic	Penicillin/Streptomycin and Gentamicin (Invitrogen/GIBCO BRL)
Selective	G418 (Geneticin) and Hygromycin B (Paa laboratories), Puromycin (SIGMA-Aldrich) and Zeocin (Invitrogen/GIBCO BRL).
Supplements	Fetal Calf Serum and L-Glutamine (Invitrogen/GIBCO BRL). Fetal Bovine Serum Superior (Biochrom), 7.5% Sodium Bicarbonate (GIBCO)
Others	Trypsin-EDTA (TE), Dulbecco PBS (+Ca, +Mg) and Dulbecco PBS (-Ca,-Mg) (Invitrogen/GIBCO BRL), DMSO and EDTA (Sigma-Aldrich).

### 2.1.8 Enzymes and proteins

**Table 2-10 Enzymes and proteins with their respective sources**

Enzyme/Protein	Firms
Gateway <sup>®</sup> BPII Clonase <sup>®</sup> Enzyme Mix	Invitrogen, Carlsbad, USA
Gateway <sup>®</sup> LR Clonase <sup>®</sup> Enzyme Mix	Invitrogen, Carlsbad, USA
DNase I	Roche, Grenzach-Wyhlen, Germany
Takara-Taq-Polymerase	TaKaRa Bio Inc., Otsu, Japan
Expand High Fidelity Taq-Polymerase	Roche, Grenzach-Wyhlen, Germany

Fetal calf serum (FCS)	PAA, Pasching, Austria
Horse serum	Carlsbad, USA
Bovine serum albumin	(BSA) Sigma-Aldrich, St. Louis, USA
Trypsin-EDTA solution	Invitrogen/Gibco, Carlsbad, USA
Restriction enzymes	Roche, Grenzach-Wyhlen and NEB, Germany

### 2.1.9 Molecular markers

**Table 2-11 Molecular markers and their sources**

Molecular markers	Sources
DNA gel electrophoresis	GeneRuler™ 1 kb DNA Ladder (MBI Fermentas, St. Leon-Roth, Germany)
DNA gel electrophoresis	O'GeneRuler™ Low Range DNA Ladder, ready to use (MBI Fermentas, St. Leon-Roth, Germany)
Polyacrylamide gel electrophoresis	Prestained High Range 161-0373 (Bio-Rad, Hercules, USA)
Polyacrylamide gel electrophoresis	Prestained Protein Molecular Weight Marker, SM0441 (MBI Fermentas, St. Leon-Roth, Germany)

### 2.1.10 Chemicals and reagents

BBL Brucella Broth (BD Falcon), Fluoroprep (BioMeriux), Coomassie Brilliant Blue G250 (Biomol), Acrylamide/Methylenbisacrylamide 30% (29:1), X-Gal (Roth), Streptomycin, Trimethoprim, Vancomycin, Nystatin, Ampicillin, Phorbol-12-myristat-13-acetate (PMA), 5-Bromo-4-chloro-3-indolylphosphate (BCIP), Ionomycin, Guanidine-HCL, Ethidium Bromide, Leupeptin, Sodium orthovanadate, Glutaraldehyde, Pepstatin, Triton X-100, Tween 20, DMSO, Dansylcadaverine, Methyl- $\beta$  Cyclodextrin (Heptakis), Ammonium chloride (Sigma-Aldrich), Chloramphenicol (Serva), Kanamycin, Phenylmethylsulfonyl fluoride (PMSF) (Merck), GC Agar, LB Agar, LB broth (Oxoid), Brucella Broth (BD BBL™), Precision Plus Protein Standards All Blue (BioRad), L-glutamine (Gibco®), Trypsin, G-418 sulfate (PAA), Tetracycline (Sigma-Aldrich), Hygromycin B (Invitrogen), Blastidicin (Invitrogen), Doxycycline (Sigma-Aldrich), Sodium bicarbonate (Gibco®), HEPES (Gibco®), Glucose (Roth), Sodium pyruvate (Gibco®),

FCS (tetracycline free) (Clontech), Calcium/Magnesium free PBS (Gibco®), LB broth (Invitrogen), Glycerol (Roth), Coomassie Brilliant Blue G250 (Roth), Phosphoric Acid (Roth), Acrylamide (Roth), SDS (Schwarz/Mann Biotech) Coomassie destaining solution (Roth), Methanol (Sigma-Aldrich), Acetic Acid (Roth), Coomassie Brilliant Blue R250 (Merck), Ammonium chloride (NH<sub>4</sub>Cl) (FLUKA Chemika), HCl (Roth), Biocoll separating solution 1.077 (Biochrom AG), Heparin (Merck), Lithium Acetate (Sigma-Aldrich) and PMSF (Sigma-Aldrich, St. Louis, USA).

All other organic and inorganic chemicals were from Merck, Roth and Sigma-Aldrich. Other specific reagents are listed with the methods.

### 2.1.11 Consumables and equipments

#### 2.1.11.1 Consumables

X-Ray film (Fuji, A. Hastenstein), Dialysis membranes (Medicell), Dialysis membranes for small volumes (Pierce), ELISA Maxisorp plates (Nunc), Cell scrappers (Falcon), FACS tubes (Becton Dickinson), Freezing Tubes 2 ml (Nalgene), PVDF membrane (Bio-Rad), High Range Protein Marker (Bio-Rad), Cell culture treated plates (Corning), 0.2 µm- Sterilefilters (Millipore), Cell culture treated bottles (75 cm<sup>2</sup> and 175 cm<sup>2</sup>) (BD Falcon), Filter paper (Whatman), Cell culture inserts 3 µm pores (Corning), Parafine pellets (Fluka), 75 cm<sup>2</sup> cell culture flask (BD Biosciences), BD Falcon™ (BD Biosciences), Neubauer Chamber (BLAUBRAND®), Micro Beads and Column LS (Miltenyi Biotec).

#### 2.1.11.2 Equipments

Thermo Scientific Heraeus® Megafuge 3.0R, Freezer -70 Thermo Scientific, Microscope-Hund Wetzlar, PAGE-Mini Gel System, Voltage Units PowerPac 300, PowerPac 1000 (Bio-Rad), Incubator (Binder), Incubator *Ultima* (Revco), Microincubator MI22C (Scholzen), Gel documentation System (Bio-Rad), Absorbance Reader Sunrise (TECAN systems), Spectrophotometer DR/2000 (Hach), Agarose Gel Electrophoresis chamber (Bio-Rad), Centrifuge Biofuge 15 R and Megafuge 3.0R (Heraeus), Centrifuge Mikro 20 (Hettich), Magnetic Stirrer MR 3001 (Heidolph), Medical Film Processor FPM-100A (Fijifilm), Microscope DM IRB (Leica), Live cell imaging Microscope (Perkin-Elmer) and TCS Software (LEICA), PCR Thermocycler (ThermoHybaid), PCR Thermocycler Microcycler Personal (Eppendorf), Pipette Transferpette-8 (20-200 µl and 0.5-10 µl) (Brand), Scales (Fischer Biotech), pH Meter (WTW),

Sterile Hood (BDK), Vacuum Centrifuge Speed-Vac DNA 110 (Savant), Vortex Gene 2 (Scientific Industries), Water Bath (GFL) and MidiMACS™ Separator (Miltenyi Biotech).

### 2.1.12 Computer programmes

Dnaman 6, CLC DNA workbench 6, GraphPad prism 5, Image J, Volocity software and Endnote programme.

## 2.2 Methods

### 2.2.1 Work with Bacteria

#### 2.2.1.1 Growth and cultivation of *E. coli*

*Escherichia coli* was grown on LB-agar for selection of transformants. All complemented with their respective antibiotic and/or inducer.

Medium      LB Agar      32 g/l Lennox-L Agar

LB Media      20 g/l Lennox-L Medium

Antibiotics      Ampicillin 100 mg/l, Chloramphenicol 30 g/l, Kanamycin 50 mg/l

#### 2.2.1.2 Freezing of *E. coli*

Bacteria were grown overnight in LB broth and 750 µl of overnight grown culture were mixed with 750 µl of a sterile 70% (v/v) glycerol solution, the bacteria were frozen in -70°C storage.

#### 2.2.1.3 Growth and cultivation of *H. pylori*

*H. pylori* was grown on a GC agar plate containing serum and appropriate antibiotics for 24 h and passaged again for next 3 day. The bacterial culture was then used for preparation of liquid cultures. Liquid cultures were prepared in Brucella medium as required and supplemented with cholesterol (1:250, Gibco) and appropriate antibiotics. The growth conditions for *H. pylori* were at 37°C in an atmosphere composed of 85% N<sub>2</sub>, 10% CO<sub>2</sub> and 5% O<sub>2</sub>. In the case of growth in serum free media, bacteria were grown minimum two passages before using them in the experiments.

#### 2.2.1.4 Freezing of *H. pylori*

Bacteria were grown on GC agar plates and mixed with 1.5 ml freezing medium containing 10% FCS, 20% Glycerol and 70% Brucella Broth. The medium is sterile filtered before use. The bacteria were stored in -70°C storage.

#### 2.2.1.5 Determination of optical density of bacteria

Optical density (OD) of bacteria was measured after making suspension of bacterial culture from an agar plate in a desired medium or 1× PBS. The suspension was then resuspended in an aliquot of a taken liquid culture. The determination of the optical density was carried out by appropriate dilution in plastic cuvettes in a spectrophotometer at a wavelength of  $\lambda=550$  nm (OD<sub>550</sub>) against the respective blank.

#### 2.2.1.6 Production of chemical competent *E. coli* cells

Chemical competent bacterial cells were produced by the rubidium chloride method. In this method, an overnight culture of *E. coli* were inoculated in 100 ml of LB liquid medium and grown up to an OD<sub>550</sub> of 0.5 to 0.6 at 37°C in a shaking incubator (180 rpm). The cultivated culture was chilled on ice for 30 min and centrifuged at 4000 rpm for 15 min at 4°C. The cell pellet was resuspended in 40 ml of TFB I buffer (30 mM potassium acetate CH<sub>3</sub>COOH, 100 mM RbCl, 10 mM CaCl<sub>2</sub>, 50 mM MnCl<sub>2</sub>, 15% (v/v) glycerol, pH 5.2 adjusted with 0.2 M CH<sub>3</sub>COOH, sterilized). After 5 min incubation on ice, cells were again centrifuged. The sedimented cells were then resuspended in 4 ml of TFB buffer II (10 mM MOPS, 75 mM CaCl<sub>2</sub>, 10 mM RbCl, 15% (v/v) glycerol, pH 6.5 with KOH, sterilized). Cells were aliquoted to 50 µl and frozen in liquid nitrogen. The cells were further stored at -70°C.

#### 2.2.1.7 Transformation of chemical competent cells

An aliquot of previously stored (at -70°C) chemical competent *E. coli* bacteria was defrosted slowly in ice. DNA (500 ng) was added to the bacteria for 30 min in ice. The bacteria were then incubated at 42°C for 45s, immediately in ice cooled and added 1 ml warm LB media. Then bacteria were incubated for one h at 37°C, pulse centrifuged, supernatant discarded and pellet resuspended in 50 µl LB media. Bacteria were then plated onto LB agar plates containing the antibiotics in the concentrations needed.

## 2.2.2 Work with yeast

### 2.2.2.1 Growth and cultivation of *Saccharomyces cerevisiae*

*Saccharomyces cerevisiae* was cultivated on yeast extract-peptone-dextrose medium (YPD medium) and minimal medium (SD-base). For liquid cultures, yeasts were cultivated in an appropriate medium without the addition of agar at 30°C aerobically in a shaking incubator (180 rpm). The selection and expression of yeasts were performed on minimal medium lacking amino acid (leucine or tryptophan). Glycerol stocks were created for strain maintenance after mixing 600 µl of a good grown liquid culture with 500 µl 80% glycerol (sterile) and were stored at -70°C.

### 2.2.2.2 Determination of the optical density of yeasts

Optical density of *Saccharomyces cerevisiae* was determined using a cell suspension with appropriate dilutions in the plastic cuvette. The optical density at 600 nm (OD<sub>600</sub>) was determined in spectrophotometer against the corresponding blank.

### 2.2.2.3 Preparation of yeast competent cells

To prepare competent yeasts, 30 ml overnight culture was inoculated into the 150 ml of YPD medium. The cells were grown at 30°C for 4.5 h upto an OD<sub>600</sub> of 0.6. The culture was centrifuged at 4°C with 1000 xg for 5 min. After centrifugation, the cell pellet was washed in 30 ml of H<sub>2</sub>O and resuspend in freshly prepared sterile 1 ml 1x TE/LiAc. The yeast suspension was aliquoted in 100 µl each and stored in liquid nitrogen frozen at -70°C.

1x TE/LiAc    1 ml of 10x TE buffer and 1ml of 10x Lithium acetate.

10 x TE buffer        0.1 M Tris-HCl, 10 mM EDTA, adjust pH to 7.5, and autoclave.

10x LiAc        1 M Lithium acetate (Sigma), adjust pH to 7.5 with dilute acetic acid, and autoclave.

### 2.2.2.4 Transformation of yeast competent cells (Geitz protocol)

The transformation of competent yeast strains for the yeast two-hybrid assay was carried out by heat shock method. For this purpose, 1 µg of plasmid DNA was added to an aliquot of given competent yeast and mix. After mixing, 0.6 ml sterile PEG/LiAc solution was added to the cells

and incubated at 30°C for 30 min with shaking (200 rpm). After shaking, DMSO to 10% (70 µl) was added and mix gently by inversion and heat shock at 42°C for 15 min was performed. The cells were chilled on ice for 2 min. The cells were harvested by centrifugation (2700 xg, 2 min) and resuspended the pellet in 0.5 ml 1x TE buffer. An aliquot of 200 µl of the mixture was applied to the corresponding selective agar plates and incubated aerobically for 3-6 days.

1x PEG/LiAc solution            8 ml of 50% PEG, 1 ml of 10x TE buffer and 1ml of 10x Lithium acetate, 50% PEG (Sigma), autoclave.

#### 2.2.2.5 Production of diploid yeast strains (Uetz *et al.*, 2006)

Yeast cells can be haploid as well as diploid. For the generation of diploid yeast strains, the "mating" was performed between *Saccharomyces cerevisiae* type a (CG1945 strain) and type  $\alpha$  (Y187 strain). After mating, the yeast cells contain both mating types (type a and type  $\alpha$ ). In the first step, the haploid strain of *S. cerevisiae* was transformed with corresponding expression plasmids in "prey" (pGADT7) or "bait" (pGBKT7) vectors. The "prey" plasmid is transformed into the strain CG1945 and used for the genes coding for the leucine biosynthesis, whereas the "bait" plasmid was transformed into the strain Y187 that contains genes for tryptophan biosynthesis. The haploid expression plasmid-carrying *S. cerevisiae* strain is selected on minimal medium in which corresponding amino acid is missing. For the mating, 5 ml of the generated haploid strains of *S. cerevisiae* mating type a and  $\alpha$  were combined in rich medium agar plate and incubated for 24 h at 30°C. Subsequently, for the selection of diploid yeast cells, the cells were inoculated to double selective drop out medium lacking Leucine and Tryptophan (SD -Leu/Trp). After selection of diploid *S. cerevisiae* strains, the liquid culture was passaged in three times in a double selective dropout medium before culture for further experimentation or was used for strain maintenance.

#### 2.2.2.6 Test for protein-protein interaction in *Saccharomyces cerevisiae* (Busler *et al.*, 2006)

The interaction of proteins in the yeast cells (encoded with prey and bait plasmids) was tested on triple selective drop out medium for the histidine auxotrophic *S. cerevisiae* strains. In addition to the leucine and tryptophan, the triple selective dropout medium was also lacking histidine (SD -Leu/Trp/His). A protein-protein interaction between prey and bait was determined by reconstitution of the Gal4 transcription factor when the activation (prey) and DNA binding

domain (bait) come together to induce histidine biosynthesis. Therefore, the growth on the triple selective dropout medium is possible. For the protein-protein interaction test, the generated diploid yeast strains were incubated into the liquid medium (SD -Leu/Trp) for 2 to 3 days. After the incubation, the yeast suspension was diluted upto  $10^5$  dilutions with an  $OD_{660}$  of 0.26/100  $\mu$ l dilution and plated on SD -Leu/Trp and SD -Leu/Trp/His agar plates with 10  $\mu$ l per dilution (in 3 parallels). The plates were then incubated at 30°C in incubator and grown for 3 to 6 days. The viability of the diploid *S. cerevisiae* strains were determined by yeast growth on SD -Leu/Trp and the interaction was confirmed by yeast growth on SD-Leu/Trp/His.

### 2.2.3 Work with DNA

#### 2.2.3.1 Primer design for yeast plasmid cloning

Primers (forward and reverse) were designed by software Dnaman 6. The internal forward primer used comprises 12 bp of *attB1*, a translational consensus sequence (KOZAK) with start codon and 18-25 bp of the respective 5' specific ORF sequence. The internal reverse primer contains 12 bp of *attB2* sites, a stop codon and 18-25 bp of the 3' end of respective ORF sequence complementary to the coding region.

#### 2.2.3.2 Polymerase Chain Reaction

The specific DNA sequence was amplified by polymerase Chain Reaction (PCR) (Mullis *et al.*, 1986). The *in vitro* method for the specific amplification of selected gene segment requires two oligonucleotides (18-25 bp). In the first step of PCR, the double-strand DNA template is denatured by heat to the complementary single-stranded DNA (template). After denaturation, two oligonucleotides bind in the region to be amplified (annealing). DNA polymerase (Takara Taq polymerase, Promega) binds to the template at the starting region for extension (elongation) along with two oligonucleotides. This process takes place by a catalytic reaction in the reaction buffer containing deoxyribonucleotide triphosphates (dNTPs). For amplification of the DNA, the DNA fragments produced by each elongation step are again denatured and amplified. The 3'-5' proofreading function of the polymerase ensures a low error probability of the amplified DNA fragments.

Plasmid DNA (1:10 dilution) was used as a template for all PCR reactions. The PCR reactions were performed in a total volume of 25  $\mu$ l containing 0.25  $\mu$ l of 100 ng/ $\mu$ l template DNA, 100 pmol each of oligonucleotide per 20 nmol dATP/dGTP/dTTP/dCTP, 2.5 mM  $MgCl_2$ , and 2 U

Taq polymerase. The duration of the elongation step was determined by the length of the gene to be amplified (1000 bp/min). The duration of the time cycles and temperature for the particular application is shown in table 2-12. The amplified PCR product was determined and purified by agarose gel electrophoresis (See 2.2.3.4).

**Table 2-12 PCR protocol**

The PCR reaction was performed with variation of the annealing temperature, elongation temperature (Takara: 68°C) and time as indicated.

Step	Reaction temperature	Time	Cycles
Primary denaturation	94°C	5 min	1x
Denaturation	94°C	30 s	30x
Annealing	48-55°C	1 min	
Elongation	68°C	1 min/1000 bp	
Final elongation	68°C	10 min	1x

### 2.2.3.3 Purification and quantitative estimation of DNA concentration

The purity and concentration of DNA was determined by measuring the UV absorbance by Nano Drop 1000 Spectrophotometer (Nano Drop Technologies) at optical density of 260 and 280 nm. The concentration of the DNA was calculated using the formula. The purity of the DNA was determined using the OD<sub>260</sub>/OD<sub>280</sub> ratio.

$$\text{DNA concentration } (\mu\text{g/ml}) = (\text{OD}_{260}) \times (\text{dilution factor}) \times (50 \mu\text{g DNA/ml}) / (1 \text{ OD}_{260} \text{ unit})$$

For transfection experiments, highly purified and concentrated DNA was used. For this purpose the concentrated DNA is further purified by Phenol–chloroform extraction method. This method is widely used for removing the impurity e.g. protein for isolation of DNA. In the method, phenol/chloroform (50%/ 50%; v/v) was used for extraction. After vortexing, the mixture was centrifuged at 13000 rpm for 10 min at room temperature. The upper phase was collected in a new tube and 3 M sodium acetate was added to 1/10 of the volume collected. 100% ethanol were added and mixed. The solution was further centrifuged at 13000 rpm at 4°C for 5 min. Supernatant was removed carefully. The pellet was washed with 70% ethanol and centrifuged at 13000 rpm at 4°C for 1 min. Ethanol was pipette out and pellet was dried. Pellet was dissolved in 50 µl TE buffer and used further for transfection experiments.

#### 2.2.3.4 DNA gel electrophoresis

DNA fragments were loaded on horizontal 1-2% agarose gels in 1× TAE buffer (40 mM Tris, 20 mM Acetic acid, 1 mM EDTA). The fragments were separated for 50 min at 70 V. Before loading to the agarose gels, DNA samples were mixed with ¼ volume of GEBS buffer (20% (v/v) glycerol, 50 mM EDTA, 0.05% (w/v) bromophenol blue, 0.5% (w/v) N-Lauryl sarcosyl). The DNA fragment sizes were determined with the help of the standard-DNA marker. After separation, the DNA fragments in agarose gels were detected after being stained with ethidium bromide solution (1 mg/l). The detection was performed under UV exposure at 260 nm using a video system (Molecular Imager Gel Doc XR System, Bio-Rad).

#### 2.2.3.5 Extraction and isolation of DNA from agarose gel

The DNA fragments obtained by PCR were separated on 1% agarose gels and the correct size was determined by 0.1% methylene blue staining solution (1 g/l of methylene blue). The correct size was cut out from the gel using a sharp razor blade. The DNA fragments were extracted from the gel by a Gel Band Purification Kit according to manufacturer's instructions (GE Healthcare). The DNA was eluted by adding 50 µl sterile distilled water.

##### 2.2.3.5.1 Isolation of plasmid DNA of *E. coli* by QIAGEN Miniprep

For the preparation of plasmid DNA, transformed bacteria were grown overnight at 37°C in TB media under constant shaking. TB components were sterile mixed short before inoculation in a proportion 1:10 (Solution 2: Solution 1). After growth, bacteria were centrifuged at 4000 rpm for 20 min at 4°C, and the supernatant discarded. Using the mini (midi or maxi) prep kit from QIAGEN with some modifications, DNA was obtained. Shortly, for 250 ml culture pallet, the Maxi-prep kit (QIAGEN) was used. Pallet resuspended in 10 ml buffer P1, then added 10 ml of buffer P2 and neutralizing with buffer N3. Separation of debris from DNA suspension at 4000 rpm for 40 min followed the collection of supernatant and addition of this one onto a pre-equilibrated column with QBT buffer. After the binding occurs, the column was washed 3 times with wash buffer and the DNA collected from the column using TE buffer as elution solution. DNA concentrations were estimated at OD<sub>260</sub>.

P1 Buffer      50 mM Tris HCl pH 8.0, 10 mM EDTA, 100 µg/ml RNase

P2 Buffer      200 mM NaOH, 1% SDS

N3 Buffer 30 M Potassium acetate; adjust pH with Glacial acetic acid to pH 5.5

QBT Buffer 750 mM NaCl, 50 mM MOPS pH 7; 15% Isopropanol, 0.15% Triton X-100

Wash Buffer 1 M NaCl, 50 mM MOPS pH 7.0, 15% v/v Isopropanol

#### 2.2.3.6 DNA restriction

The restriction of DNA was performed using restriction enzymes (Roche and NEB, Schwalbach) and their corresponding buffer. The selected incubation temperature and time for various restriction enzymes were used according to manufacture's protocol. After restriction, purification of the DNA was performed with the illustra GFX PCR DNA and Gel Band purification kit. For plasmid DNA, restriction was performed in a total volume of 10  $\mu$ l. About 2-5 U of appropriate enzymes were used for the hydrolysis of about 0.1-0.5  $\mu$ g of DNA at 37°C for 1.5 h. For making a vector, the enzyme mixture was taken in a volume of 40-50  $\mu$ l (10-15 U of enzyme) and incubated for 4 h. After incubation, the enzymes were deactivated by adding GEBS (1/4 of the total volume) and DNA bands were purified using the illustra GFX PCR DNA and Gel Band Purification Kit.

#### 2.2.3.7 Ligation

Ligation of DNA fragments were performed in a mixture of 0.8  $\mu$ l of T4 DNA ligase and 1.2  $\mu$ l of 10x ligation buffer (Roche Applied Science) having a total volume of 12  $\mu$ l. The ratio of cut plasmid and DNA fragment was 1:3 respectively. The ligation mixture was incubated for 4 h at 16°C or overnight at 4°C. After ligation, 5  $\mu$ l of the ligation mixture was used for transformation in *E. coli*.

#### 2.2.3.8 Colony PCR

For quick checking of *E.coli* clones "colony PCR" was performed. The respective cells were taken with pipette tip and dissolved in 14.75  $\mu$ l of water. PCR was performed according to standard protocol.

#### 2.2.3.9 Gateway cloning

Gateway<sup>®</sup> cloning is a very efficient cloning technology developed by Invitrogen. This method is based upon sequence-specific recombination system of the bacteriophage lambda, and enables rapid and highly efficient integration of DNA sequences into different vector systems. For this

purpose, DNA fragments are amplified with "attachment sites" (*attB1* and *attB2*) in two steps by "nested"-PCR and are inserted into a donor vector with attachment sites (*attP1* and *attP2*) by reaction called BP Clonase™. This reaction generates an entry vector with attachment sites (*attL1* and *attL2*). A recombination reaction is then carried out between *attL* sites of an entry vector and *attR* sites of a destination vector to create an expression vector by reaction LR Clonase™.

The Gateway® cloning technology was used in this work to test for protein-protein interaction by yeast two-hybrid (Y2H) assay. For this purposes, the genes encoding these proteins were inserted into the vectors of the Matchmaker system (Clontech, California, USA), pGADT7 and pGBKT7.

#### 2.2.3.9.1 "nested"-PCR

The first step of two-stage "nested"-PCR was performed with one set of oligonucleotides, an internal forward and reverse sequence with *attB* sites and contain a gene sequence to be cloned. The PCR reaction was performed in a total volume of 50 µl containing 1 µl Template DNA, 10 pmol of each oligonucleotide, 7 nmol of dNTP, 1.5 mM to 3 mM MgCl<sub>2</sub> and 2 U Taq polymerase. In table 2-13, the reaction cycles and conditions are listed for the first step of the "nested"-PCR.

**Table 2-13 Protocol for "nested"-PCR step-I**

The first stage of the "nested" PCR reaction was performed with following variations in temperature and time for each step.

Step	Reaction temperature	Time	Cycles
Primary denaturation	94°C	5 min	1 x
Denaturation	94°C	45 s	30 x
Annealing	56°C	30 s	
Elongation	68°C	1 min 30 s	
Final elongation	68°C	5 min	1 x

The second step of the "nested" PCR was performed using gene specific amplified product obtained from the first PCR reaction and used as template. For this purpose, a set of external forward and reverse oligonucleotides were used for all experiments, Since all templates contain regions of the *attB* sites (Table 2-5). The second step of the "nested"-PCR completes the amplification of specific recombination sites, *attB1* and *attB2*. The PCR reaction is performed in a total volume of 50 µl containing 10 µl of the first step PCR reaction product as Template DNA, 16 pmol of each oligonucleotide, 7 nmol of each dNTP, 1.5 mM to 3 mM MgCl<sub>2</sub> and 2 U Taq polymerase. Reaction cycles and duration for the second step of the "nested" PCR is shown in table 2-14.

**Table 2-14 Protocol for "nested"-PCR step-II**

The second stage of the "nested" PCR reaction was performed with following variations in temperature and time for each step.

Step	Reaction temperature	Time	Cycles
Primary denaturation	94°C	3 min	1 x
Denaturation	94°C	45 s	25 x
Annealing	54°C	30 s	
Elongation	68°C	1 min	
Final elongation	68°C	3 min	1 x

PCR amplified products obtained from second step are analysed by agarose gel electrophoresis and the right PCR-products are subsequently used for BP Clonase™-reaction

### 2.2.3.9.2 BP Clonase™-Reaction

BP reaction was performed according to the manufacturer's protocol using Gateway® BP Clonase™ enzyme mix (Invitrogen). The BP Clonase™ enzyme mix contains the Lambda integrase recombination proteins, and the *E. coli* protein subunits "Integration Host Factors" (IHF). The attachment sites *attP1* and *attP2* flanking donor vector consists of a chloramphenicol resistance and the *ccdB* gene. By the recombination of B and P "attachment sites", the gene of interest is exchanged with the chloramphenicol resistance and *ccdB* gene cassette (Figure 2-1). After this reaction, a vector is formed containing the integrated DNA fragment flanked by new "attachment sites" (*attL1* and *attL2*). This entry vector is transformed into *E. coli*, and the viable clones were tested for chloramphenicol sensitivity and gentamycin resistance. Plasmids were verified by restriction analysis with appropriate restriction enzymes.

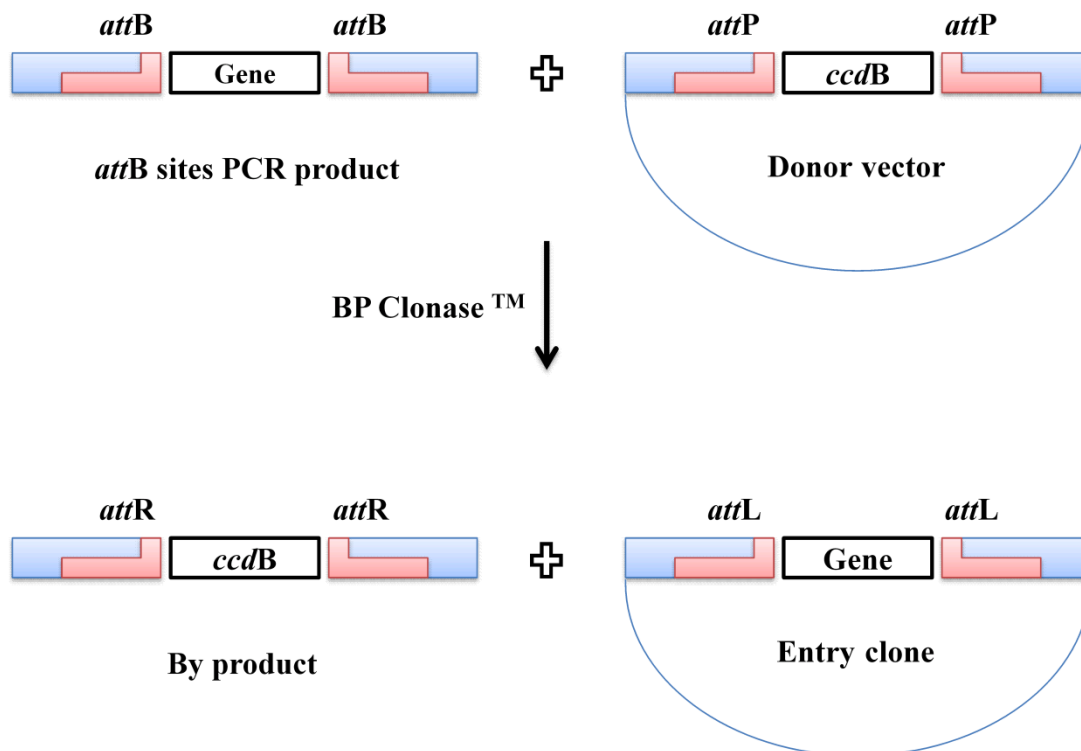


**Figure 2-1 BP Clonase™-Reaction.**

BP recombination reaction is mediated between *attB*-flanked DNA fragment (gene) and *attP*- flanked *ccdB* cassette of donor vector to generate an entry clone.

#### 2.2.3.9.4 LR Clonase™-Reaction

The LR reaction was performed according to the manufacturer's protocol using Gateway® LR Clonase™ Enzyme Mix (Invitrogen). The vectors for LR reaction were yeast two-hybrid (YTH) plasmids, pGADT7 and pGBKT7 (Clontech). These vectors contain *attR* sites and gateway cassette (GW) that is flanked by gene cassette of entry clone to generate expression clone (Uetz *et al.*, 2006) (Figure 2-2).

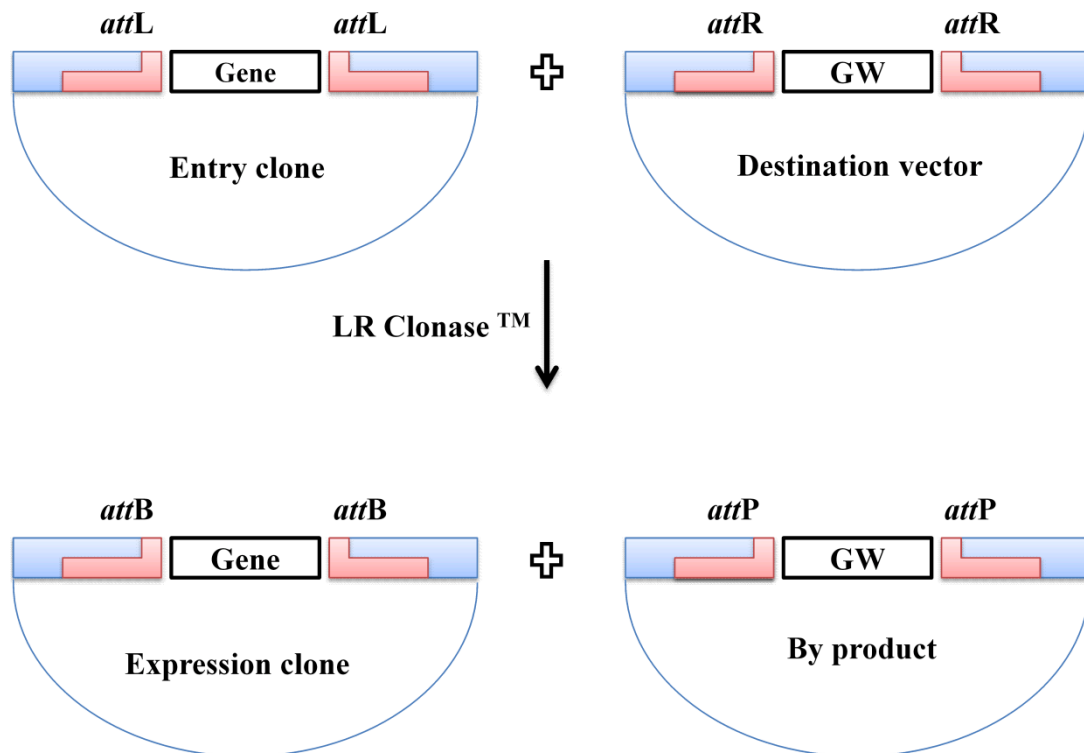


**Figure 2-2 LR Clonase™-Reaction.**

LR recombination reaction occurs between an entry clone containing *attL*-flanking gene and a destination vector containing *attR*-flanking gateway cassette to generate an expression clone.

#### 2.2.3.10 DNA sequencing

DNA sequencing was performed by companies MWG-Biotech (Ebersberg, Germany) and GATC (Kempton, Germany). Oligonucleotides were selected using standard or specific primers for the corresponding DNA sequence. The analysis of sequences was performed in the DNAMAN program (Lynnon software).

## 2.2.4 Work with cell culture

### 2.2.4.1 Cell counting with Neubauer counting chamber

To determine the viable cell numbers, the cell counting was done in the Neubauer Counting chamber. The viable cells were counted in four quadrants of the Neubauer Counting chamber and the mean value calculated. To count the number of viable cells per ml, the mean value is multiplied by dilution factor and the chamber's factor ( $10^4$ ).

### 2.2.4.2 Cultivation of adherent cells

#### 2.2.4.2.1 Cultivation of HEK-293 cells

HEK-293 cells were cultured in 75 cm<sup>2</sup> cell culture flask (Thermo Fisher Scientific, Langenselbold) in 12 ml DMEM supplemented with 10% FCS and 2 mM L-glutamine at 37°C and 5% CO<sub>2</sub>. Before the cells form a confluent lawn, they were used for trypsinization. They were firstly washed with Calcium/Magnesium free PBS to remove the serum and incubated with 3 ml of pre warmed trypsin/EDTA solution for 3 min at 37°C and 5% CO<sub>2</sub>. Cells were observed under inverted microscope. Once the monolayer of cells were detached from the bottom of the cell culture flask, a single cell suspension obtained by adding 5 ml of DMEM medium containing 10% heat inactivated FCS. The cell suspension was transferred into 15 ml sterile falcon tube and spins the cells down at 1100 rpm for 10 min. The pellet was resuspended with DMEM containing 10% FCS and 2 mM L-glutamine. The cell number was determined using a Neubauer Chamber and cells were seeded in ratio of 1:3 to make the final concentration of  $\sim 2 \times 10^5$  cells/ml. Rest of the suspension used for experiments..

#### 2.2.4.2.2 Cultivation of HEK-293 cells expressing mCherry-STIM1

HEK-293 cells expressing mCherry-STIM1 were cultured in 75 cm<sup>2</sup> cell culture flask (Thermo Fisher Scientific, Langenselbold) in 12 ml DMEM supplemented with 10% FCS, 2 mM L-glutamine and G-418 sulfate (antibiotic selection) 100 µg/ml at 37°C and 5% CO<sub>2</sub>. When the cells were viable, they rinse down by adding complete medium to detach. Cells were seeded in ratio of 1:5 every third day.

### 2.2.4.2.3 Cultivation of HEK-293 cells expressing eGFP-myc-ORAI1

HEK-293 cells expressing eGFP-myc-ORAI1 were cultured in 75 cm<sup>2</sup> cell culture flask (Thermo Fisher Scientific, Langenselbold) in 12 ml DMEM supplemented with 10% FCS (tetracycline free), 50 µg/ml Hygromycin B, 15 µg/ml Blasticidin S and 2 mM L-glutamine at 37°C and 5% CO<sub>2</sub>. When the cells were viable, 1 µg/ml doxycycline or tetracycline added to the flask for selection. The cells were rinse down by adding complete medium to detach from bottom of the flask. Cells were seeded in ratio of 1:5 every third day.

### 2.2.4.3 Cultivation of suspension cells

#### 2.2.4.3.1 Cultivation of Jurkat E6.1 cells

Jurkat E6.1 cells were cultured in 75 cm<sup>2</sup> cell culture flask (Thermo Fisher Scientific, Langenselbold) in 12 ml RPMI 1640 supplemented with 10% FCS, 10 mM HEPES, 1 mM sodium pyruvate, 4.5 g/l Glucose, 1.5 g/l Sodium bicarbonate, and 2 mM L-glutamine at 37°C and 5% CO<sub>2</sub>. The cell suspension was transferred into 15 ml sterile falcon tube and spins the cells down at 1100 rpm for 5 min. The pellet was resuspended with fresh culture medium. The cells were every third day with 1:5 passaged.

### 2.2.4.4 Transfection of adherent cells

#### 2.2.4.4.1 Generation of Flp-In™ T-REx designed HEK-293 cells stably expressing eGFP-myc-ORAI1

Flp-In™ T-REx system was used to generate HEK-293 cells stably expressing eGFP-myc-ORAI1 according to manufactures protocol. Two plasmids, the pOG44 and pcDNA™5/FRT/TO vector containing eGFP-myc-ORAI1, were cotransfected into the HEK-293 cells. A homologous recombination event occurs between the Flp recombinase expressed from pOG44 and the FRT sites (integrated into the genome and on pcDNA™5/FRT/TO). The Flp-In™ T-REx™ generated HEK-293 cells expressing eGFP-myc-ORAI1 were selected with Blasticidin and Hygromycin resistance and eGFP-myc-ORAI1 expression was induced by 1 µg/ml doxycycline or tetracycline.

#### 2.2.4.4.2 Generation of HEK-293 cell stably expressing mCherry-STIM1

HEK-293 cells stably expressing mCherry-STIM1 were generated by transfection with a mCherry-STIM1-encoding plasmid carrying the *neo* gene. Cells were transfected by using lipofectamine 2000 according to manufactures protocol. After transfection, cells were treated with G418 sulfate with varying concentrations. Cell death occurs rapidly allowing the selection of HEK-293 cells with mCherry-STIM1. Cells were then passed in fresh DMEM medium containing G418 sulphate (100 µg/ml). After few days, only few HEK-293 cells survived which had incorporated the mCherry-STIM1 plasmid carrying the *neo* gene. The survived HEK-293 carrying mCherry-STIM1 plasmids were transferred in fresh DMEM medium containing G418 sulphate (100 µg/ml) and were used for further experiments.

#### 2.2.4.4.5 Isolation of human CD<sup>4+</sup> T-lymphocytes

Human CD<sup>4+</sup> T-lymphocytes were isolated by positive selection with the MACS technology. The purified PBLC were obtained in the cell density of  $1 \times 10^7$  cells per 80 µl of MACS buffer. In the cell density of  $1 \times 10^7$ , 20 µl of MACS CD<sup>4+</sup> Micro Beads (Miltenyi Biotec) was added and the cells were incubated for 15 min at 4°C and shaken every 5 min. The cells were then washed with 20 ml MACS buffer, resuspended in 1 ml MACS buffer and applied to MACS buffer equilibrated column LS, combined with MidiMACS™ Separator. The column was then washed with 2 times 4 ml each MACS buffer. The Column was then removed from MidiMACS™ Separator to elute the cells with 3 ml MACS buffer. The cells were centrifuged at 200 xg for 5 min and resuspended in 10 ml RPMI supplemented with 10% FCS. Cells were seeded with cell density of  $1 \times 10^6$  cells/ml. MACS buffer PBS, 0.5% BSA, 2 mM EDTA

#### 2.2.4.4.6 Lymphocyte purification from normal human peripheral blood

PBLC (peripheral blood lymphocytes) were isolated by density gradient centrifugation from human blood. Firstly, freshly prepared blood was collected from a human volunteer and heparinized (1:100). The collected blood was diluted with 3 volumes of PBS. The diluted blood (whole volume 37.5 ml) was added gently to 12.5 ml Biocoll separating solution of density 1.077 (Biochrom AG). After centrifugation (400 ×g, 30 min, without brake, Thermo Scientific Heraeus® Megafuge 3.0R) at the interface between blood and Biocoll, layer of lymphocytes, monocytes and platelets were collected. Washed the cells once with 50 ml PBS/2 mM EDTA

(4°C). For the separation of the platelets, cells were washed twice with PBS/2 mM EDTA and centrifuged at 300 ×g.

#### 2.2.4.7 Calcium assay

Fluo-4 NW calcium assay solution was prepared by mixing component A (Fluo-4 NW dye mix), component B (probenecid) and component C (1X HBSS, 20 mM HEPES) according to manufactures protocol. After mixing all the components, solution was kept at 4°C for 30 min. Cells were incubated in black, clear bottom, sterile 96 well Poly-D-Lysine coated plate. Cells were then used for experiment and Fluo-4 NW calcium assay solution was loaded for 1 h prior to fluorescence measurement. Cells were evaluated by fluorescence measurement (excitation at 494 nm and emission at 516 nm) in a fluorescence microplate reader (FLUOstar OPTIMA).

#### 2.2.4.8 Cryopreservation of cells

Cryopreservation of cells was done by storage in liquid nitrogen. Cells were preserved in cryovials (Thermo Fisher Scientific, Langenselbold) in a cell density of  $5 \times 10^5$  cells in 1 ml of freezing medium.

#### 2.2.4.9 Cell thawing

For the cultivation cryopreserved cells, the freezing medium containing cells were thawed at 37°C and then immediately mixed with 10 ml of prewarmed cell culture medium to dilute harmful DMSO concentration. Thawed cells were palleted at 800 xg for 5 min. Thereafter, cells were washed three times with 10-20 ml. Cell pallet was resuspended with the culture medium after centrifugation at 500 xg for 5 min.

#### 2.2.4.10 Microscopy

##### 2.2.4.10.1 Live cell imaging

HEK cells ( $0.5 \times 10^6$  cells/ml) expressing mCherry-STIM1 or eGFP-myc-ORAI1 or both were incubated in DMEM medium with 1 µg/ml acid activated VacA labelled with Alexa<sup>647</sup> for 4 h at 37°C and 5% CO<sub>2</sub>. Cells were washed carefully once with 1 ml PBS. After washing with PBS, cells were carefully resuspended in DMEM medium and live cell imaging was performed. eGFP expression was analysed by Excitation/Emission at 488/509 nm, mCherry at 587/610 nm and Alexa<sup>647</sup> dye at 652/668 nm.

## 2.2.5 Work with Protein

### 2.2.5.1 Protein estimation by Bradford assay

To determine the protein concentration of a sample, 100 µl of the suspension (Diluted in defined volume of PBS with 1 ml Bradford Reagent (Bradford, 1976) was added and mixed. After 15 min incubation at room temperature in the dark, the absorbance of the sample at 595 nm measured against zero value in Spectrophotometer. For Standard calibration curve known concentration of BSA (100 mg/ml) was measured.

Bradford Reagent      0.01% Coomassie Brilliant Blue G250, 5% Ethanol, 8.5% Phosphoric Acid

### 2.2.5.2 Ammonium sulphate precipitation and concentration of VacA from culture supernatant

The *H. pylori* strains 60190 were grown in Brucella broth medium with cholesterol (1:250, Gibco) under microaerophilic conditions (10% CO<sub>2</sub>/ 85% N<sub>2</sub>/ 5% O<sub>2</sub>) at 37°C. The bacterial suspension was centrifuged at 6000 rpm for 20 min at 4°C. The supernatant was then sterile filtered. A saturated ammonium sulfate solution ((NH<sub>4</sub>)<sub>2</sub>SO<sub>4</sub> saturated) was added to the proteins and were precipitated overnight at 4°C with gentle stirring. Subsequently, the proteins precipitated at 13000 rpm for 30 min (4°C) were palleted and resuspended in 15-30 ml PBS. To ensure a sufficient solubility, the proteins were incubated overnight at 4°C. For the subsequent gel-filtration, the volume having a filtration unit (Amicon Ultra Centrifugal Filter 100 kD cut-off size, Millipore) was concentrated to 4 ml. The separation of proteins was carried out according to their size by gel filtration.

The gel filtration of proteins were performed using a Sephacryl S300 16/60-column. For the chromatography, either a FPLC or HPLC method with 100 mM NaCl, 50 mM NaPO<sub>4</sub> (pH 7.4) was used as running buffer.

### 2.2.5.3 Acid activation of VacA

The required concentrations of purified VacA 2 µg and 0.25 µg for the respective experiment in the eppendorf tube were taken. The volume of 0.25 fold of 0.3 M HCl into the required concentration of purified VacA was added and incubated at 37°C for 20 min. After incubation, the volume of 0.25 fold of 0.3 M NaOH (the same volume as HCl to neutralize the effect of acid) was added immediately before mixing to the cells.

#### 2.2.5.4 Cell vacuolating activity induced by VacA

Cells ( $0.5 \times 10^6$  cells/ml) were incubated with various concentrations of acid activated VacA for 3 h at 37°C in 5% CO<sub>2</sub>. Ammonium chloride (NH<sub>4</sub>Cl) was then added at the final concentration of 2 mM and incubated further for 1 h. Cell vacuolation was quantified by neutral red uptake assay. Cells were washed once with 1 ml ice cold PBS and incubated in RPMI medium containing 10% FCS and 0.008% neutral red for 10 min at room temperature. After washing twice with 1 ml each with PBS containing 0.5% BSA, cells were lysed with 70% ethanol and 0.37% HCl, and transferred into 96-well plates. Neutral red was determined photometrically at a wavelength of 534 nm (reference: 405 nm) and was quantified in Absorbance reader (Sunrise).

#### 2.2.5.5 Detection of protein in SDS polyacrylamide gel electrophoresis

SDS polyacrylamide gel electrophoresis was performed with Mini-Protein III™ using Bio-Rad system with 10% gels (80 x 50 x 1 mm). The separating gel (10% gel) was prepared, mixed and poured between the glass plates and covered with distilled water. After polymerisation for 30 min, the distilled water was removed. The stacking gel (5% gel) was then poured and the 10 wells comb was inserted. The samples were loaded on the gel along with the protein marker. The separation was done for 15 min at 80 V and 1 h at 120 V.

10% Separation gel: 4.95 ml Acrylamide/Bisacrylamide (37.5:1), 3.75 ml 1.5 M Tris pH 8.8, 75 µl 10% SDS, 6.15 ml Distilled water, 75 µl 10% APS and 7.5 µl TEMED

5% Stacking gel: 1.35 ml Acrylamide/Bisacrylamide (37.5:1), 0.625 ml 1 M Tris pH 6.8, 25 µl 10% SDS, 1.53 ml Distilled water, 12.5 µl 10% APS and 2.5 µl TEMED

Electrophoresis buffer (10 x) (1L): 50 mM Tris, 84 mM Glycine and 0.1% SDS

#### 2.2.5.6 Staining of proteins by Coomassie Blue

The separated proteins from the sample in Acrylamide-SDS gel was submerged into 50 ml of coomassie staining solution for 30 min on rotating shaker. The Acrylamide-SDS gel was washed 3 times with 50 ml coomassie destaining solution for 30 min each on rotating shaker. Once the bands were visualized and detected, the gel was finally washed with distilled water and dried for 45 min at 80°C in a Gel dryer.

Staining Solution: 0.5% (w/v) Coomassie Brilliant Blue R250, 50% (v/v) Methanol, 10% (v/v) Acetic Acid

Destaining Solution: 20% (v/v) Methanol, 10% (v/v) Acetic Acid

#### 2.2.5.7 Fluorescent staining of VacA

The purified VacA was labelled (by covalent binding) with fluorescent Alexa Fluor 488 dye, Alexa Fluor 555 dye or Alexa Fluor 647 dye (molecular probes). The purified VacA to be labelled was taken in eppendorf and stained according to manufacture's protocol (Invitrogen/Molecular probes). After labelling, they were dialysed with PBS for overnight and later for 4 h at 4°C. The labelled VacA were store at -20°C until its use.

#### 2.2.6 Statistical analysis

All values were mean +/- standard deviation of at least three independent experiments. Statistical significance was determined by Student's t-test or Mann-Whitney U-test and was indicated for the corresponding experiment.

### 3. Results

#### 3.1 Growth of *H. pylori* and purification of VacA

##### 3.1.1 Growth of *H. pylori* in solid and liquid culture

*H. pylori* 60190 strain, which produces the VacA protein was grown on GC agar plates in the CO<sub>2</sub> incubator or anaerobic chambers with 5% O<sub>2</sub> and 10% CO<sub>2</sub> in a microaerobic atmosphere for 24 h. The bacteria were transferred into Brucella broth supplemented with cholesterol, nystatin, trimethoprim and vancomycin. The effect of cholesterol on *H. pylori* growth and purification of VacA were shown in this study (Jimenez-Soto *et al.*, 2012). Supplementation of Brucella Broth with cholesterol resulted in a better growth of bacteria and a longer exponential phase of *H. pylori* especially after long-term growth (>40 h) (Figure 3-1).

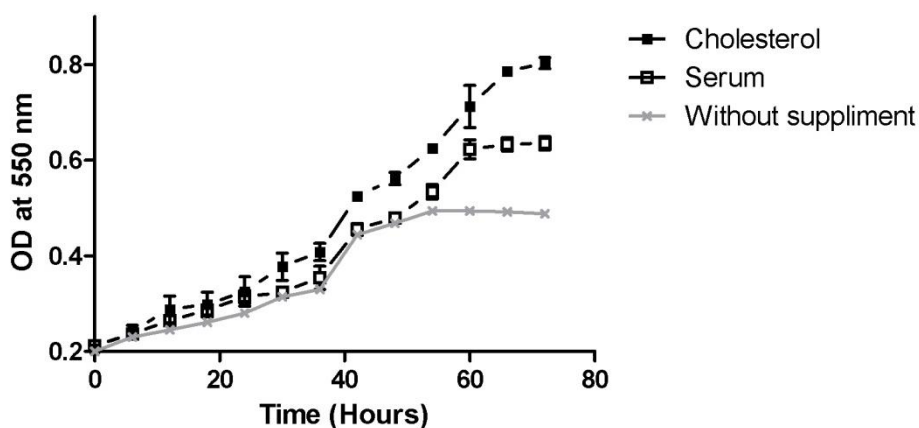


**Figure 3-1** Growth curve of *H. pylori* 60190 in liquid culture.

The growth of *H. pylori* strain 60190 was evaluated by OD<sub>550</sub> measurement of liquid culture in Brucella broth media without any supplement, with serum and with cholesterol complementation.

##### 3.1.2 *H. pylori* 60190 VacA protein precipitation and purification through Gel filtration

The VacA protein isolated from strain *H. pylori* 60190 was used in this study. *H. pylori* 60190 strain is type *s1m1*, which produces relatively high amount of VacA. *H. pylori* 60190 was grown in solid and liquid culture. The proteins in the culture supernatant were precipitated using ammonium sulfate. VacA was purified from precipitated proteins using gel filtration chromatography (Sephacryl S300) column, as described in the materials and methods. The

purified VacA fractions were separated by SDS- PAGE and analyzed by Coomassie Brilliant Blue staining (Figure 3-2 A).

A VacA mutant (VacA  $\Delta$ 6-27 designated here as VacA M) protein was also used for AGS cell infection experiments. The VacA M- producing mutant *H. pylori* strain was constructed by deletion of the strong hydrophobic region near the amino-terminus (amino acids 6-27) resulting in loss of vacuolation activity of the toxin. The VacA M protein is comparatively less ion-selective and forms slower ion-conductive channels. The purification procedure for both VacA WT and VacA M were compared by SDS-PAGE and analyzed by Coomassie Brilliant Blue staining (Figure 3-2 B).

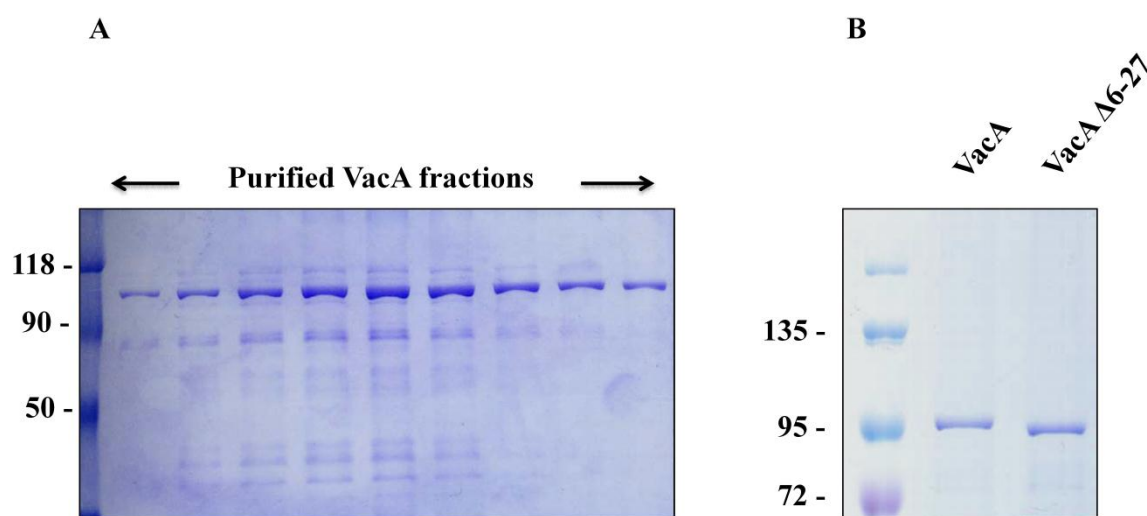


**Figure 3-2 Purified VacA protein after Gel filtration and comparison of the sizes of VacA proteins purified from culture supernatant of *H. pylori* 60190 VacA WT and VacA M strain.**

(A) The protein in culture supernatant of *H. pylori* 60190 is precipitated by ammonium sulphate (44%) and purified through gel filtration chromatography. VacA wild type protein purified fractions were analyzed by SDS-PAGE (10%) after staining with Coomassie Brilliant Blue. (B) The purified VacA WT and VacA M proteins are loaded on SDS- PAGE (10%). The sizes of both proteins were compared after staining with Coomassie Brilliant Blue. The size of VacA WT is slightly larger as compared to VacA M.

### 3.2 Quantification of VacA induced cell vacuolation in human Jurkat E6.1 T-cell line

In order to check the activity of VacA, the purified VacA (both VacA WT and VacA M) was tested by using the vacuolation assay. Normally, the purified VacA is poorly active and needs to be acid activated by 0.3 M HCl and the acid is neutralized by 0.3 M NaOH (see methods; 2.2.5.3).

The human Jurkat E6.1 T-cell line used in our lab is derived from Jurkat FHCRC (Fred Hutchinson Cancer Research Center, Seattle, WA) cell lines. Human Jurkat E6.1 T-cells produce large amounts of IL-2, human alpha interferon after stimulation with phorbol 12-myristate 13-acetate (PMA) or anti-CD3/CD28 antibodies.

The Jurkat E6.1 are cells growing in suspension and they are pseudo diploid. The cells are maintained in culture in RPMI 1640 containing 2 mM Glutamine and 10% Foetal Bovine Serum (FBS). Upon resuscitation, single cells can be observed, but during culture most cells grow as aggregates.

In order to check the activity of VacA by vacuolation assay, Jurkat E6.1 T-cells ( $0.5 \times 10^6$  cells/ml) were incubated for 4 h at 37°C and 5% CO<sub>2</sub> with different concentrations of acid activated VacA (VacA WT and VacA M). A final concentration of 2 mM NH<sub>4</sub>Cl was added and further incubated for 1 h at 37°C and 5% CO<sub>2</sub>. The cell vacuolation was determined by quantification of neutral red staining of cells. The cells were centrifuged and washed. These cells were incubated with 0.008% neutral red in RPMI medium supplemented with 10% FCS for 10 min at room temperature. The cells were then washed 2 times with 1 ml PBS containing 0.5% BSA. The neutral red was extracted by 70% ethanol and 0.37% HCl and immediately transferred into 96-well plates. The neutral red was at a wavelength of 534 nm (reference: 405 nm) photometrically quantified (Figure 3-3).

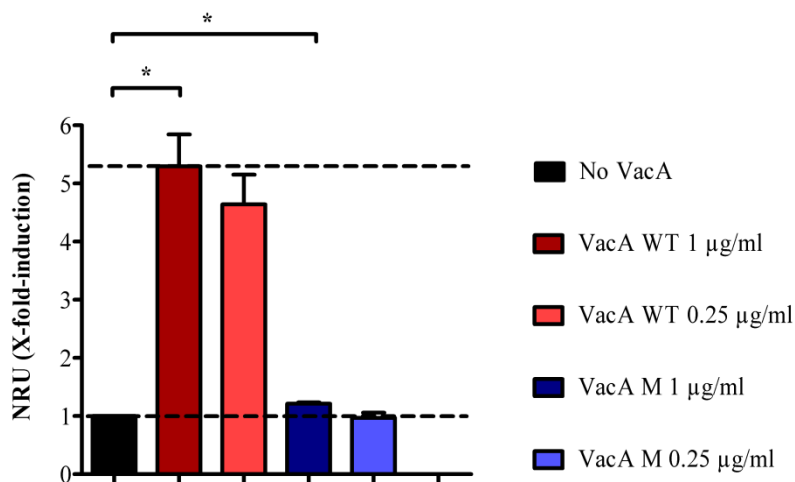


**Figure 3-3 Neutral red uptake assay of Jurkat E6.1 cells**

Jurkat E6.1 were treated with different concentrations (0.25 µg/ml and 1 µg/ml) of acid activated VacA (VacA WT and VacA M). The vacuolation assay was determined by neutral red uptake (NRU). The amount of neutral red in the vacuoles was quantified (NRU: "neutral red units") at a wavelength of 534 nm (reference: 405 nm). The dark black bar indicates a control value with no VacA corresponding 1-NRU. The values of red and blue bars show induction of

vacuoles as x fold to 1-NRU of VacA WT and VacA M respectively. Data shows the mean values and standard deviation from three independent experiments. Statistical significance was evaluated using a t-Test. \*P<0.05.

### **3.3 VacA inhibits the increase of cytosolic free Ca<sup>2+</sup> in response to stimulation by ionomycin and thapsigargin in T-lymphocytes**

*H. pylori* VacA binds to the receptor on the surface of target cells and is internalized. Once inside the cell, VacA alters the cytosolic calcium concentration thereby allowing the toxin to modulate cell function. The involvement of VacA in calcium influx in RBL-2H3 cells was previously described (de Bernard *et al.*, 2005). Our *in vitro* investigations reveal that VacA suppresses the increase of the cytosolic free calcium concentration after stimulation by the calcium ionophore ionomycin and thapsigargin.

#### **3.3.1 Effect of VacA on increase of cytosolic free Ca<sup>2+</sup> concentration in human Jurkat E6.1 T-cell line**

##### **3.3.1.1 *H. pylori* VacA inhibits calcium influx in human Jurkat E6.1 T-cell line after stimulation by ionomycin**

Ionomycin is an effective calcium ionophore (Liu & Hermann, 1978). Ionomycin raises the intracellular level of calcium (Ca<sup>2+</sup>). In order to increase the calcium influx, ionomycin acts as a Ca<sup>2+</sup> carrier across the membrane. This increase of Ca<sup>2+</sup> influx is achieved by direct stimulation of store-regulated cation entry across biological membranes (Morgan & Jacob, 1994). At the micromolar level, ionomycin is able to activate Ca<sup>2+</sup>/Calmodulin dependent protein kinases (CaMK) including CaMKII and CaMKIV to stimulate gene expression (Lobo, Zanjani, Ho, Chatila, & Fuleihan, 1999). Ionomycin induces hydrolysis of phosphoinositides and activates PKC to mediate T-cell activation in human cells (Chatila, Silverman, Miller, & Geha, 1989).

To measure the intracellular level of calcium, Fluo-4 NW calcium assay was used. Fluo-4 NW is a fluorescent Ca<sup>2+</sup> indicator with high sensitivity and high fluorescence. Its fluorescence is increased upon binding of Ca<sup>2+</sup> in the cytoplasm of the cells. Fluo-4 is an acetoxymethyl (AM) ester, which is cell membrane permeable. When cells are incubated with the dye, the dye is taken up by cells. Once inside the cells, Fluo-4 AM is hydrolyzed by intracellular esterases resulting in the negatively charged membrane impermeable form which is capable of binding Ca<sup>2+</sup> and emits fluorescence (Figure 3-4).

Several  $\text{Ca}^{2+}$  chelators were used to inhibit  $\text{Ca}^{2+}$  influx by binding extracellular as well as intracellular free  $\text{Ca}^{2+}$  for our experiments. EDTA and EGTA act as powerful chelating agents, which bind to divalent cations such as  $\text{Ca}^{2+}$  or  $\text{Mg}^{2+}$  with EGTA having a higher affinity than EDTA. Both are impermeable to the membranes, therefore, a combination of EDTA-EGTA were used to inhibit  $\text{Ca}^{2+}$  influx by binding extracellular free  $\text{Ca}^{2+}$ . In contrast to EDTA-EGTA, BAPTA AM was used to bind intracellular free  $\text{Ca}^{2+}$ . BAPTA AM is a membrane permeable intracellular calcium chelator. Once inside the cell, BAPTA AM is cleaved by intracellular esterases and binds  $\text{Ca}^{2+}$  in the cytoplasm of the cells (Figure 3-4).

The effect of VacA was measured in the human Jurkat E6.1 T-cell line and primary human  $\text{CD}^{4+}$  T-cells in the presence and absence of calcium chelators.

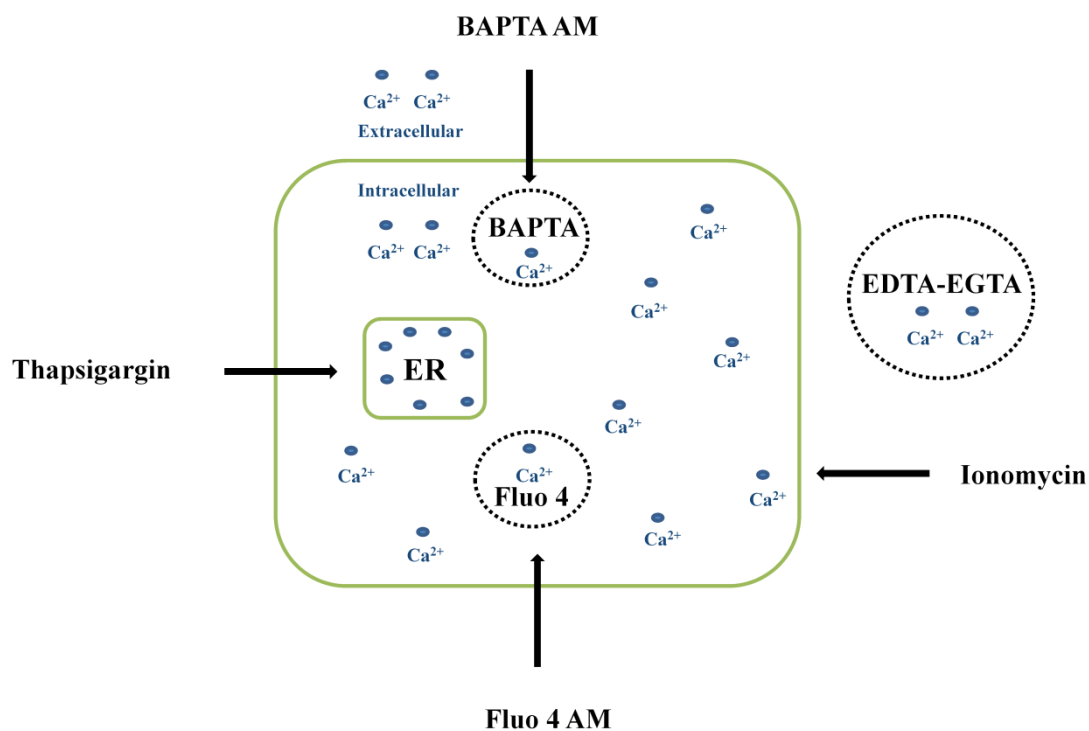


**Figure 3-4 Mechanism of action of  $\text{Ca}^{2+}$  ionophores and inhibitors**

Ionomycin is an effective calcium ionophore. Ionomycin increases  $\text{Ca}^{2+}$  influx by acting as a  $\text{Ca}^{2+}$  carrier and stimulates store regulated cation entry across the membrane. Thapsigargin is a membrane permeable enzyme. Thapsigargin blocks the sarcoplasmic/endoplasmic reticulum calcium ATPase (SERCA) and thereby causes depletion of the ER calcium store. This results in an increase of cytoplasmic  $\text{Ca}^{2+}$  concentration and an increase in  $\text{Ca}^{2+}$  influx. A combination of EDTA-EGTA inhibits  $\text{Ca}^{2+}$  influx by binding extracellular free  $\text{Ca}^{2+}$ . BAPTA AM is a membrane permeable  $\text{Ca}^{2+}$  chelator, which binds to cytoplasmic free  $\text{Ca}^{2+}$  upon cleavage by intracellular esterases.

In the first approach to evaluate the effect of VacA on ionomycin stimulated Jurkat E6.1 cells, the cells ( $1.75 \times 10^6$  cells/ml) were pre-incubated with purified acid activated VacA WT and VacA M for 3 h at 37°C and 5% CO<sub>2</sub> and then were loaded with Fluo-4 NW calcium assay dye and incubated for further 1 h at 37°C and 5% CO<sub>2</sub>.

For this purpose, Jurkat E6.1 cells were pre-incubated with VacA WT and VacA M at two different concentrations (2 µg/ml and 0.25 µg/ml). In order to sequester extracellular Ca<sup>2+</sup>, a combination of EDTA-EGTA (final concentration 2 mM and 500 µM, respectively) was used. BAPTA AM was used at the final concentration of 50 µM to sequester intracellular Ca<sup>2+</sup>. Additionally, EDTA-EGTA and BAPTA AM both together were used to sequester all free Ca<sup>2+</sup>. After 4 h of incubation, Jurkat E6.1 cells were evaluated by fluorescence measurement (excitation at 494 nm and emission at 516 nm) in a fluorescence micro plate reader (FLUOstar OPTIMA).

In the first step, the baseline fluorescence of resting cells (before stimulation) was measured for 10 cycles. Addition of ionomycin at the final concentration 0.5 µM to the cells led to Ca<sup>2+</sup> influx, showing the highest peaks of measured fluorescence in this experiment. Treatment of the cells with EDTA-EGTA before ionomycin stimulation greatly reduced this Ca<sup>2+</sup> influx by chelating extracellular Ca<sup>2+</sup>. BAPTA AM pretreated cells showed an increased level of intracellular Ca<sup>2+</sup> after stimulation because BAPTA AM only binds intracellular Ca<sup>2+</sup>, but does not prevent Ca<sup>2+</sup> influx into the cell. Administration of both EDTA-EGTA and BAPTA AM at the same time completely abolished Ca<sup>2+</sup> influx after ionomycin stimulation and showed the lowest fluorescence signal in this experiment (Figure 3-5 A).

A slight reduction of calcium influx induced by ionomycin was observed when the cells were pre-incubated with VacA WT and VacA M as compared to cells without VacA treatment. The effect of VacA WT and VacA M on calcium influx was consistent even after 35 min and 60 min of ionomycin stimulation (Figure 3-5 B&C).

The two different concentrations (2 µg/ml and 0.25 µg/ml) of VacA WT and VacA M were tested. Both VacA WT and VacA M had an effect on the increase of calcium influx with concentrations as low as 0.25 µg/ml. As noticed in figure 3-5 B&C, the effect of VacA WT and VacA M was similar. Ionomycin acts as a Ca<sup>2+</sup> carrier across the membrane suggesting both type of VacA may inhibit calcium influx extracellularly. The negative control measurements were taken with the cells treated with EDTA-EGTA, BAPTA AM and EDTA-EGTA & BAPTA AM

with and without stimulation by ionomycin. The cells with only stimulation by ionomycin were taken as positive control (Figure 3-5 A, B&C).

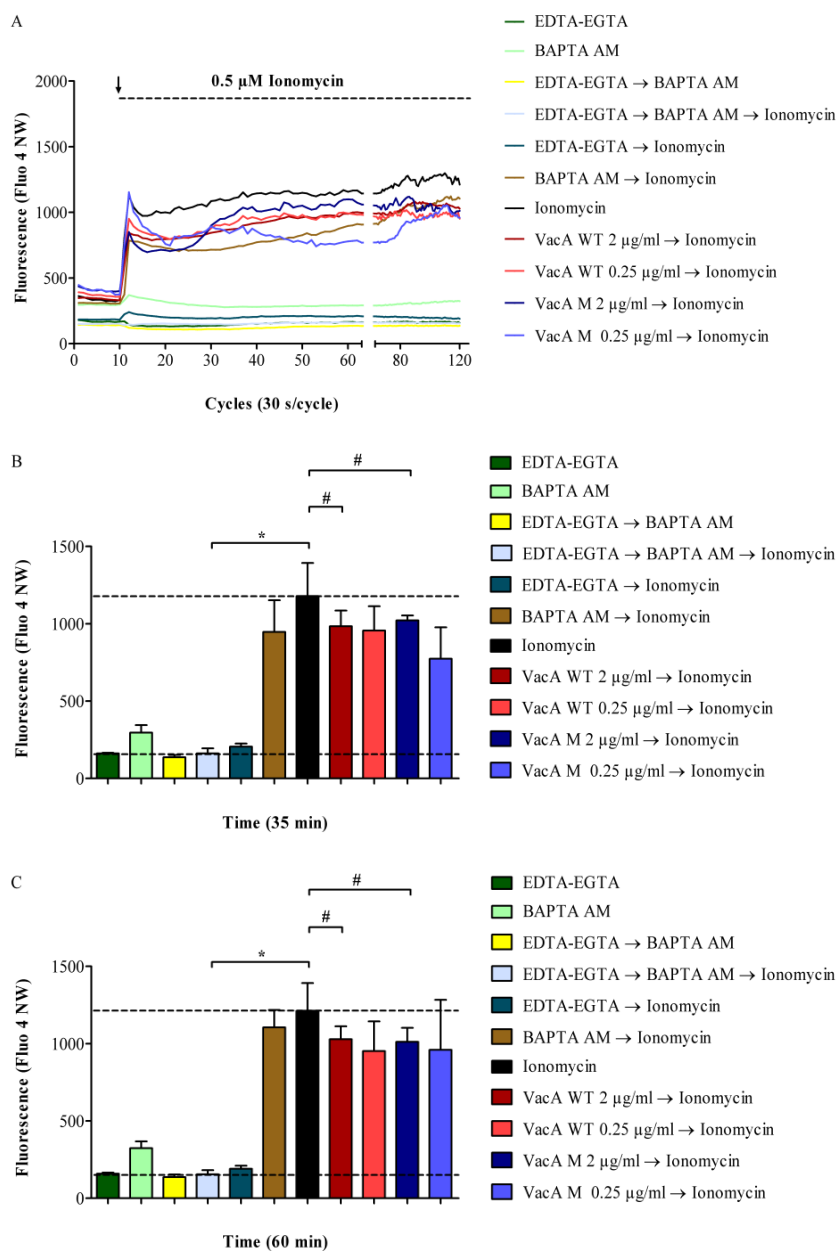


**Figure 3-5 Measurement of  $\text{Ca}^{2+}$  influx stimulated by ionomycin and the effect of VacA on the increase of the cytosolic free  $\text{Ca}^{2+}$  concentration in Jurkat E6.1 cells.**

(A) Each line in the graph displays fluorescence intensity measurements for 60 min in Jurkat E6.1 cells loaded with Fluo-4 NW. Ten baseline fluorescence measurements were taken prior to stimulation with 0.5  $\mu$ M ionomycin. The time point of ionomycin stimulation is indicated by a black vertical arrow. Measurements were performed in the presence of EDTA-EGTA (final concentration 2 mM and 500  $\mu$ M, respectively), BAPTA AM (50  $\mu$ M), EDTA-EGTA and BAPTA AM, VacA WT and VacA M. The cells were pre-incubated with both VacA WT and VacA M at two different concentrations (2  $\mu$ g/ml and 0.25  $\mu$ g/ml) indicated in red and blue, respectively. (B) The degree of inhibition of calcium influx by VacA WT and VacA M at 35 min depicted as bar graphs. (C) Bars represent the average measurement obtained at 60 min. The horizontal arrows indicate the order of pre-incubation to stimulation.

---

Each graph was compiled from data obtained in three independent experiments. Error bars are standard deviations. Statistical significance was evaluated using a t-Test. \*P<0.05, # No significance.

In addition to the above experiments, the effect of VacA WT and VacA M on the increase of Ca<sup>2+</sup> influx stimulated by ionomycin was also measured in cells which were treated (before stimulation) with EDTA-EGTA, BAPTA AM and ionomycin.

In order to measure the effect of VacA on Ca<sup>2+</sup> influx, Jurkat E6.1 cells were incubated for 4 h with VacA and then treated with EDTA-EGTA and ionomycin, prior to measuring the baseline fluorescence.

No increase of Ca<sup>2+</sup> influx stimulated by ionomycin was observed, when the cells were pre-incubated with VacA WT and VacA M and were treated with EDTA-EGTA and ionomycin (Figure 3-6A).

This suggests that EDTA-EGTA alone is able to bind all extracellular Ca<sup>2+</sup>, thereby not allowing ionomycin to induce Ca<sup>2+</sup> influx. It was also noticed that a later treatment with ionomycin does not increase Ca<sup>2+</sup> influx after stimulation by ionomycin for measurement.

Furthermore, it was confirmed that when cells were pre-incubated with VacA WT and VacA M and treated with BAPTA AM and ionomycin, baseline Ca<sup>2+</sup> levels were elevated. This was due to the effect of ionomycin before measurement, where BAPTA AM was not able to block the calcium influx caused by ionomycin treatment (Figure 3-6 B) as noticed earlier. No significant difference was observed between VacA WT and VacA M effects on calcium influx in these experiments.

As a further control experiment, it was necessary to confirm that no increase of calcium influx occurs when the cells were pre-incubated with VacA WT and VacA M and treated with EDTA-EGTA, BAPTA AM and ionomycin. As expected, ionomycin stimulation of VacA WT and VacA M pre-incubated cells was not observed (Figure 3-6 C). This effect was caused by EDTA-EGTA alone and not by BAPTA AM.

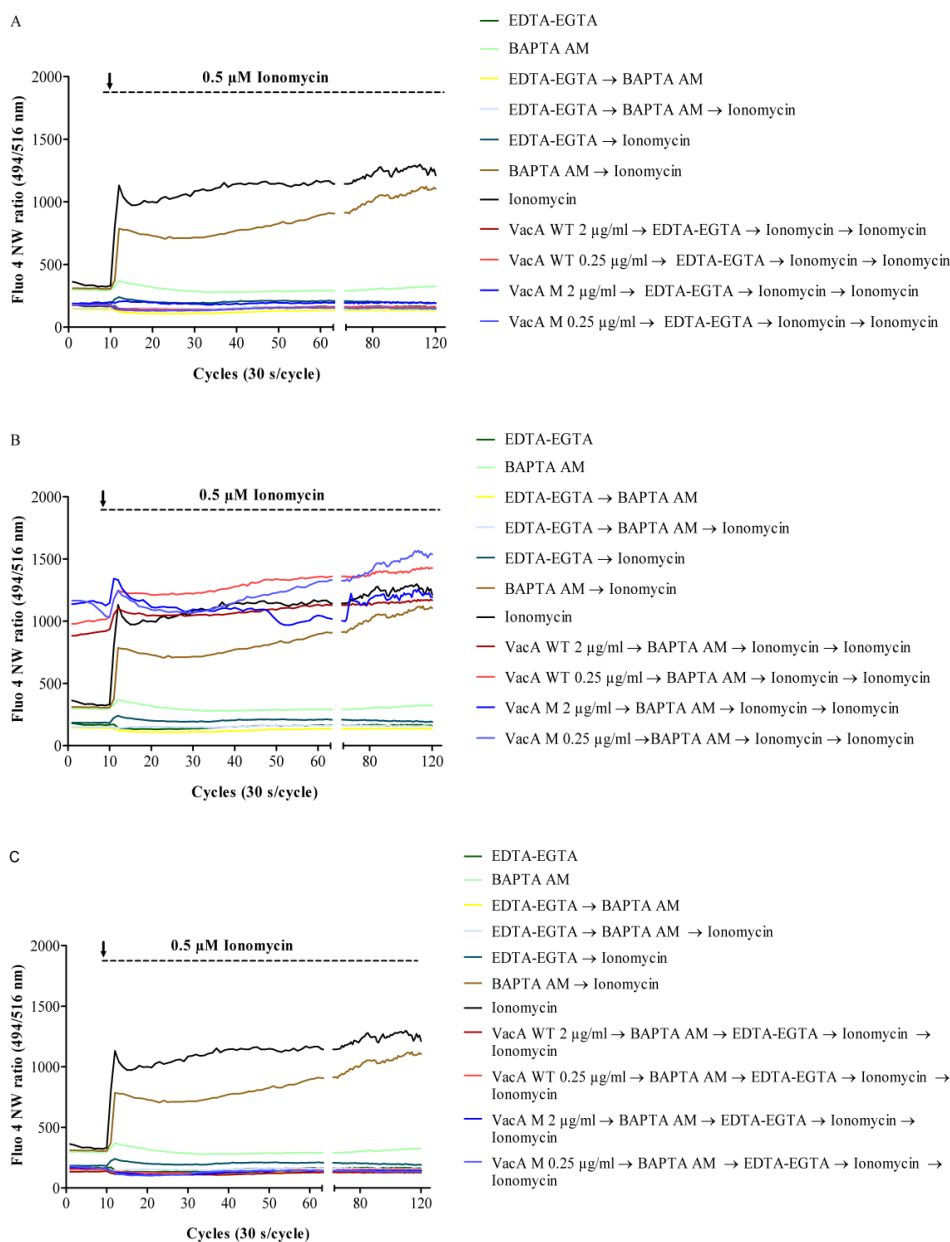


**Figure 3-6 Measurement of  $\text{Ca}^{2+}$  influx evoked by ionomycin and the effect of VacA on the increase of the cytosolic free calcium concentration in Jurkat E6.1 cells.**

Each line in the graph displays fluorescence intensity measurements in Jurkat E6.1 cells loaded with Fluo-4 NW. The cells were pre-incubated with VacA WT and VacA M (indicated in red and blue, respectively). (A) The cells were then treated with EDTA-EGTA and ionomycin. (B) The cells were then treated with BAPTA AM and ionomycin. (C) The cells were then treated with BAPTA AM, EDTA-EGTA and ionomycin. The cells were stimulated by 0.5  $\mu$ M ionomycin (black vertical arrow) after measuring the baseline fluorescence. The horizontal arrows indicate the order of pre-incubation to treatment and stimulation. Each graph was compiled from data obtained in three independent experiments.

In addition to the above experiments, no effect on the calcium influx of VacA WT and VacA M pre-incubated cells together with BAPTA AM was measured (Figure 3-7 A). Elevated baseline  $\text{Ca}^{2+}$  influx was measured in the VacA WT and VacA M pre-incubated cells treated with ionomycin. However, no significant difference regarding the effect on  $\text{Ca}^{2+}$  influx between VacA WT and VacA M was observed (Figure 3-7 B).

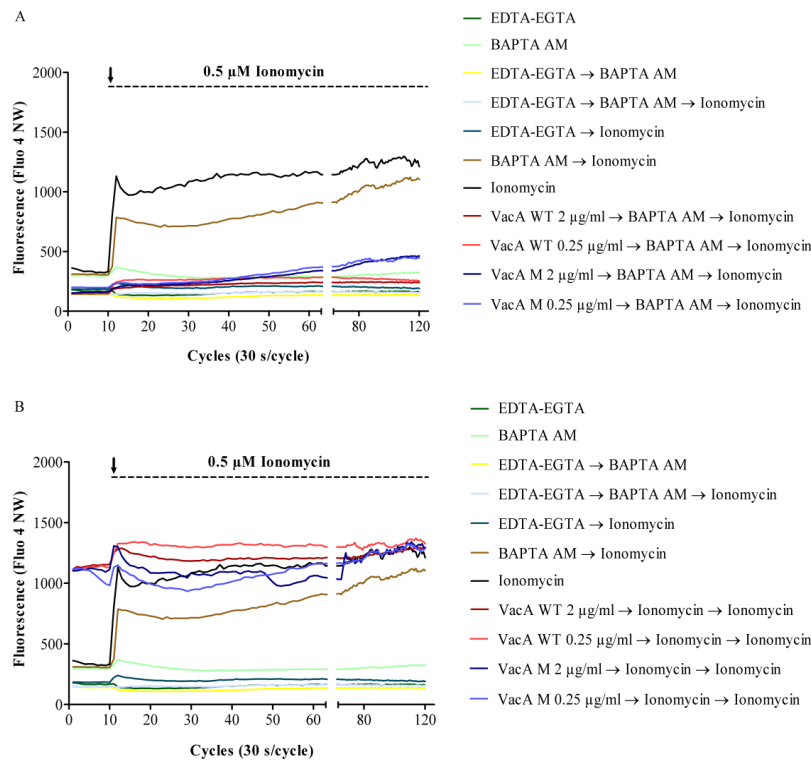


**Figure 3-7 Measurement of  $\text{Ca}^{2+}$  influx evoked by ionomycin and the effect of VacA on the increase of the cytosolic free calcium concentration in Jurkat E6.1 cells.**

Each line in the graph displays fluorescence intensity measurements in Jurkat E6.1 cells loaded with Fluo-4 NW. The cells were pre-incubated with VacA WT and VacA M (indicated in red and blue, respectively). (A) The cells were then treated with BAPTA AM. (B) The cells were then treated with ionomycin. The cells were stimulated by 0.5  $\mu\text{M}$  ionomycin (black vertical arrow) after measuring the baseline fluorescence. The horizontal arrows indicate the order of pre-incubation to treatment and stimulation. Each graph was compiled from data obtained in three independent experiments.

### 3.3.1.2 *H. pylori* VacA inhibits the increase of cytosolic free Ca<sup>2+</sup> in human Jurkat E6.1 T-cell line after stimulation by thapsigargin

We wanted to see whether VacA WT and VacA M had a similar effect on calcium influx and increase of cytosolic free Ca<sup>2+</sup> stimulated by thapsigargin, so we performed similar experiments with thapsigargin and measured the fluorescence. We thought to use thapsigargin in our experiments because of its specificity in increase of cytosolic free Ca<sup>2+</sup> by endoplasmic reticulum (ER) Ca<sup>2+</sup> store depletion (Lytton, Westlin, & Hanley, 1991). Thapsigargin is a potent inhibitor of a class of enzymes known as SERCA (Sarco/endoplasmic reticulum calcium ATPase) (Rogers, Inesi, Wade, & Lederer, 1995). It is a tumor promoter in mammalian cells (Hakii *et al.*, 1986). Thapsigargin raises the cytoplasmic calcium concentration by blocking the SERCA pump causing calcium stores to become depleted. Store depletion consequently activates plasma membrane calcium channels, allowing an influx of calcium into the cytosol.

In order to evaluate the effect of VacA on Jurkat E6.1 cells stimulated by thapsigargin, the cells (1.75 x 10<sup>6</sup> cells/ml) were pre-incubated with purified acid activated VacA WT and VacA M (2 µg/ml and 0.25 µg/ml) for 3 h and then were loaded with Fluo-4 NW calcium assay dye for further 1 h in at 37°C and 5% CO<sub>2</sub>. The cells were then evaluated by fluorescence measurement for excitation at 494 nm and emission at 516 nm in fluorescence micro plate reader. The experiments were conducted as described in 3.3.1.1.

In the first step, the baseline fluorescence was measured for 10 cycles. Thapsigargin at a final concentration of 1 µM was then added to the cells. The effect of thapsigargin treatment of Jurkat E6.1 cells can be seen in figure 3-8 A, B and C. A strong reduction of the increase of cytosolic free Ca<sup>2+</sup> was observed when the cells were pre-incubated with VacA WT. The effect of VacA WT was statistically significant even with a low concentration of VacA WT (0.25 µg/ml), however in the case of VacA M (Figure 3-8 A), a significant but comparatively lesser reduction was observed. The effect of VacA WT to inhibit the increase of cytosolic free Ca<sup>2+</sup> was consistent even after 35 min and 60 min after thapsigargin stimulation (Figure 3-5 B&C).

In order to inhibit the Ca<sup>2+</sup> influx into the cells, a mixture of EDTA-EGTA (final concentration 2 mM and 500 µM, respectively) and BAPTA AM (50 µM) were added and the control measurements were taken.

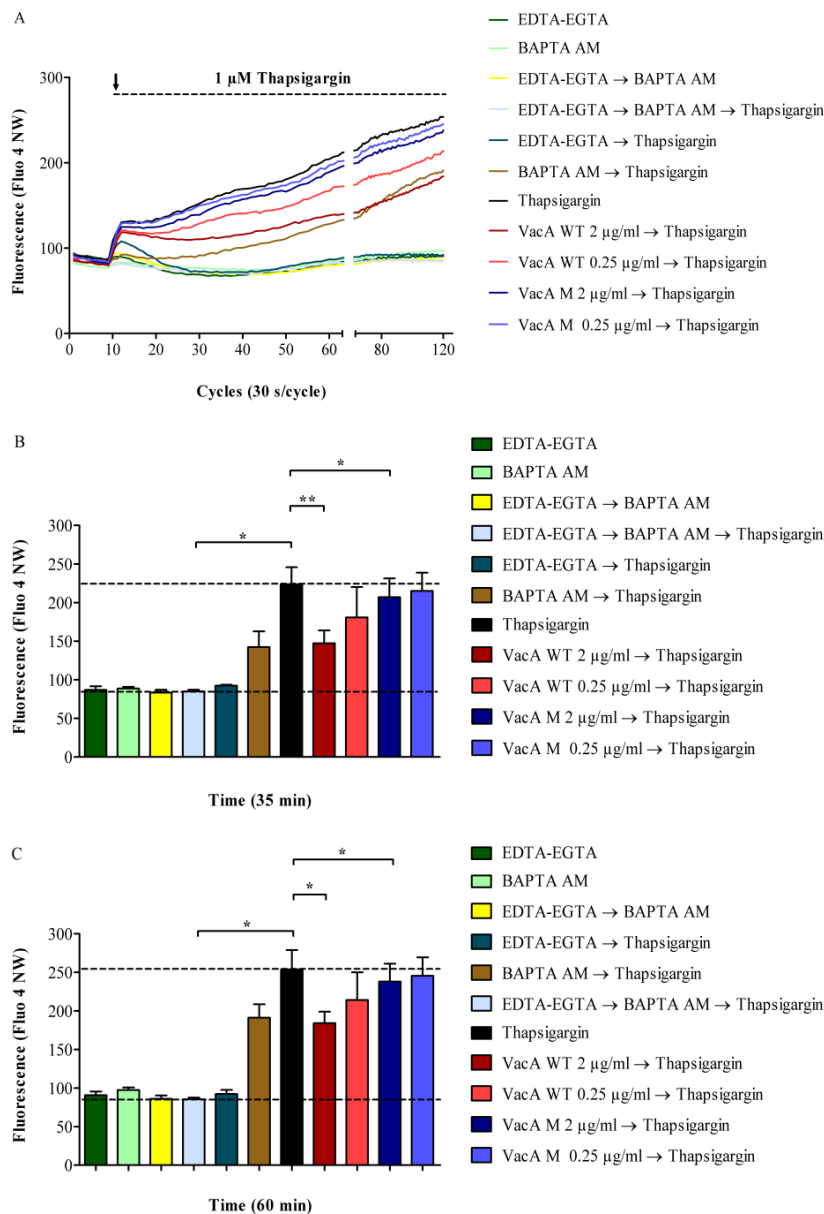


**Figure 3-8 Measurement of  $\text{Ca}^{2+}$  influx evoked by thapsigargin and the effect of VacA on the increase of the cytosolic free calcium concentration in Jurkat E6.1 cells.**

(A) Each line in the graph displays fluorescence intensity measurements over the period of 100 min in Jurkat E6.1 cells loaded with Fluo-4 NW. Ten baseline fluorescence measurements were taken prior to stimulation with 1  $\mu$ M thapsigargin. The time point of thapsigargin stimulation is indicated by a black vertical arrow. Measurements were performed in the presence of EDTA-EGTA (final concentration 2 mM and 500  $\mu$ M, respectively), BAPTA AM (50  $\mu$ M), EDTA-EGTA and BAPTA AM, VacA WT and VacA M. The cells were pre-incubated with both VacA WT and VacA M at two different concentrations (2  $\mu$ g/ml and 0.25  $\mu$ g/ml) indicated in red and blue, respectively. (B) The degree of inhibition in the increase of the cytosolic free  $\text{Ca}^{2+}$  by VacA WT and VacA M at 35 min depicted as bar graphs. (C) Bars represent the averaged measurement obtained at 60 min. The horizontal arrows indicate the order of pre-incubation to stimulation. Each graph was compiled from data obtained in three independent experiments. Error bars are standard deviations. Statistical significance was evaluated using a t-Test. \* $P < 0.05$ , \*\* $P < 0.01$ .

As observed in figure 3-8, VacA WT and VacA M have a significant effect on the increase of cytosolic free  $\text{Ca}^{2+}$  after stimulation by thapsigargin. This effect of VacA WT is much higher than VacA M, which seems to have similar effect as BAPTA AM on the cells. This suggests that the high concentration of 2  $\mu\text{g/ml}$  of VacA WT is able to block up to 40% of the increase of cytosolic free  $\text{Ca}^{2+}$  in Jurkat E6.1 cells.

Since, thapsigargin acts intracellularly, it could be interesting to see if extracellular calcium was first blocked by EDTA-EGTA and then treated by thapsigargin in the cells with pre-incubated VacA. The cells were then stimulated by thapsigargin after measuring the baseline fluorescence. As expected, EDTA-EGTA was able to block calcium influx by chelating extracellular  $\text{Ca}^{2+}$  completely causing no increase of cytosolic free  $\text{Ca}^{2+}$  to be measured and therefore VacA inhibition on increase of calcium influx was not observed (Figure 3-9 A, B&C).

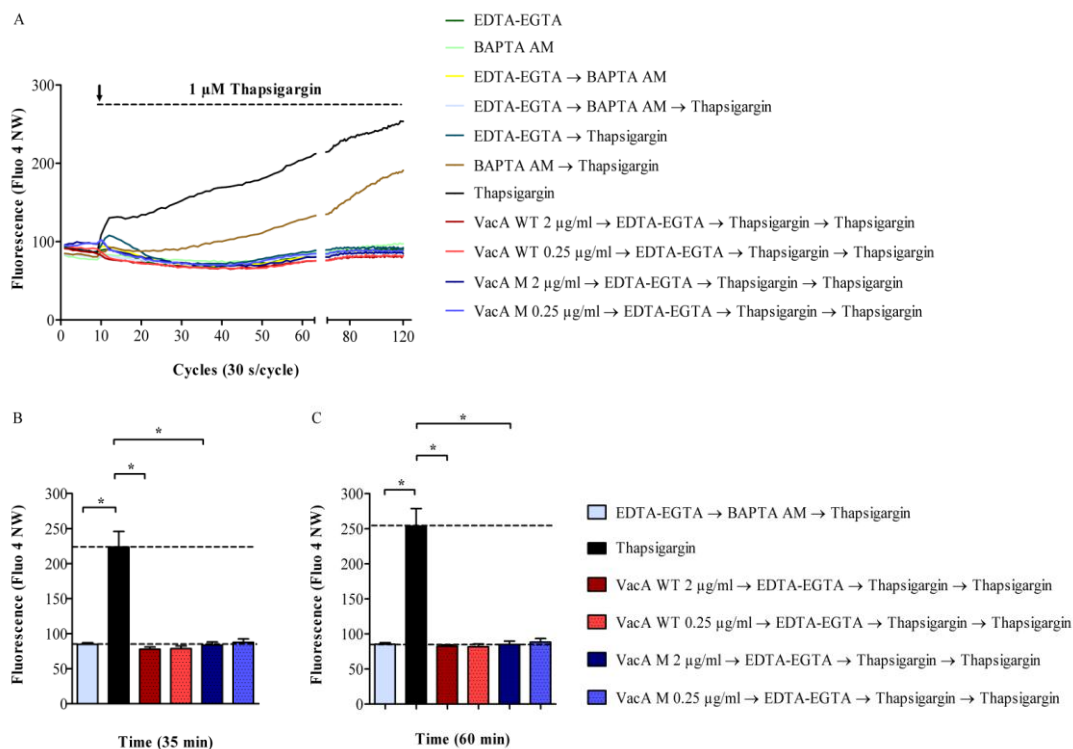


**Figure 3-9 Fluorescence measurement of  $\text{Ca}^{2+}$  influx evoked by thapsigargin and the effect of VacA on the increase of the cytosolic free calcium concentration in Jurkat E6.1 cells treated with EDTA-EGTA and thapsigargin.**

(A) Each line in the graph displays fluorescence intensity measurements in Jurkat E6.1 cells loaded with Fluo-4 NW. The cells were pre-incubated with VacA WT and VacA M (indicated in red and blue, respectively) and treated with EDTA-EGTA and thapsigargin. The cells were then stimulated by 1  $\mu\text{M}$  thapsigargin (black vertical arrow) after measuring the baseline fluorescence. (B) The degree of inhibition on the increase of the cytosolic free  $\text{Ca}^{2+}$  by VacA WT and VacA M at 35 min depicted as bar graphs. (C) Bars represent the averaged measurement obtained at 60 min. The horizontal arrows indicate the order of pre-incubation to treatment and stimulation. Each graph was compiled

from data obtained in three independent experiments. Error bars are standard deviations. Statistical significance was evaluated using a t-Test. \* $P < 0.05$ .

Similarly to the previous experiments using EDTA-EGTA, now BAPTA AM was used to sequester only cytosolic free  $\text{Ca}^{2+}$  in cells that had been pre-incubated with VacA and further treated by thapsigargin and after measuring the baseline fluorescence and then again stimulated by thapsigargin. As observed in figure 3-10, VacA and BAPTA AM were not able to block  $\text{Ca}^{2+}$  influx completely as compared to VacA and EDTA-EGTA in previous experiments.

Since increase of free  $\text{Ca}^{2+}$  in the cytoplasm by thapsigargin occurs via intracellular stores and a  $\text{Ca}^{2+}$  influx from the extracellular milieu was not abolished, in this experiment the measured fluorescence was increased after stimulation by thapsigargin even though BAPTA AM previously bound all cytosolic free  $\text{Ca}^{2+}$ . However, BAPTA AM could not block the influx of extracellular free  $\text{Ca}^{2+}$ . In addition, we can show that only VacA WT and BAPTA AM, but not VacA M and BAPTA AM were able to inhibit significantly the increase of cytosolic free  $\text{Ca}^{2+}$  by the influx of free  $\text{Ca}^{2+}$  from the extracellular milieu (Figure 3-10 A, B&C).

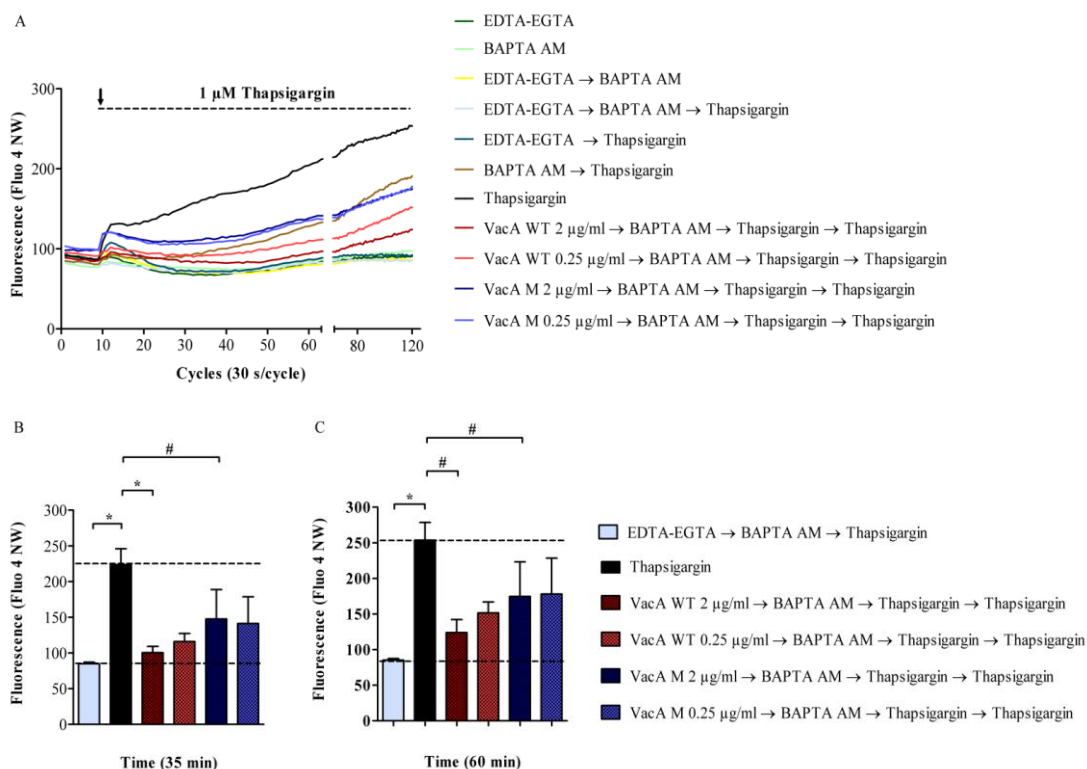


**Figure 3-10** Fluorescence measurement evoked by thapsigargin and the effect of VacA on the increase of the cytosolic free calcium concentration in Jurkat E6.1 cells treated with BAPTA AM and thapsigargin.

(A) Each line in the graph displays fluorescence intensity measurements in Jurkat E6.1 cells loaded with Fluo-4 NW. The cells were pre-incubated with VacA WT and VacA M (indicated in red and blue, respectively) and treated with BAPTA AM and thapsigargin. The cells were then stimulated by 1  $\mu\text{M}$  thapsigargin (black vertical arrow) after measuring the baseline fluorescence. (B) The degree of inhibition in the increase of the cytosolic free  $\text{Ca}^{2+}$  by VacA WT and VacA M at 35 min depicted as bar graphs. (C) Bars represent the averaged measurement obtained at 60 min. The horizontal arrows indicate the order of pre-incubation to treatment and stimulation. Each graph was compiled from data obtained in three independent experiments. Error bars are standard deviations. Statistical significance was evaluated using a t-Test. \* $P < 0.05$ , # No significance.

Knowing that VacA WT inhibits the increase of the cytosolic free  $\text{Ca}^{2+}$  concentration and not the  $\text{Ca}^{2+}$  efflux from the ER as a result of stimulation by thapsigargin, it was important to confirm this in Jurkat E6.1 cells pre-incubated with VacA WT and VacA M and then treated with EDTA-EGTA, BAPTA AM and thapsigargin. After measuring the baseline fluorescence, the cells were then again stimulated by 1  $\mu\text{M}$  thapsigargin. As expected, the increase of the cytosolic free  $\text{Ca}^{2+}$  concentration and  $\text{Ca}^{2+}$  influx were completely blocked, and no rise in fluorescence was measured (Figure 3-11 A, B&C). This effect of chelating free  $\text{Ca}^{2+}$  was due to EDTA-EGTA extracellularly and BAPTA AM intracellularly, therefore the effect of VacA was not seen.

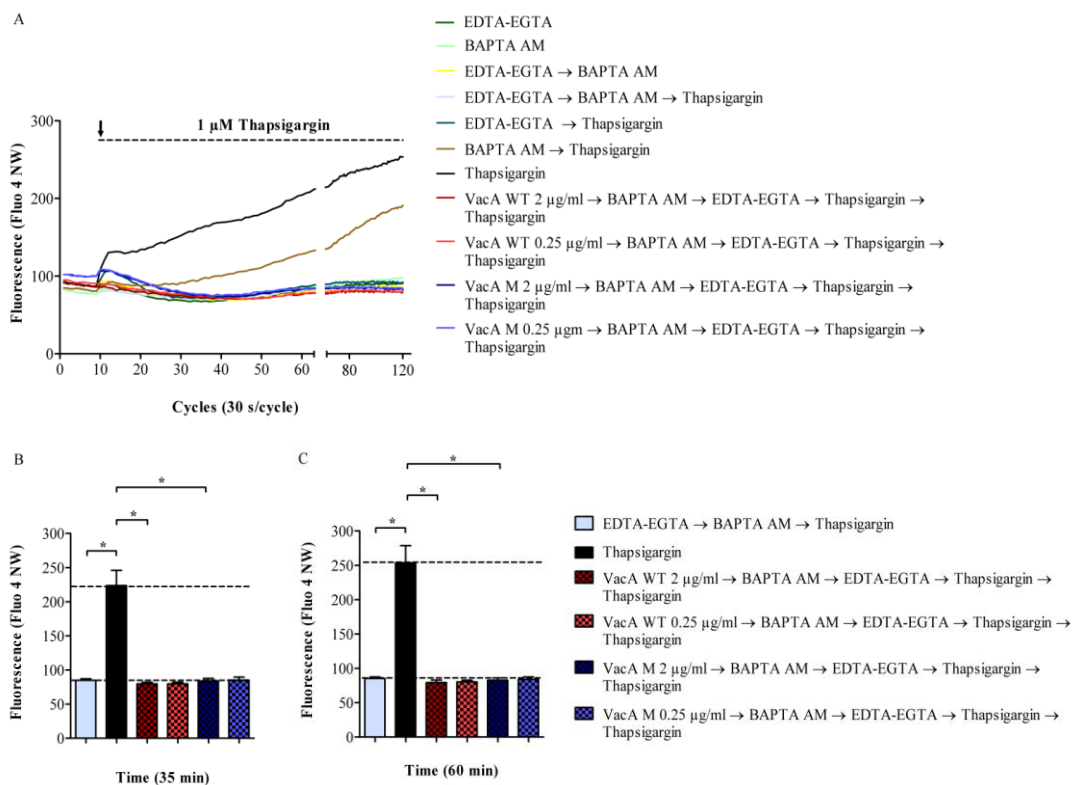


**Figure 3-11** Fluorescence measurement evoked by thapsigargin and the effect of VacA on the increase of the cytosolic free calcium concentration in Jurkat E6.1 cells treated with EDTA-EGTA, BAPTA AM and thapsigargin.

(A) Each line in the graph displays fluorescence intensity measurements in Jurkat E6.1 cells loaded with Fluo-4 NW. The cells were pre-incubated with VacA WT and VacA M (indicated in red and blue, respectively) and treated with EDTA-EGTA BAPTA AM and thapsigargin. The cells were then stimulated by 1  $\mu$ M thapsigargin (black vertical arrow) after measuring the baseline fluorescence. (B) The degree of inhibition in the increase of the cytosolic free  $\text{Ca}^{2+}$  by VacA WT and VacA M at 35 min depicted as bar graphs. (C) Bars represent the averaged measurement obtained at 60 min. The horizontal arrows indicate the order of pre-incubation to treatment and stimulation. Each graph was compiled from data obtained in three independent experiments. Error bars are standard deviations. Statistical significance was evaluated using a t-Test. \* $P < 0.05$ .

The next step was to confirm this in Jurkat E6.1 cells that were pre-incubated with VacA WT and VacA M and treated with BAPTA AM without thapsigargin. The cells were then stimulated by 1  $\mu$ M thapsigargin after measuring the baseline fluorescence. A strong and significant reducing effect by VacA WT together with BAPTA AM on the increase of the cytosolic free  $\text{Ca}^{2+}$  concentration was observed (Figure 3-12 A). The effect of VacA WT and BAPTA AM was consistent even after 35 min and 60 min after thapsigargin stimulation (Figure 3-12 B&C).

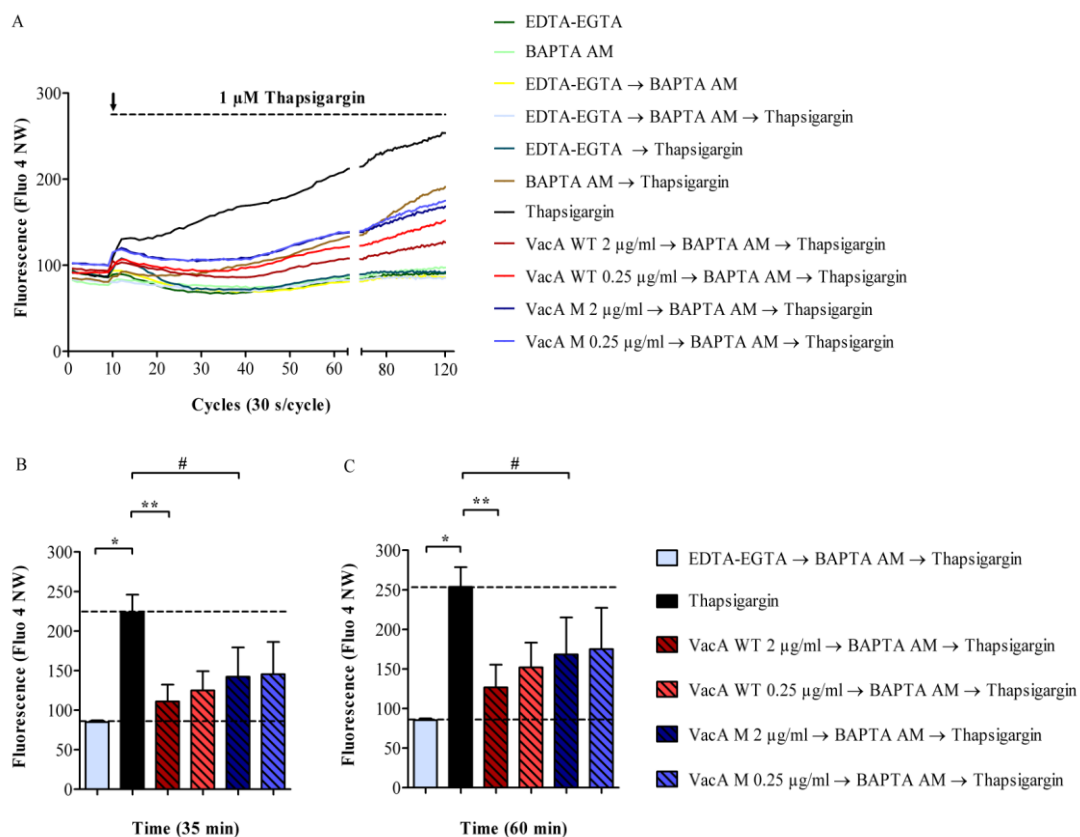


**Figure 3-12 Fluorescence measurement evoked by thapsigargin and the effect of VacA on the increase of the cytosolic free calcium concentration in Jurkat E6.1 cells treated with BAPTA AM.**

(A) Each line in the graph displays fluorescence intensity measurements in Jurkat E6.1 cells loaded with Fluo-4 NW. The cells were pre-incubated with VacA WT and VacA M (indicated in red and blue, respectively) and treated with BAPTA AM. The cells were then stimulated by 1  $\mu$ M thapsigargin (black vertical arrow) after measuring the baseline fluorescence. (B) The degree of inhibition in the increase of the cytosolic free  $\text{Ca}^{2+}$  by VacA WT and VacA M at 35 min depicted as bar graphs. (C) Bars represent the averaged measurement obtained at 60 min. The horizontal

arrows indicate the order of pre-incubation to treatment and stimulation. Each graph was compiled from data obtained in three independent experiments. Error bars are standard deviations. Statistical significance was evaluated using a t-Test. \*P<0.05, \*\*P<0.01, # No significance.

It was also important to confirm the effect of VacA WT on the increase of cytosolic free  $\text{Ca}^{2+}$  in Jurkat E6.1 cells when the cells were pre-incubated with VacA WT and treated with thapsigargin. Once the cells were stimulated by 1  $\mu\text{M}$  thapsigargin after measuring the baseline fluorescence (Figure 3-13 A), the effect of VacA WT as compared to VacA M to inhibit the increase of cytosolic free  $\text{Ca}^{2+}$  was high and significant with thapsigargin treatment (Figure 3-13 B&C).

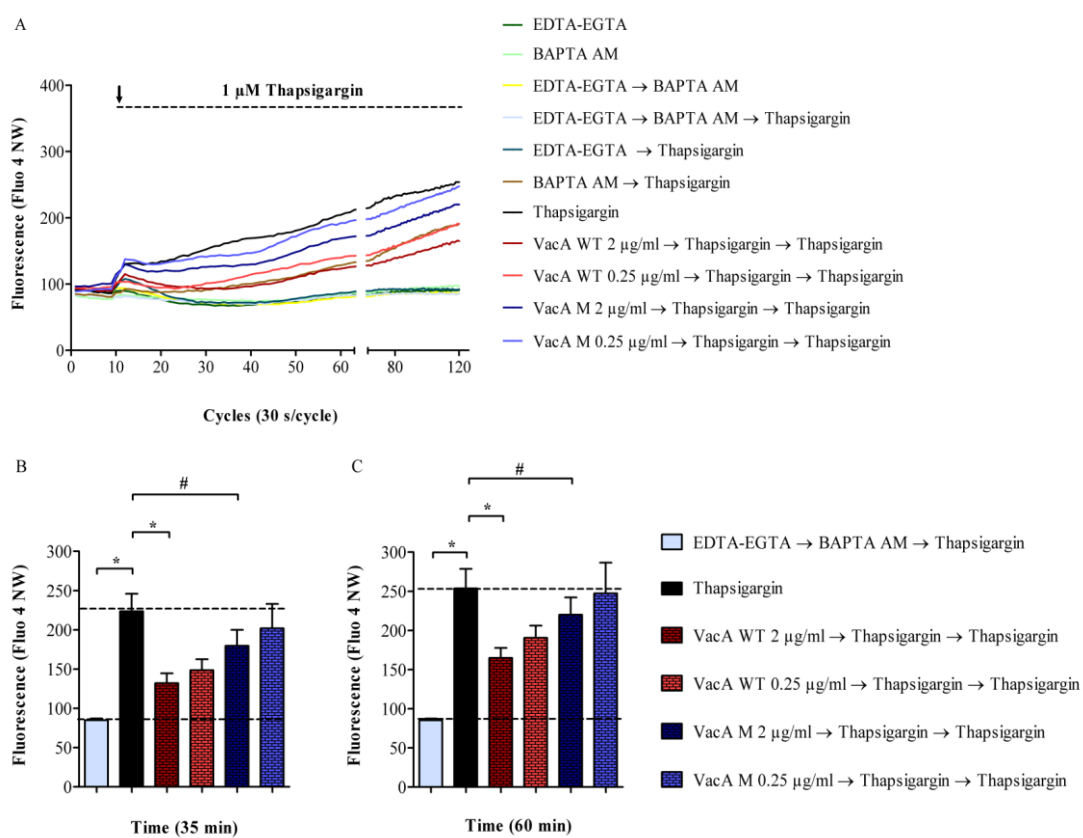


**Figure 3-13 Fluorescence measurement of  $\text{Ca}^{2+}$  influx in the effect of VacA on the increase of the cytosolic free calcium concentration in Jurkat E6.1 cells treated with two times thapsigargin.**

(A) Each line in the graph displays fluorescence intensity measurements in Jurkat E6.1 cells loaded with Fluo-4 NW. The cells were pre-incubated with VacA WT and VacA M (indicated in red and blue, respectively) and treated with thapsigargin. The cells were then stimulated by 1  $\mu\text{M}$  thapsigargin (black vertical arrow) after measuring the baseline fluorescence. (B) The degree of inhibition in the increase of the cytosolic free  $\text{Ca}^{2+}$  by VacA WT and VacA M at 35 min depicted as bar graphs. (C) Bars represent the averaged measurement obtained at 60 min. The horizontal arrows indicate the order of pre-incubation to treatment and stimulation. Each graph was compiled from data obtained in three independent experiments. Error bars are standard deviations. Statistical significance was evaluated using a t-Test. \*P<0.05, # No significance.

### 3.3.2 Effect of VacA on increase of cytosolic free Ca<sup>2+</sup> concentration in human CD<sup>4+</sup> T-cells

*H. pylori* VacA inhibits calcium influx and the increase of cytosolic free Ca<sup>2+</sup> concentration in Jurkat E6.1 cells after stimulation by ionomycin and thapsigargin. Most important, VacA WT but not VacA M largely affected the increase of cytosolic free Ca<sup>2+</sup> concentration stimulated by thapsigargin (Figure 3-8). It was also observed that this effect of VacA WT as compared to VacA M was much higher and significant after subsequent thapsigargin treatment (Figure 3-13).

An important question was now whether there is a similar effect of VacA WT and VacA M on calcium influx evoked by ionomycin and increase of cytosolic free Ca<sup>2+</sup> concentration stimulated by thapsigargin in PMA activated CD<sup>4+</sup> T-cells with similar experimental conditions as described in 3.3.1.1 with Jurkat E6.1 cells.

#### 3.3.2.1 *H. pylori* VacA inhibits calcium influx in human CD<sup>4+</sup> T-cells after stimulation by ionomycin

Therefore the intracellular calcium in CD<sup>4+</sup> T-cells was measured using the Fluo-4 NW calcium assay. The same Ca<sup>2+</sup> chelators were used to inhibit Ca<sup>2+</sup> influx by binding extracellular as well as intracellular free Ca<sup>2+</sup> for the experiments as described with Jurkat E6.1 cells (see 3.3.1.1). The effect of VacA was measured in primary human CD<sup>4+</sup> T-cells after activation by PMA.

Firstly, fresh prepared human blood was collected and PBLC (peripheral blood lymphocytes) were isolated by density gradient centrifugation (see 2.2.4.6). Primary human CD<sup>4+</sup> T-cells were isolated by positive selection with the MACS technology as described in 2.2.4.5.

The primary human CD<sup>4+</sup> T-cells were then seeded with a cell density of 1x 10<sup>6</sup> cells/ml. Cells were activated by 2 nM PMA for 1 h and then used for experiments. Similar to the previous experiments with Jurkat E6.1 cells as described in 3.3.1.1, the primary human CD<sup>4+</sup> T-cells were pre-incubated with purified acid-activated VacA WT and VacA M with concentrations of 2 µg/ml or 0.25 µg/ml for 3 h at 37°C and 5% CO<sub>2</sub> and then were loaded with Fluo-4 NW calcium assay dye and incubated for another h at 37°C and 5% CO<sub>2</sub>. After 4 h of total incubation, cells were evaluated by fluorescence measurement (excitation at 494 nm and emission at 516 nm) in a fluorescence microplate reader (FLUOstar OPTIMA). The baseline fluorescence of resting cells (before stimulation) was measured for 10 cycles and then cells were stimulated by ionomycin at a final concentration of 0.5 µM.

A significant reduction of calcium influx induced by ionomycin was observed when the cells were pre-incubated with VacA WT (2  $\mu\text{g}/\text{ml}$ ) (Figure 3-14 A). This effect was consistent even after 100 min of ionomycin stimulation. No significant reduction of calcium influx was observed in cells pre-incubated with VacA M (Figure 3-14 B&C).

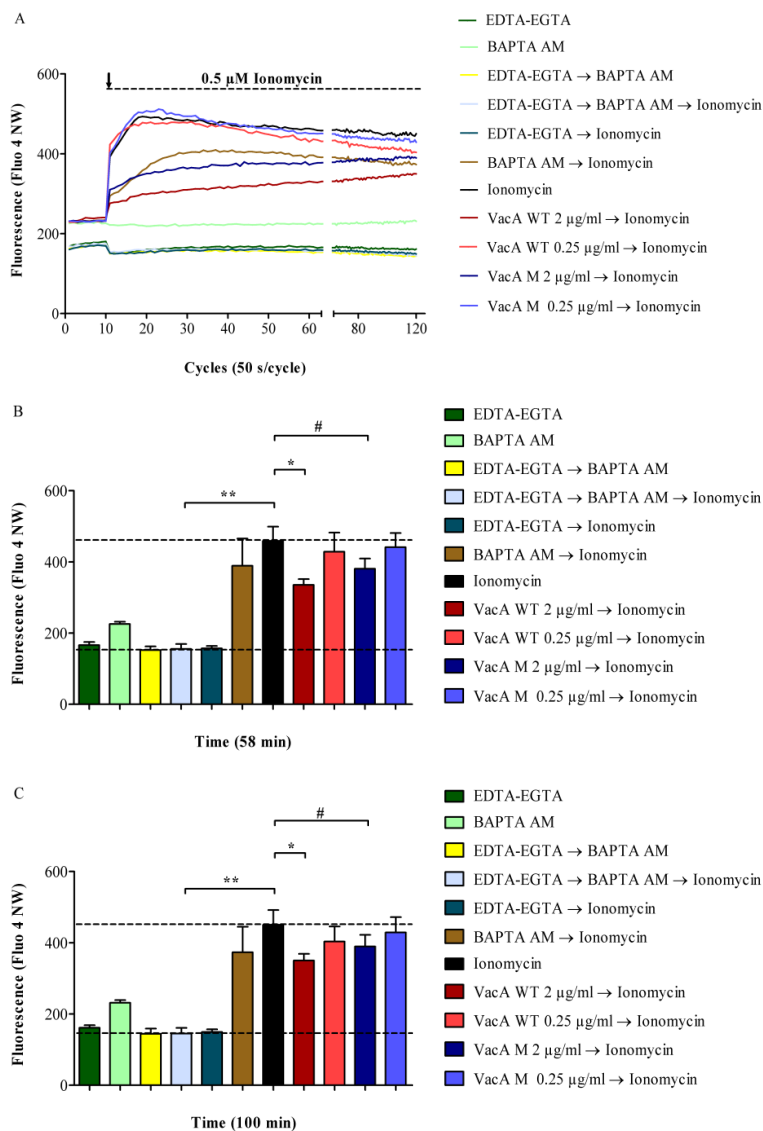


**Figure 3-14 Measurement of  $\text{Ca}^{2+}$  influx evoked by ionomycin and the effect of VacA on  $\text{Ca}^{2+}$  influx in  $\text{CD}^{4+}$  T-cells.**

(A) Each line in the graph displays fluorescence intensity measurements over the period of 100 min in  $\text{CD}^{4+}$  T-cells. After ten baseline fluorescence measurements, 0.5  $\mu\text{M}$  ionomycin was added to the cells. The time point of ionomycin stimulation is indicated by a black vertical arrow. For control measurements EDTA-EGTA, BAPTA AM, and EDTA-EGTA and BAPTA AM were added to the cells. The cells were pre-incubated with both VacA WT and VacA M at two different concentrations (2  $\mu\text{g}/\text{ml}$  and 0.25  $\mu\text{g}/\text{ml}$ ) indicated in red and blue, respectively. (B) The degree of inhibition of calcium influx by VacA WT and VacA M at 58 min depicted as bar graphs. (C) Bars represent

the average measurement obtained at 100 min. The horizontal arrows indicate the order of pre-incubation to stimulation. Each graph was compiled from data obtained in three independent experiments. Error bars are standard deviations. Statistical significance was evaluated using a t-Test. \*P<0.05, \*\*P<0.01, # No significance.

### 3.3.2.2 *H. pylori* VacA inhibits the increase of cytosolic free Ca<sup>2+</sup> in CD4<sup>+</sup> T-cells after stimulation by thapsigargin

As seen in figure 3-8 in Jurkat E6.1 cells, VacA WT had a much higher and significant effect on the increase of cytosolic free Ca<sup>2+</sup> concentration than VacA M after stimulation by thapsigargin. To test whether VacA WT and VacA M have similar effects in CD4<sup>+</sup> T-cells after stimulation by thapsigargin, similar experimental conditions with CD4<sup>+</sup> T-cells were applied.

Therefore, we first activated CD4<sup>+</sup> T-cells by 2 nM PMA for 1 h. After activation, cells were pre-incubated with purified acid activated VacA WT and VacA M (2 µg/ml and 0.25 µg/ml) as described in 3.3.1.2. Furthermore, CD4<sup>+</sup> T-cells were also treated with EDTA-EGTA and BAPTA AM alone, as well as stimulated by thapsigargin as control. After measuring the baseline fluorescence, a final concentration of 1 µM thapsigargin was added to the cells. The cells were then evaluated for the effect of VacA on the increase of cytosolic free Ca<sup>2+</sup> after stimulation by thapsigargin.

The effect of thapsigargin treatment of CD4<sup>+</sup> T-cells can be seen in figure 3-15 A, B and C.

VacA WT caused a strong significant reduction of the increase of cytosolic free Ca<sup>2+</sup> concentration in PMA activated CD4<sup>+</sup> T-cells after the addition of thapsigargin. This effect was observed right after stimulation by thapsigargin and remained unchanged throughout the thapsigargin treatment upto 100 min. For the positive control, the PMA activated CD4<sup>+</sup> T-cells were only stimulated by thapsigargin and as negative control, the extracellular as well as intracellular free Ca<sup>2+</sup> were sequestered together with a mixture of EDTA-EGTA and BAPTA AM and then stimulated by thapsigargin. As observed in figure 3-15 B, the inhibitory effect of VacA WT at the higher concentration (2 µg/ml) at 58 min of thapsigargin treatment was upto 40% of the cells without pre-incubation with VacA. This percentage of inhibition was calculated by comparing the effect of VacA WT in the increase of cytosolic free Ca<sup>2+</sup> with the effect in resting cells treated with EDTA-EGTA and BAPTA AM (negative control) and the effect in cells stimulated by thapsigargin (positive control). The fluorescence measured in negative control was considered zero value as there occurred no increase of cytosolic free Ca<sup>2+</sup>. The positive control was taken as 100%. However, as seen in figure 3-15 C, a slight but significant reduction of VacA

M was observed after 100 min of thapsigargin treatment, although no significant reduction was observed by VacA M after 58 min of thapsigargin treatment (Figure 3-15 B).

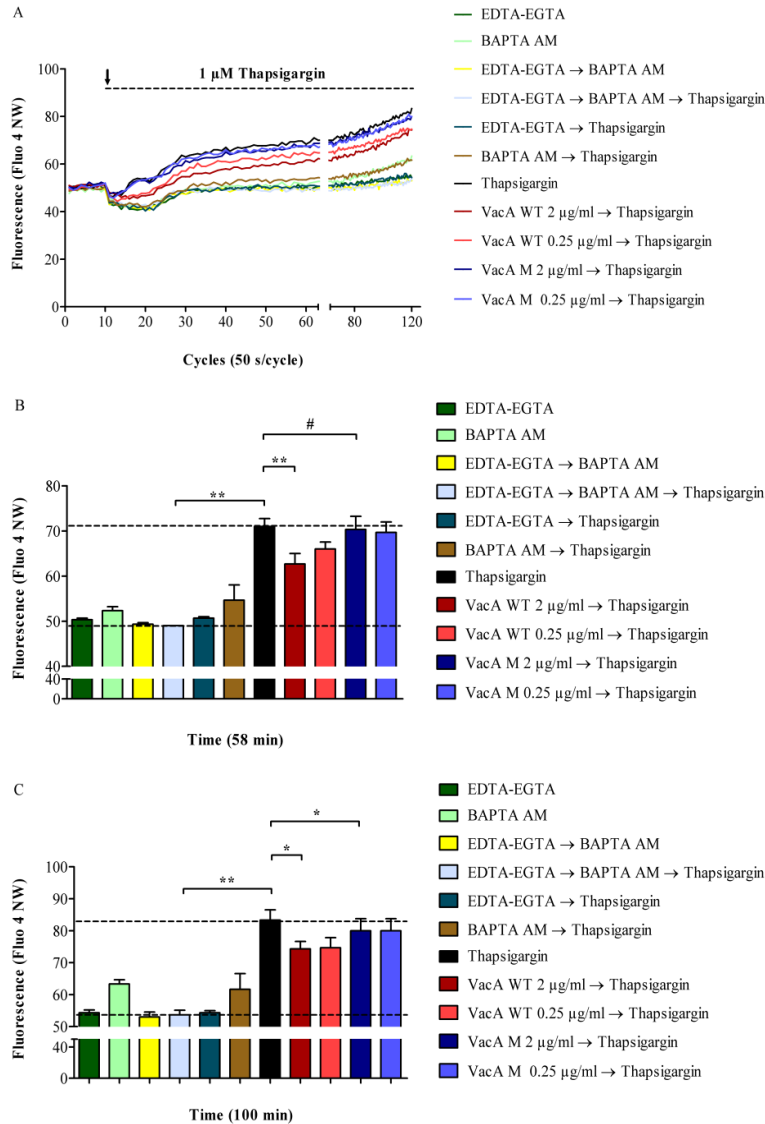


**Figure 3-15** Measurement of the increase of the cytosolic free calcium concentration in CD<sup>4+</sup> T-cells pre-incubated with VacA and then stimulated by thapsigargin.

(A) Each line in the graph displays fluorescence intensity measurements over the period of 100 min in CD<sup>4+</sup> T-cells. Ten baseline fluorescence measurements were taken prior to stimulation with 1  $\mu$ M thapsigargin. The time point of thapsigargin stimulation is indicated by a black vertical arrow. The cells were pre-incubated with both VacA WT and VacA M at two different concentrations (2  $\mu$ g/ml and 0.25  $\mu$ g/ml) indicated in red and blue, respectively. Control measurements were performed in the presence of EDTA-EGTA, BAPTA AM, EDTA-EGTA and BAPTA AM, and thapsigargin treatment. (B) The degree of inhibition in the increase of the cytosolic free Ca<sup>2+</sup> by VacA WT and VacA M at 58 min depicted as bar graphs. (C) Bars represent the averaged measurement obtained at 100 min. The horizontal arrows indicate the order of pre-incubation to stimulation. Each graph was compiled from data obtained in three independent experiments. Error bars are standard deviations. Statistical significance was evaluated using a t-Test. \*P<0.05, \*\*P<0.01, # No significance.

Since the effect on inhibition of VacA WT on increase of cytosolic free  $\text{Ca}^{2+}$  was increased after two times thapsigargin treatment in Jurkat E6.1 cells figure 3-13, it was also interesting to see a similar effect in  $\text{CD}^{4+}$  T-cells. Therefore, PMA activated  $\text{CD}^{4+}$  T-cells were pre-incubated with VacA WT and VacA M and treated with 1  $\mu\text{M}$  thapsigargin. After measuring the baseline fluorescence, cells were then again stimulated by 1  $\mu\text{M}$  thapsigargin (Figure 3-16 A). As expected, VacA WT was able to inhibit upto 50% of the increase of cytosolic free  $\text{Ca}^{2+}$  in PMA activated  $\text{CD}^{4+}$  T-cells. This effect of VacA WT was evaluated at time points 58 min and 100 min (Figure 3-16, B&C). Besides, a slight but significant effect of VacA M was also observed after two times thapsigargin treatment (Figure 3-16 A, B&C).

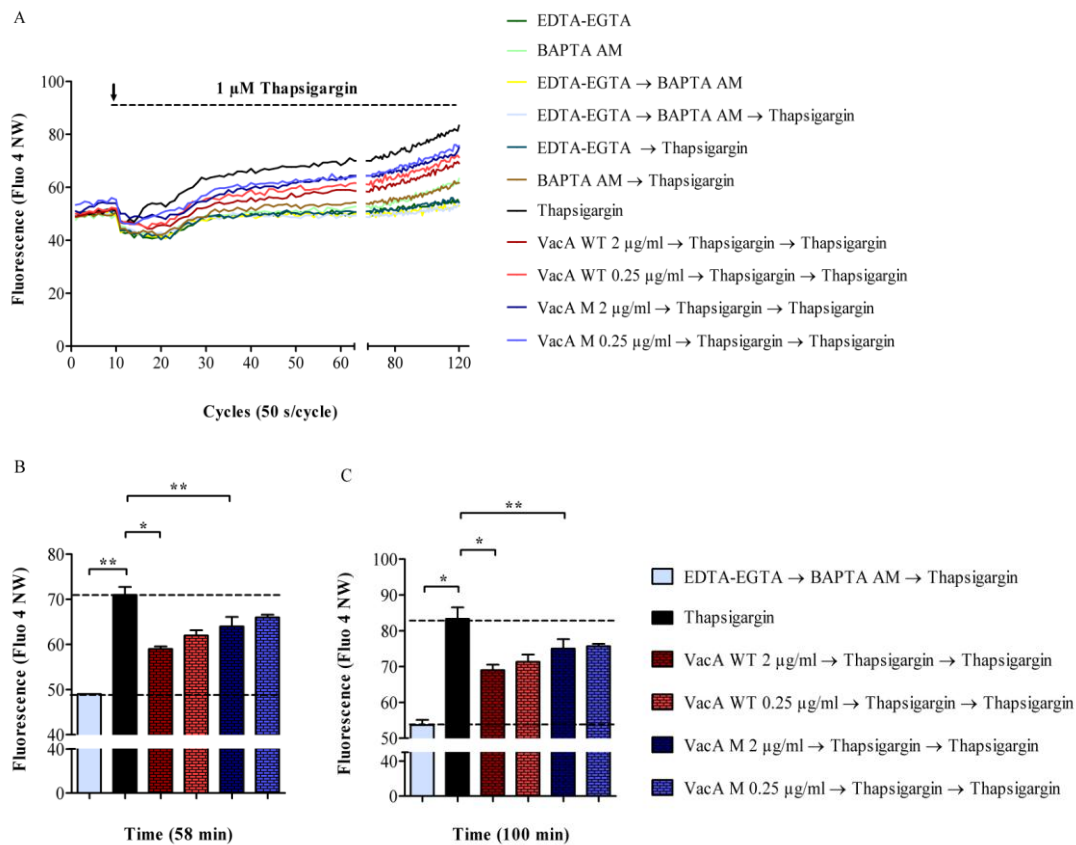


**Figure 3-16 Measurement of the increase of the cytosolic free calcium concentration in  $\text{CD}^{4+}$  T-cells pre-incubated with VacA and then stimulated by two times thapsigargin.**

(A) Each line in the graph displays fluorescence intensity measurements over the period of 100 min in  $\text{CD}^{4+}$  T-cells. The time point of thapsigargin stimulation is indicated by a black vertical arrow. The cells were pre-incubated with both VacA WT and VacA M at two different concentrations (2  $\mu\text{g/ml}$  and 0.25  $\mu\text{g/ml}$ ) indicated in red and blue, respectively. Cells were then treated with thapsigargin and ten baseline fluorescence measurements were taken. After measuring the baseline fluorescence, 1  $\mu\text{M}$  thapsigargin was again added to the cells. Control measurements were performed in the presence of EDTA-EGTA, BAPTA AM, EDTA-EGTA and BAPTA AM, and thapsigargin treatment. (B) The degree of inhibition in the increase of the cytosolic free  $\text{Ca}^{2+}$  by VacA WT and VacA M at 58 min

depicted as bar graphs. (C) Bars represent the averaged measurement obtained at 100 min. The horizontal arrows indicate the order of pre-incubation to stimulation. Each graph was compiled from data obtained in three independent experiments. Error bars are standard deviations. Statistical significance was evaluated using a t-Test. \* $P < 0.05$ , \*\* $P < 0.01$ .

As a further control experiment to confirm that no increase of cytosolic free  $\text{Ca}^{2+}$  occurred, PMA activated  $\text{CD}^{4+}$  T-cells were pre-incubated with VacA and then treated with both EDTA-EGTA and BAPTA AM. As observed in figure 3-17, EDTA-EGTA and BAPTA AM together sequester extracellular as well as intracellular free  $\text{Ca}^{2+}$  respectively thereby not allowing the increase of cytosolic free  $\text{Ca}^{2+}$  after stimulation by thapsigargin.

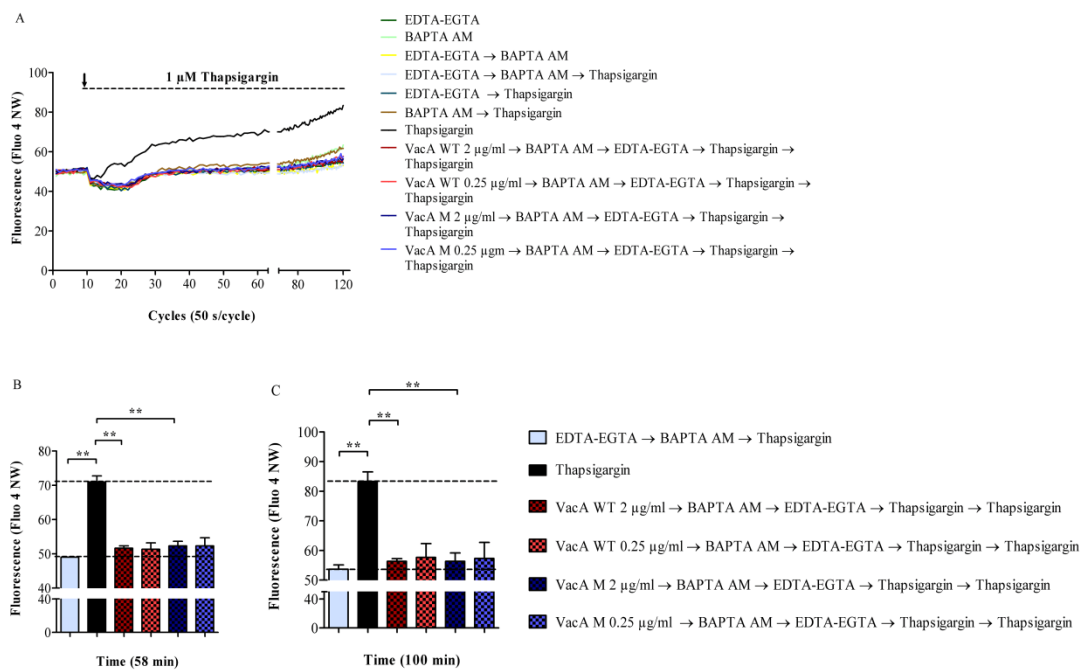


**Figure 3-17 Fluorescence measurement of  $\text{CD}^{4+}$  T-cells pre-incubated with VacA and treated with EDTA-EGTA, BAPTA AM and thapsigargin.**

(A) Each line in the graph displays fluorescence intensity measurements over the period of 100 min in  $\text{CD}^{4+}$  T-cells. The time point of thapsigargin stimulation is indicated by a black vertical arrow. The cells were pre-incubated with both VacA WT and VacA M at two different concentrations (2  $\mu\text{g}/\text{ml}$  and 0.25  $\mu\text{g}/\text{ml}$ ) indicated in red and blue, respectively. Cells were then treated with both EDTA-EGTA and BAPTA AM. Ten baseline fluorescence measurements were taken. After measuring the baseline fluorescence, 1  $\mu\text{M}$  thapsigargin was again added to the cells. (B) The degree of inhibition by VacA, EDTA-EGTA and BAPTA AM at 58 min depicted as bar graphs. (C) Bars represent the averaged measurement obtained at 100 min. The horizontal arrows indicate the order of pre-incubation to stimulation. Each graph was compiled from data obtained in three independent experiments. Error bars are standard deviations. Statistical significance was evaluated using a t-Test. \*\* $P < 0.01$ .

Taking together all the data of calcium assays done in the human Jurkat E6.1 T-cells and primary human CD<sup>4+</sup> T-cells, it was confirmed that VacA protein inhibits calcium influx and an increase of cytosolic free Ca<sup>2+</sup> after both ionomycin and thapsigargin treatment. The effect of VacA WT in the human Jurkat E6.1 T-cells and primary human CD<sup>4+</sup> T-cells was stronger and much more significant in the case of thapsigargin treatment and increased after subsequent thapsigargin stimulation. The question arised now why only VacA WT and not VacA M had a strong effect after thapsigargin stimulation in the human Jurkat E6.1 T-cell line and primary human CD<sup>4+</sup> T-cells? When VacA is once inside the cells, the VacA M protein is comparatively less ion-selective and forms slower ion-conductive channels as compared to VacA WT, resulting in a loss of vacuolating activity of VacA M. Therefore, a strong effect of only VacA WT was expected in the calcium assay in the case of thapsigargin treatment, since thapsigargin stimulates the increase of cytoplasmic free Ca<sup>2+</sup> concentration from intracellular stores, such as ER. We further asked whether VacA WT inhibits the increase of cytosolic free Ca<sup>2+</sup> after stimulation by thapsigargin through direct effects, such as a binding to the calcium channel proteins STIM1 or ORAI1 of store operated calcium entry.

### 3.4 Cellular processes that are essential for store operated calcium entry

Since *H. pylori* VacA WT inhibits the increase of cytosolic free Ca<sup>2+</sup> concentrations in Jurkat E6.1 T-cell line and primary human CD<sup>4+</sup> T-cells, based on our results with the calcium assay, we further evaluated the role of VacA WT in calcium signalling by thapsigargin in T-cells. It has been shown that thapsigargin raises the cytosolic free Ca<sup>2+</sup> concentration by blocking the ability of the cell to pump Ca<sup>2+</sup> into the ER, which causes ER Ca<sup>2+</sup> stores to become depleted. The ER store-depletion in result activates store operated calcium entry into the cytosol (Lytton, Westlin, & Hanley, 1991). We therefore speculated that two proteins of store operated calcium entry called STIM1 and ORAI1 might be involved in this effect of VacA on the increase of cytosolic free Ca<sup>2+</sup> evoked by thapsigargin.

As observed with the calcium assay in Jurkat E6.1 cells and CD<sup>4+</sup> T-cells, the effect of VacA after stimulation by thapsigargin was statistically significant. Therefore, given the fact that the mechanism of the increase of cytosolic free Ca<sup>2+</sup> concentrations after stimulation by thapsigargin in T-cells is by ER store-depletion, we first wanted to see how thapsigargin raises cytosolic free Ca<sup>2+</sup> concentration in T-cells by live cell imaging and then decided to look at T-cells that had been pre-incubated with VacA WT for 4 h and stimulated by thapsigargin.

### 3.4.1 Stromal interaction molecule-1 (STIM1) clusters in response to thapsigargin treatment in T-cells

Stromal interaction molecule-1 (STIM1) has been known for its role as tumor suppressing gene product (Sabbioni, Barbanti-Brodano, Croce, & Negrini, 1997). RNAi screening experiments in *Drosophila* S2 cells (Roos *et al.*, 2005) and human-derived HeLa cells (Liou *et al.*, 2005) suggested that STIM1 plays a major role in store operated calcium entry. STIM1 is localized on the ER membrane.

Since most of the studies showed that thapsigargin-mediated depletion of ER  $\text{Ca}^{2+}$  stores causes a redistribution of STIM1 (Stathopoulos, Zheng, Li, Plevin, & Ikura, 2008), the effect of thapsigargin on STIM1 oligomerization was evaluated. HEK-293 cells were transfected with a mCherry-STIM1-encoding plasmid carrying the *neo* gene using the transfection reagent lipofectamine 2000 as described in 2.2.4.4.2. The mCherry expression of STIM1 was analysed by confocal laser scanning microscopy (CLSM) (Excitation/Emission at 587/610 nm) (Figure 3-18 A). Firstly, the cells were visualized without thapsigargin treatment. Next, thapsigargin at a concentration of 1  $\mu\text{M}$  was added to the HEK-293 cells expressing mCherry-STIM1. As observed in figure 3-18, STIM1 oligomerization occurred upon thapsigargin treatment. STIM1 oligomerization started immediately within 30s of thapsigargin treatment (Figure 3-18 B) and lasted until 1800 s (Figure 3-18 C-H).

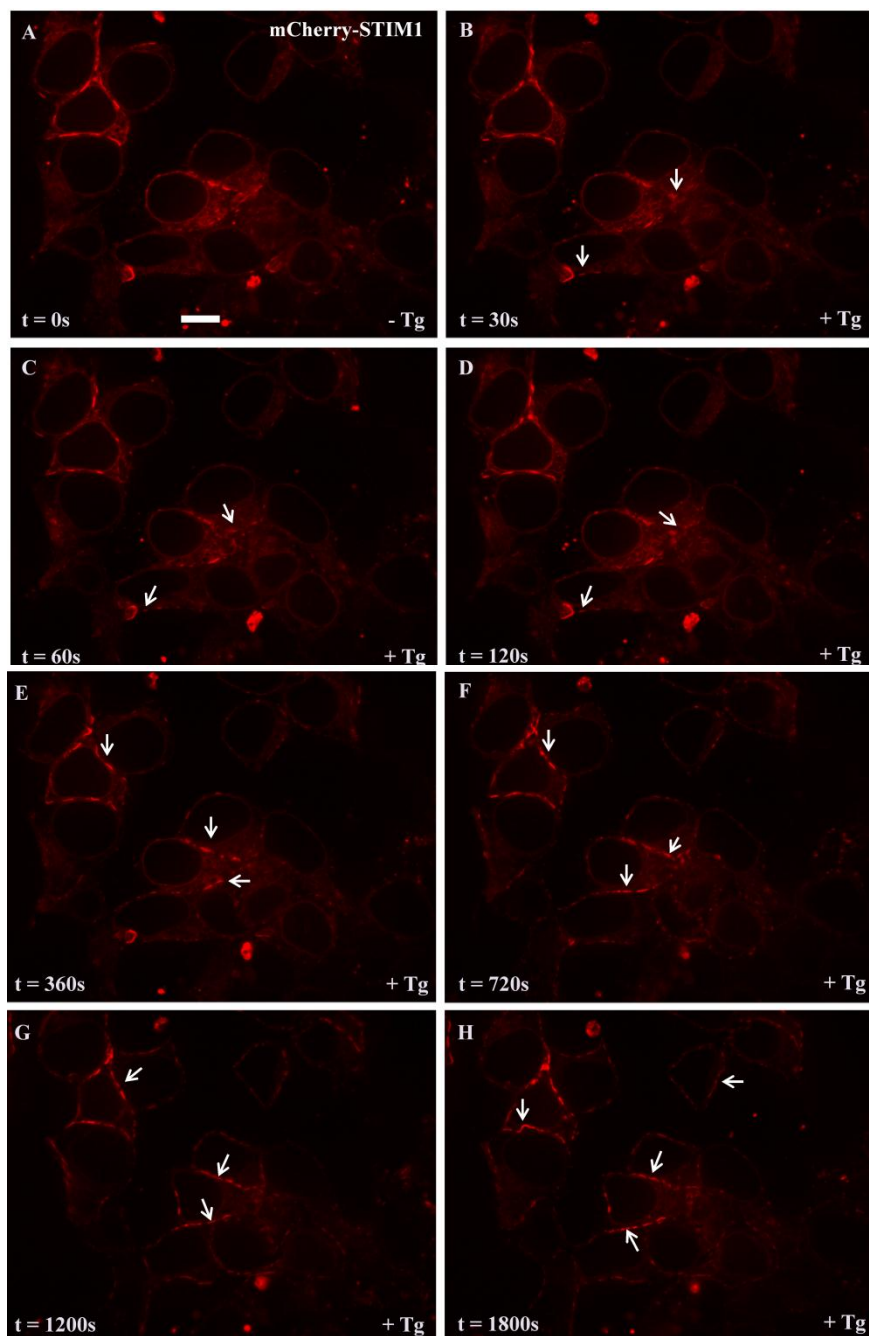


**Figure 3-18 mCherry-STIM1 oligomerization upon thapsigargin treatment in HEK-293 cells.**

(A) Live cell microscopy image from HEK-293 cells expressing mCherry-STIM1 (red) before thapsigargin treatment. (B) to (H) Cells at different time points after thapsigargin administration. The white arrows point out areas of STIM1 oligomerization. Scale bar A-H 9  $\mu$ m.

### 3.4.2 STIM1/ORAI1 coupling and store operated calcium entry

After  $\text{Ca}^{2+}$  store depletion by thapsigargin treatment, STIM1 redistributes and relocates to the junction between the ER and plasma membrane (PM) where the  $\text{Ca}^{2+}$  release-activated  $\text{Ca}^{2+}$  (CRAC) channel protein ORAI1 is localized, and forms puncta. This STIM1 redistribution is necessary for binding with ORAI1 (Wu, Buchanan, Luik, & Lewis, 2006). In addition, the direct binding of STIM1 after clustering leads to the activation of CRAC channels and extracellular  $\text{Ca}^{2+}$  influx (Park *et al.*, 2009).

In order to verify whether STIM1 clusters and relocates towards the plasma membrane localized calcium channel protein ORAI1, Two plasmids encoding mCherry-STIM1 and eGFP-myc-ORAI1 respectively were transfected into HEK-293 cells. The HEK-293 cells expressing the mCherry-STIM1 plasmid carrying the *neo* gene were selected by G418 sulfate (100  $\mu\text{g}/\text{ml}$ ) and transfection efficiency was measured. After the stable expression of mCherry-STIM1, cells were then transiently transfected with the eGFP-myc-ORAI1 plasmid using lipofectamine 2000 as a transfection reagent. The HEK-293 cells were then passed in fresh medium after 12-18 h of transient transfection with the eGFP-myc-ORAI1 plasmid and then used for live cell imaging.

mCherry-STIM1 and eGFP-myc-ORAI1 expression in resting conditions of HEK-293 cells was visualized by live cell imaging (Figure 3-19 A&B). After merging the two image channels in volocity software (Figure 3-19 C), a co-localization study was performed. No co-localization of mCherry-STIM1 and eGFP-myc-ORAI1 was observed (Figure 3-19 D). 1  $\mu\text{M}$  thapsigargin was then added to the cells. Immediately after stimulation by thapsigargin clustering of mCherry-STIM1 clearly occurred (Figure 3-19 F). This relates to the redistribution of STIM1 in the ER. We then asked the question whether this redistribution or clustering of STIM1 further leads to the formation of junctions with ORAI1. As observed in figure 3-19 H, co-localization between mCherry-STIM1 and eGFP-myc-ORAI1 was clearly visualized. The co-localized area refers to the area where STIM1 binds directly to ORAI1, forming puncta, after stimulation by thapsigargin in HEK-293 cells.

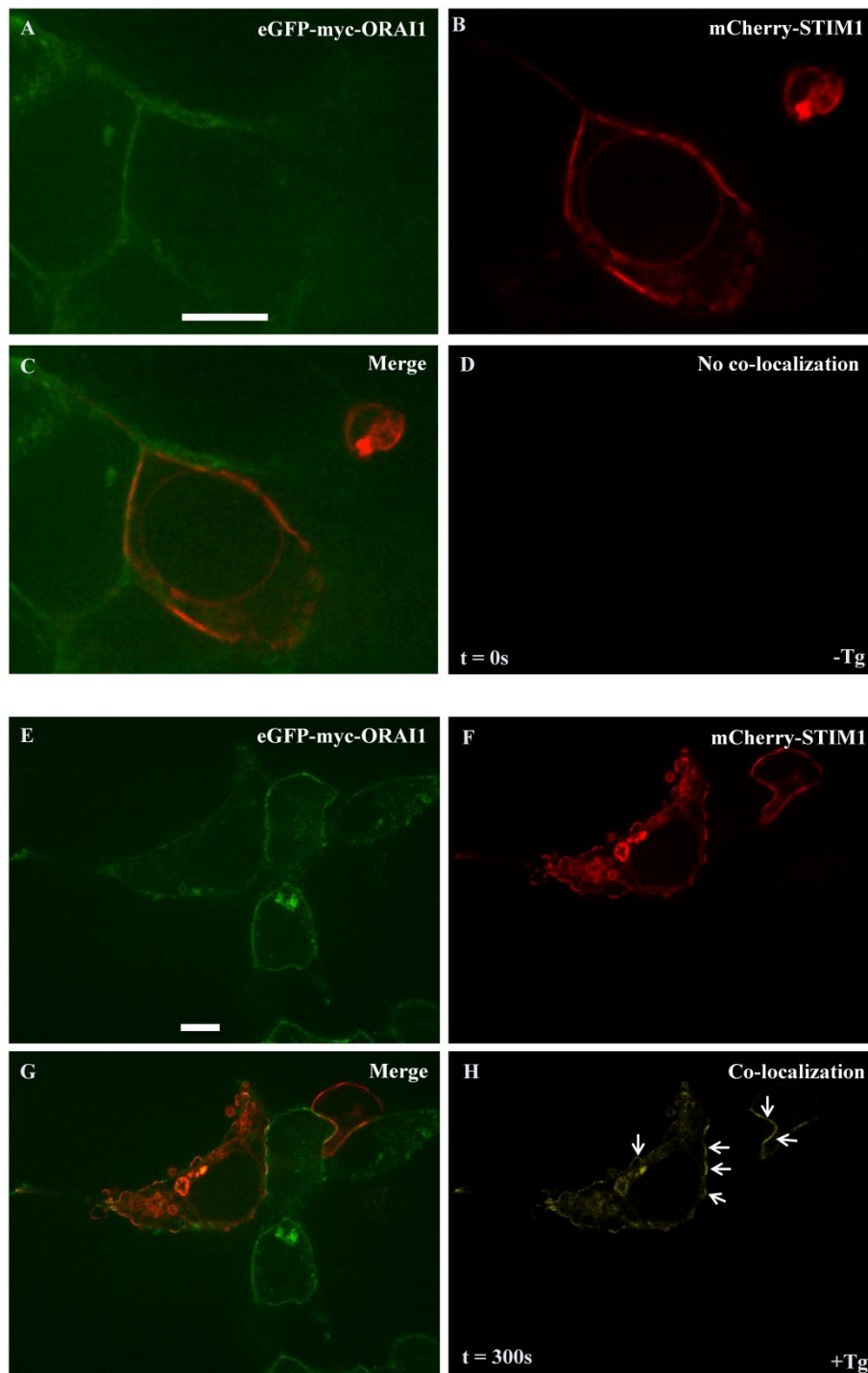


**Figure 3-19 Co-localization study of eGFP-myc-ORAI1 and mCherry-STIM1 before and after thapsigargin stimulation.**

(A) Live cell microscopy image of HEK-293 cells expressing eGFP-myc-ORAI1 (green) before thapsigargin treatment. (B) Cells expressing mCherry-STIM1 (red) before thapsigargin treatment. (C) Merged image of eGFP-myc-ORAI1 and mCherry-STIM1. (D) No co-localization was seen between eGFP-myc-ORAI1 and mCherry-STIM1 before thapsigargin treatment. (E) Cells expressing eGFP-myc-ORAI1 (green) after thapsigargin treatment (F) Cells expressing mCherry-STIM1 (red) after thapsigargin treatment. (G) Merged image of eGFP-myc-ORAI1 and mCherry-STIM1 after thapsigargin treatment. (H) Co-localization was visualized between eGFP-myc-ORAI1 and mCherry-STIM1 after thapsigargin treatment (yellow). Scale bar A-D 5  $\mu\text{m}$ , E-H 9  $\mu\text{m}$ .

### 3.4.3 *H. pylori* VacA co-localizes with STIM1 before and after thapsigargin stimulation

To investigate the possibility that VacA could interact inside the cells with STIM1 and inhibit the increase of cytoplasmic free  $\text{Ca}^{2+}$  by direct binding, we decided to visualize intracellular co-localization of these two proteins before and after thapsigargin treatment. Since STIM1 redistribution and clustering is required for CRAC channel activation, we wanted to analyze whether VacA might localize towards the area of STIM1 clustering.

In order to visualize intracellular co-localization of VacA and STIM1, mCherry-STIM1 expressing HEK-293 cells were incubated with VacA<sup>Alexa 647</sup> and live cell imaging was performed.

In the first step, highly purified VacA WT was labelled with Alexa Fluor 647 dye as described in 2.2.5.7. After checking the activity of labelled VacA<sup>Alexa 647</sup>, HEK-293 cells expressing mCherry-STIM1 were incubated with acid activated VacA<sup>Alexa 647</sup> for 4 h. After washing the cells with PBS, they were resuspended in new medium and used for live cell imaging.

The data showed that VacA<sup>Alexa 647</sup> co-localized on the area of mCherry-STIM1 (Figure 3-20 D) already before thapsigargin treatment. This co-localization image reveals that VacA localizes towards STIM1 even when no clustering of STIM1 by thapsigargin treatment occurred. This observation suggested that VacA might interfere with intracellular  $\text{Ca}^{2+}$  elevation during the process of redistribution or clustering of STIM1 after thapsigargin stimulation. Therefore, a higher degree of co-localization between VacA<sup>Alexa 647</sup> and mCherry-STIM1 in the area of redistribution of STIM1 after thapsigargin treatment was expected to be seen. The addition of a final concentration of 1  $\mu\text{M}$  thapsigargin to the cells resulted in the oligomerization of STIM1 (Figure 3-20). After merging the two image channels, the VacA<sup>Alexa 647</sup> was seen in the area of redistribution of STIM1 (Figure 3-20 G, white arrow). Interestingly, a very high degree of co-localization between VacA<sup>Alexa 647</sup> and mCherry-STIM1 was visualized after 300 s of thapsigargin treatment (Figure 3-20 H). This co-localization was strong in the area of clustering of STIM1.

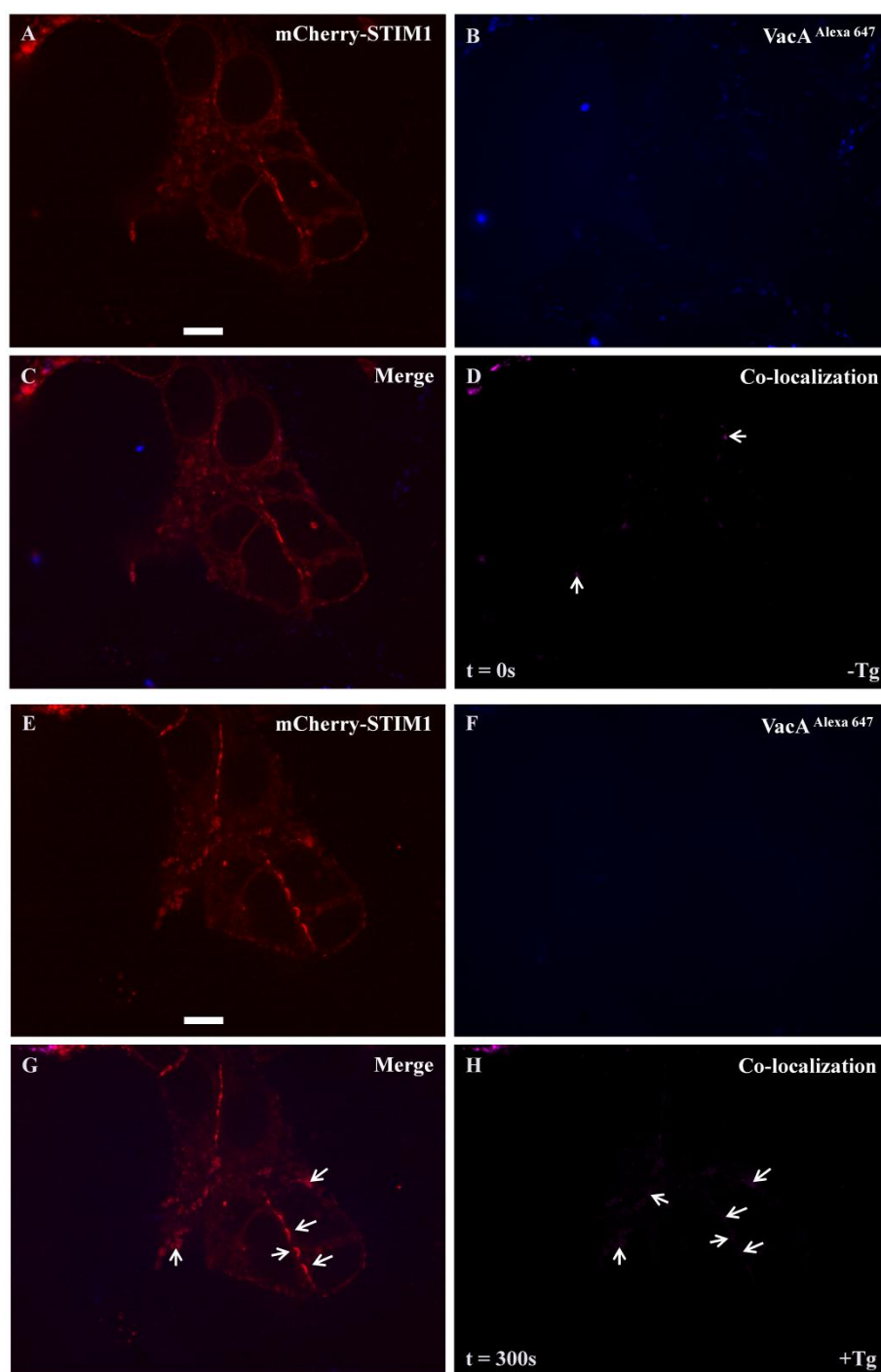


**Figure 3-20** Co-localization of mCherry-STIM1 and VacA<sup>Alexa 647</sup> before and after thapsigargin stimulation.

HEK-293 cells expressing mCherry-STIM1 (red) were incubated with VacA<sup>Alexa 647</sup> (blue) for 4 h (A)-(D) before thapsigargin stimulation (E)-(H) after thapsigargin stimulation. Areas of co-localization (magenta) and highlighted with arrows. Scale bar A-H 9  $\mu$ m.

### 3.4.4 VacA substantially reduces movement of STIM1 towards the plasma membrane protein ORAI1

After observing a strong co-localization between VacA<sup>Alexa 647</sup> and mCherry-STIM1, it was important to test if VacA also co-localizes with ORAI1 and whether the binding of VacA to STIM1 had an effect on STIM/ORAI1 coupling and consequently in store operated calcium entry. With this intention, we expressed mCherry-STIM1 and eGFP-myc-ORAI1 in HEK-293 cells and then incubated with VacA<sup>Alexa 647</sup>.

Using the method described in 3.4.2 for the expression of mCherry-STIM1 and eGFP-myc-ORAI1 together in HEK-293 cells, the cells were then incubated with VacA<sup>Alexa 647</sup> for 4 h at 37°C and 5% CO<sub>2</sub>. After checking the expression of mCherry-STIM1 and eGFP-myc-ORAI1, cells were stimulated by 1 µM thapsigargin (Figure 3-21 and Figure 3-22 A, B & C). The cells were analyzed at two different time points including 120 s and 30 min of thapsigargin treatment. After merging the images of expression of mCherry-STIM1, eGFP-myc-ORAI1 and VacA<sup>Alexa 647</sup> at 120 s and 30 min, a co-localization study was performed (Figure 3-21 & Figure 3-22 D).

As seen in figure 3-21 E, a significant degree of co-localization occurred between mCherry-STIM1 and eGFP-myc-ORAI1 in the cells containing relatively little VacA<sup>Alexa 647</sup> after 120 s of thapsigargin treatment. However, as observed in figure 3-22 E, less co-localization occurred between mCherry-STIM1 and eGFP-myc-ORAI1 in the cells with more internalized VacA<sup>Alexa 647</sup>. The clustering of STIM1 increases with time up to 30 min and co-localization of mCherry-STIM1 with VacA<sup>Alexa 647</sup> was seen (Figure 3-22 F). No co-localization was seen between eGFP-myc-ORAI1 and VacA<sup>Alexa 647</sup> (Figure 3-21 & 3-22 G).

The analysis of these co-localization images suggested that VacA may bind with STIM1 to interfere with STIM1/ORAI1 coupling during the process of calcium store depletion. As VacA co-localized already with STIM1 before stimulation by thapsigargin, VacA is also seen co-localized in the process of clustering of STIM1 after stimulation by thapsigargin.

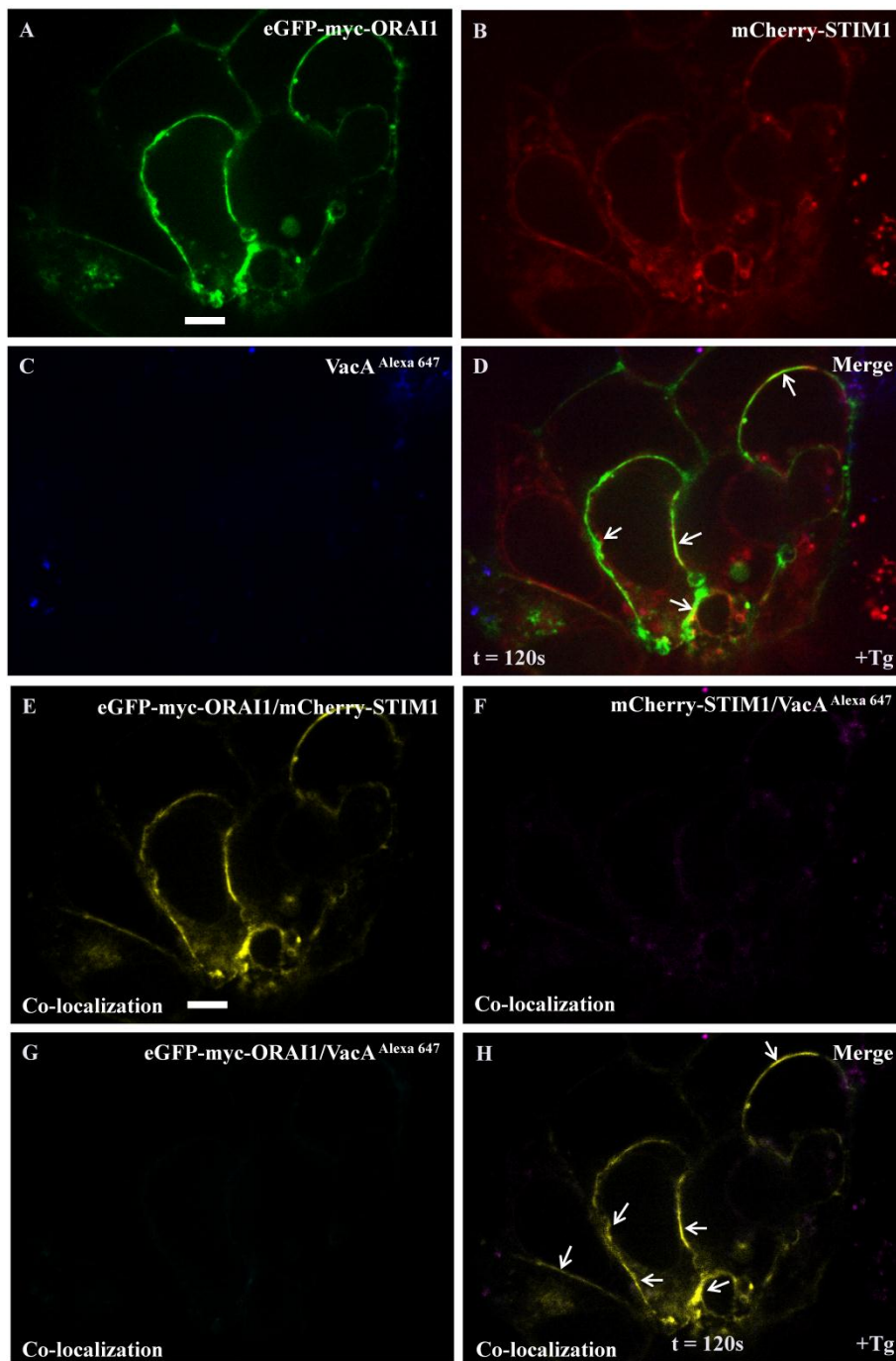


**Figure 3-21 Co-localization of eGFP-myc-ORAI1, mCherry-STIM1 and VacA<sup>Alexa 647</sup> at 120 s after stimulation by thapsigargin.**

HEK-293 cells expressing eGFP-myc-ORAI1 (green) and mCherry-STIM1 (red) were incubated with VacA<sup>Alexa647</sup> (blue) for 4 h and stimulated by thapsigargin before imaging. (A)-(D) Cells expressing eGFP-myc-ORAI1 (green), mCherry-STIM1 (red) and VacA<sup>Alexa 647</sup> (blue). (E)-(H) Areas of co-localization are shown in yellow, cyan and magenta. Scale bar A-H 9  $\mu$ m.

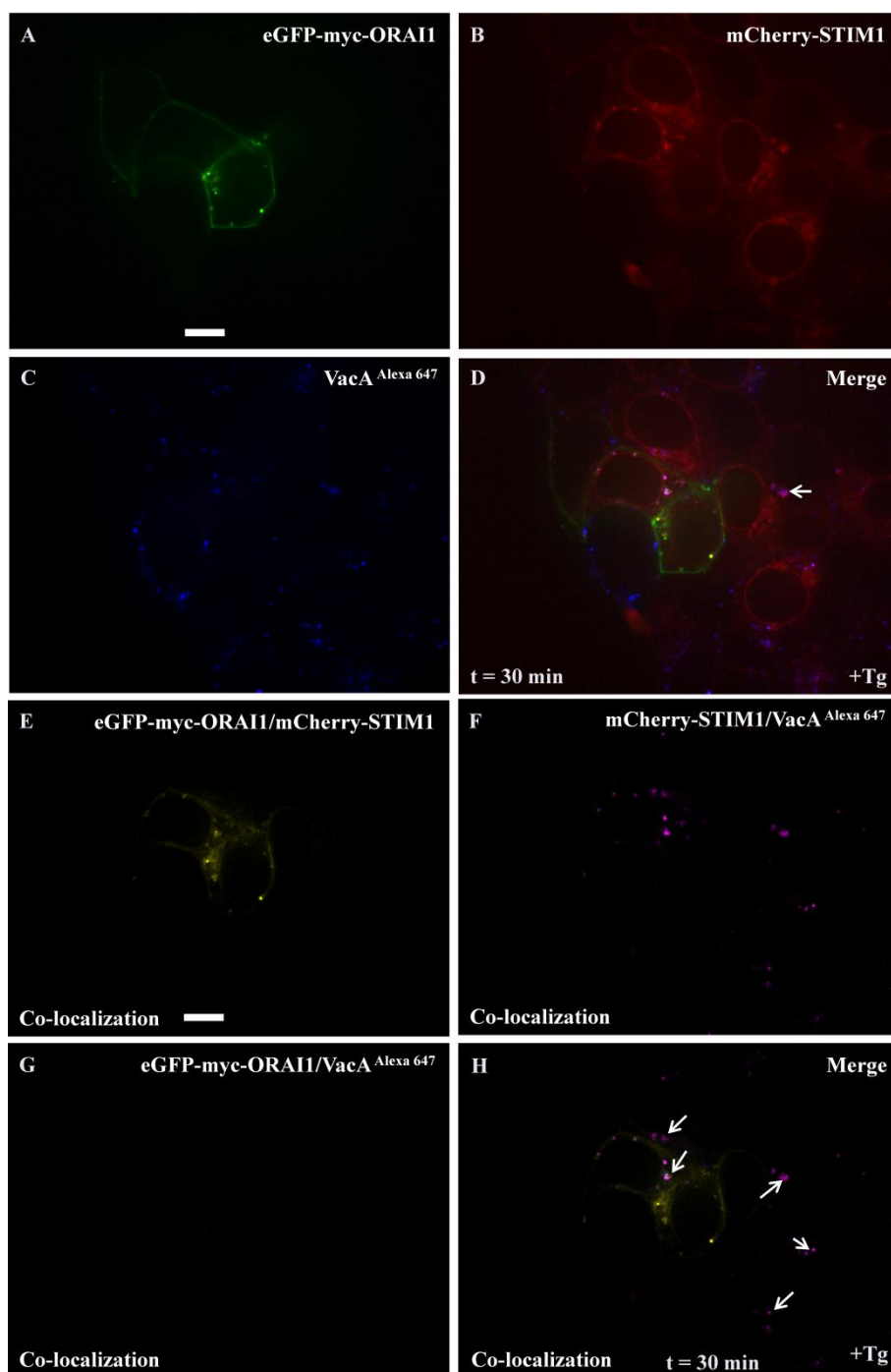


**Figure 3-22** Co-localization of eGFP-myc-ORAI1, m-Cherry STIM1 and VacA<sup>Alexa 647</sup> at 30 min after stimulation by thapsigargin.

HEK-293 cells expressing eGFP-myc-ORAI1 (green) and mCherry-STIM1 (red) were incubated with VacA<sup>Alexa647</sup> (blue) for 4 h and stimulated by thapsigargin over the period of 30 min before imaging. (A)-(D) Cells expressing eGFP-myc-ORAI1 (green), mCherry-STIM1 (red) and VacA<sup>Alexa 647</sup> (blue). (E)- (H) Areas of co-localization are shown in yellow, cyan and magenta. Scale bar A-H 9  $\mu$ m.

### 3.4.5 Co-localization of VacA with STIM1 substantially increases after stimulation by two times thapsigargin

Until this point, the co-localization between VacA with STIM1 was confirmed in HEK-293 cells expressing mCherry-STIM1 after pre-incubation with Alexa Fluor 647 labelled VacA. With these experiments, it was shown that VacA interacts with STIM1 before stimulation by thapsigargin. In addition, after stimulation by thapsigargin, VacA is visualized with a high degree of co-localization in the area of clustering and rearrangement of STIM1.

As previously observed in calcium assay data with Jurkat E6.1 cells and primary human CD<sup>4+</sup> T-cells in figures 3-13 and 3-16, the effect of inhibition of VacA WT on the increase of cytosolic free Ca<sup>2+</sup> was increased after two times thapsigargin treatment. This relevant data needed to be evaluated in co-localization studies. Therefore, mCherry-STIM1 and eGFP-myc-ORAI1 expressing HEK-293 cells after incubation with VacA<sup>Alexa 647</sup> for 4 h and stimulation by thapsigargin were used for this experiment. The cells were further stimulated by 1  $\mu$ M thapsigargin. The cells were then visualized for co-localization.

The images shown figure 3-23 A, B & C were taken after 2 times stimulation by thapsigargin. It shows that mCherry-STIM1 largely clusters with itself and around VacA<sup>Alexa 647</sup> (Figure 3-23 D). A strong co-localization was seen between mCherry-STIM1 and VacA<sup>Alexa 647</sup> (Figure 3-23 F). No co-localization was observed between eGFP-myc-ORAI1 and VacA<sup>Alexa 647</sup> (Figure 3-23 G). Furthermore, the colocalization between eGFP-myc-ORAI1 and mCherry-STIM1 was evaluated and no co-localization was seen in these cells with large clusters of mCherry-STIM1 and VacA<sup>Alexa 647</sup> (Figure 3-23 E).

The fact that the effect of VacA WT on the increase of cytosolic free Ca<sup>2+</sup> was increased in comparison to one time thapsigargin treatment in both Jurkat E6.1 cells and primary human CD<sup>4+</sup> T-cells could be explained as the result of a more intense interaction of VacA with STIM1. Co-localization of VacA with STIM1 is increased substantially after stimulation by thapsigargin, and after two times thapsigargin treatment, STIM1 clusters largely with itself and with VacA. These effects greatly inhibit binding of STIM1 to ORAI1. In these experiments, it was confirmed that VacA binding with STIM1 substantially reduces the movement of STIM1 towards ORAI1 to activate CRAC channels, thereby reducing calcium influx into the cells.

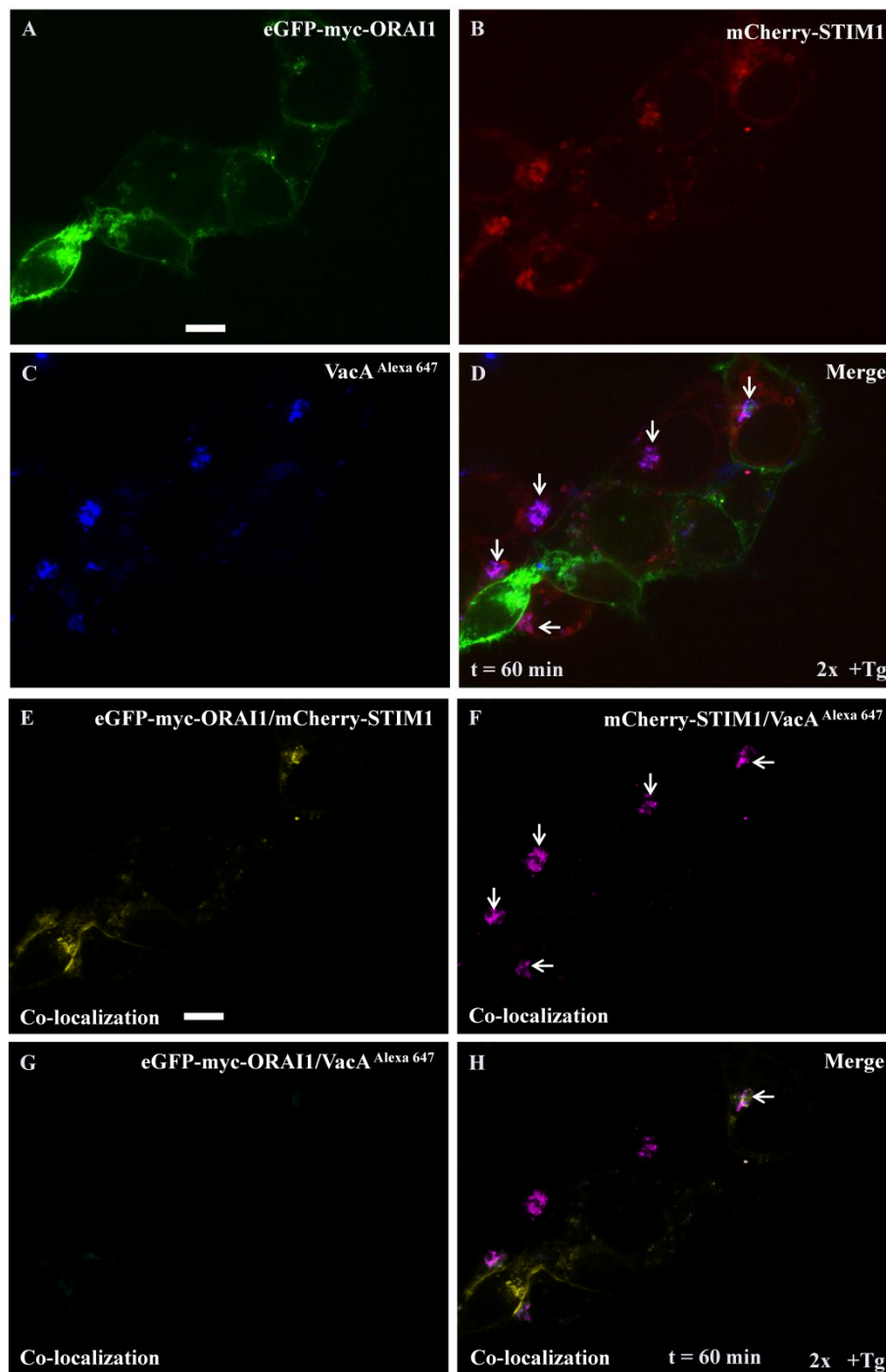


**Figure 3-23** Co-localization of eGFP-myc-ORAI1, mCherry-STIM1 and VacA<sup>Alexa 647</sup> after two times thapsigargin stimulation.

HEK-293 cells expressing eGFP-myc-ORAI1 (green) and mCherry-STIM1 (red) were incubated with VacA<sup>Alexa647</sup> (blue) for 4 h and stimulated by two times thapsigargin over the period of 60 min before imaging. (A)-(D) Cells expressing eGFP-myc-ORAI1 (green), mCherry-STIM1 (red) and VacA<sup>Alexa 647</sup> (blue). (E)- (H) Areas of co-localization are shown in yellow, cyan and magenta. Scale bar A-H 9  $\mu$ m.

### 3.4.6 VacA co-localizes with STIM1 in vicinity of ER membrane protein translocator Sec61 before and after stimulation with thapsigargin

After having shown that mCherry-STIM1 clusters and VacA interferes with this STIM1 clustering after stimulation by thapsigargin in HEK-293 cells, we further were interested to see whether this clustering of mCherry-STIM1 stimulated by thapsigargin and VacA interference with STIM1 occurred in the close vicinity of the ER membrane protein translocator Sec61. It has been shown that the Sec61 complex may act as a  $\text{Ca}^{2+}$  leak channel in the ER membrane and different cellular components are involved to limit  $\text{Ca}^{2+}$  efflux from the ER (Lang *et al.*, 2011). Therefore, a co-localization study of GFP-Sec61, m-Cherry STIM1 and VacA<sup>Alexa 647</sup> was performed.

In the first step, a GFP-Sec61 plasmid was transiently transfected in HEK-293 cells stable expressing mCherry-STIM1 using the lipofectamin 2000 transfection reagent. After checking the transfection efficiency, the cells were incubated with VacA<sup>Alexa 647</sup> for 4 h at 37°C and 5%  $\text{CO}_2$ . The cells were then washed with PBS. After resuspension in new medium, the cells were visualized for co-localization of the corresponding labelled proteins.

The localization of GFP-Sec61, m-Cherry STIM1 and VacA<sup>Alexa 647</sup> is shown in figure 3-24 A, B & C, respectively. After merging of these three image channels (GFP, m-Cherry and Alexa 647) in volocity software, co-localization was seen. As is clearly visible in figure 3-24 E, GFP-Sec61 substantially co-localizes with m-Cherry STIM1. As seen in figure 3-24 F, VacA<sup>Alexa 647</sup> hardly co-localized with GFP-Sec61. Furthermore, after merging all the co-localized channels of figure 3-24 E, F and G, VacA<sup>Alexa 647</sup> was clearly visualized in the same region as m-Cherry STIM1 and GFP-Sec61 (Figure 3-24 H).

Given the fact that VacA<sup>Alexa 647</sup> co-localized in the region of GFP-Sec61 and m-Cherry STIM1 before stimulation by thapsigargin, we expected a substantial co-localization of VacA<sup>Alexa 647</sup> with m-Cherry STIM1 and not with GFP-Sec61 after stimulation, since stimulation by thapsigargin only clusters STIM1. As expected, after stimulation by thapsigargin, GFP-Sec61 was not clustered (Figure 3-25 A). As can be observed in figure 3-25 B, C & D, m-Cherry STIM1 oligomerized and VacA<sup>Alexa 647</sup> was seen in the area of m-Cherry STIM1 clustering. After evaluating the co-localization images, it was observed that the co-localization of VacA<sup>Alexa 647</sup> with GFP-Sec61 was reduced after stimulation (Figure 3-25 F), however no change was observed in the degree of colocalization between m-Cherry STIM1 and GFP-Sec61 (Figure 3-25 E-H).

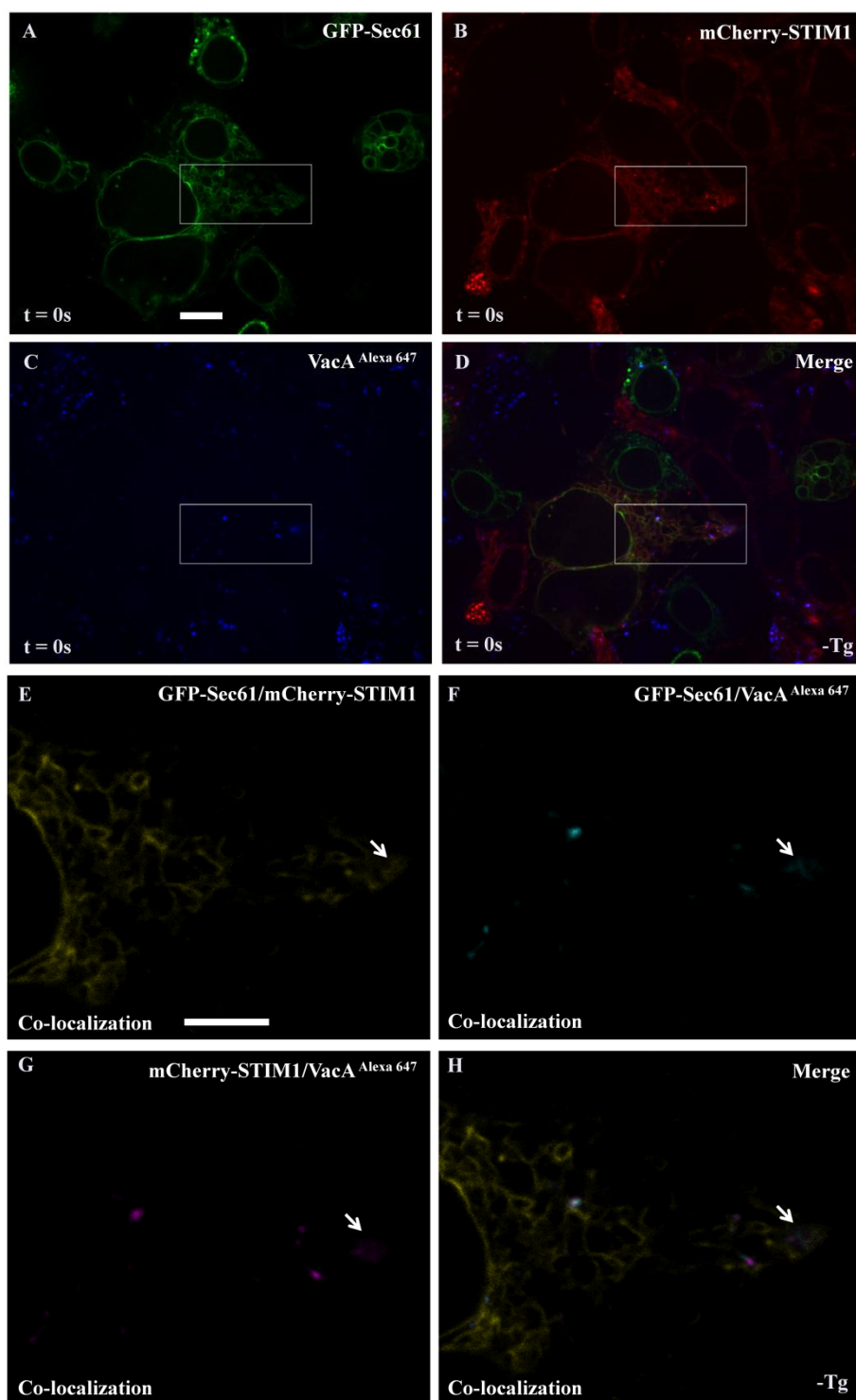


**Figure 3-24** Co-localization of GFP-Sec61, mCherry-STIM1 and VacA<sup>Alexa 647</sup> before thapsigargin stimulation.

HEK-293 cells expressing GFP-Sec61 (green) and m-Cherry-STIM1 (red) were incubated with VacA<sup>Alexa647</sup> (blue) for 4 h. (A)-(D) Cells expressing GFP-Sec61 (green), mCherry-STIM1 (red) and VacA<sup>Alexa 647</sup> (blue). (E)- (H) Areas of co-localization are shown in yellow, cyan and magenta. Scale bar A-D 10  $\mu$ m, E-H 5  $\mu$ m.

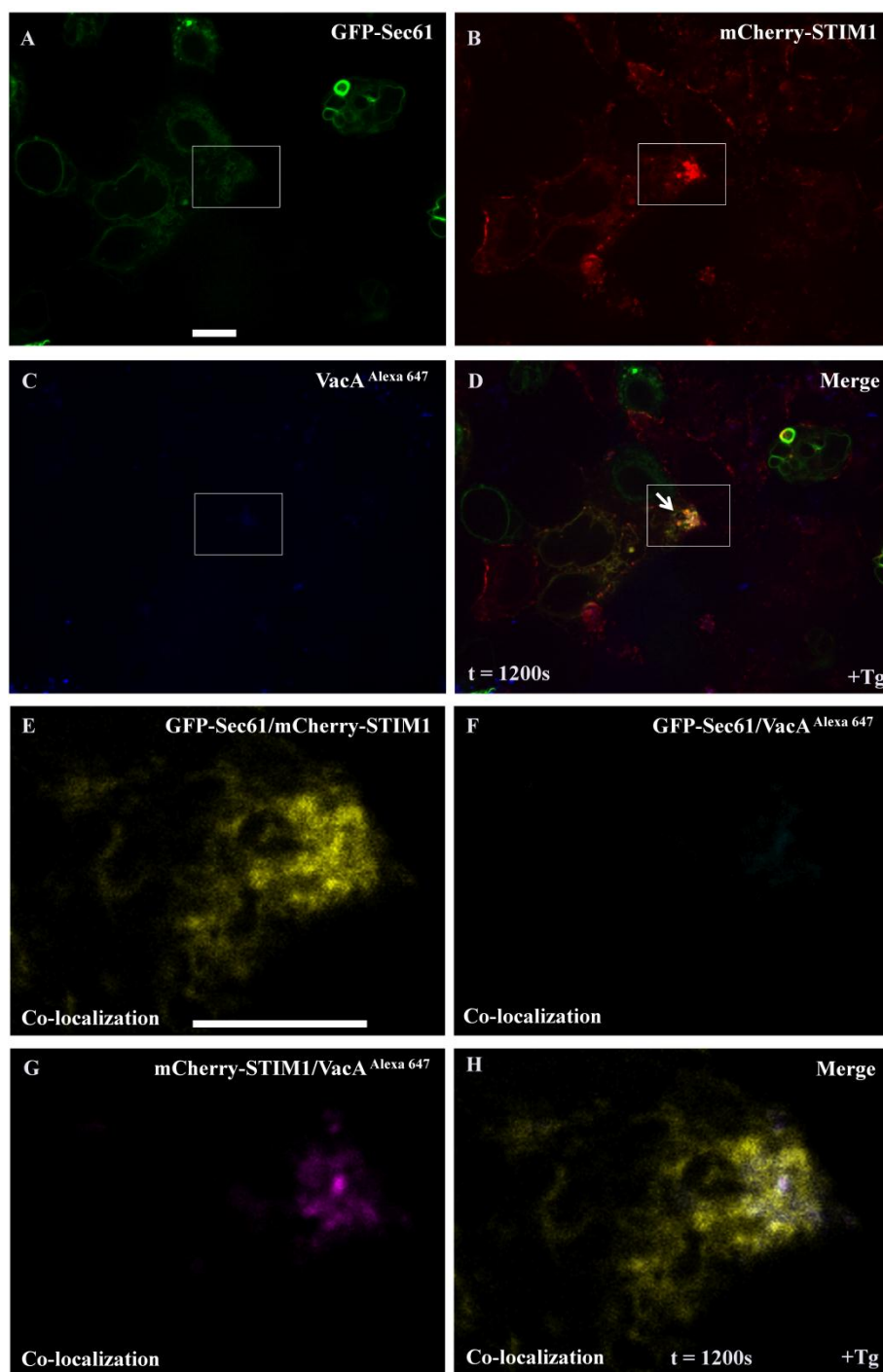


**Figure 3-25 Co-localization of GFP-Sec61, mCherry-STIM1 and VacA<sup>Alexa 647</sup> after thapsigargin stimulation.**

HEK-293 cells expressing GFP-Sec61 (green) and m-Cherry-STIM1 (red) were incubated with VacA<sup>Alexa647</sup> (blue) for 4 h and stimulated by thapsigargin. (A)-(D) Cells expressing GFP-Sec61 (green), mCherry-STIM1 (red) and VacA<sup>Alexa 647</sup> (blue). (E)- (H) Areas of co-localization are shown in yellow, cyan and magenta. Scale bar A-D 10  $\mu$ m, E-H 2.5  $\mu$ m.

### 3.5 Yeast two-hybrid assay to study the interaction between *H. pylori* VacA and different domains of STIM1 and ORAI1

*H. pylori* VacA is a major virulence factor which blocks intracellular  $\text{Ca}^{2+}$  in eukaryotic cells. The results obtained from calcium assays in the human Jurkat E6.1 T-cell line and primary human  $\text{CD}^{4+}$  T-cells activated by PMA suggested that VacA prevents the increase of cytoplasmic  $\text{Ca}^{2+}$  in T-cells after stimulation by thapsigargin. Two components of store operated calcium entry, STIM1 and ORAI1, were considered as possible targets of VacA. The live cell imaging data confirmed that VacA interacts with STIM1, which is localized in the ER. In order to search for the interacting domain of STIM1 with VacA, a yeast two-hybrid (YTH) assay was established.

The stromal interaction molecule 1 (STIM1), which is localized in the ER, contains a luminal and a cytosolic domain connected by a single transmembrane domain (TMD). The N-terminal signal peptide is cleaved during translocation. The ER-luminal N-terminal domain includes a  $\text{Ca}^{2+}$ -binding canonical EF-hand domain (cEF), a non- $\text{Ca}^{2+}$ -binding hidden EF-hand (hEF) domain and a sterile  $\alpha$ -motif (SAM). The cytosolic carboxy-terminal domain includes an Ezrin-Radixin-Moesin (ERM) like domain consisting of two coiled-coil regions called CC1 and CC2. STIM1 also contains a serin/prolin rich domain (S/P) and a polybasic lysine-rich domain (K). The CAD ( $\text{Ca}^{2+}$  release-activated  $\text{Ca}^{2+}$  (CRAC) activation domain) is the minimal sequence required for activation of ORAI1 and located in the cytosolic region (Figure 3-26 A).

ORAI1 is a plasma membrane protein with four transmembrane segments (TM1, TM2, TM3 and TM4) with intracellular amino- and carboxy- termini. ORAI1 contains a putative coiled-coil domain (CC1) at the carboxy- terminal end. This coiled-coil domain mediates dynamic coupling to STIM1 (Figure 3-26 B).

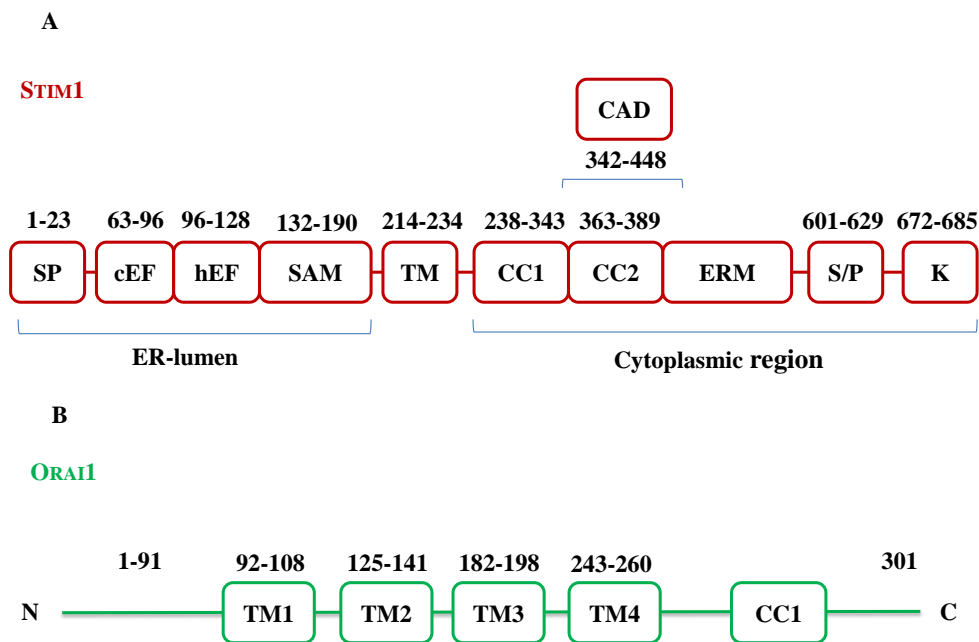


**Figure 3-26 Different domains of STIM1 and ORAI1.**

(A) STIM1 is a transmembrane ER localized  $\text{Ca}^{2+}$  sensor protein. The ER luminal N-terminal domain contains a signal peptide (SP), a  $\text{Ca}^{2+}$ -binding canonical EF-hand domain (cEF), a non- $\text{Ca}^{2+}$ -binding hidden EF-hand domain (hEF) and a sterile  $\alpha$ -motif (SAM). The cytosolic carboxy-terminal domain includes an Ezrin-Radixin-Moesin like domain (ERM) consists of two coiled-coil regions called CC1 and CC2. Furthermore, STIM1 contains a serin/proline rich (S/P) domain and a polybasic lysine-rich (K) domain. (B) ORAI1 is a four transmembrane domain protein (TM1, TM2, TM3 and TM4) with intracellular amino- and carboxy- termini. ORAI1 contains a coiled-coil domain (CC1) at the carboxy- terminal end.

In order to analyze interactions between domains of STIM1 and VacA proteins, both genes were cloned in yeast two-hybrid bait and prey vectors. Furthermore, two domains of ORAI1 were tested for their possible interaction with VacA.

The recombination cloning method used here was Gateway<sup>®</sup> cloning.

### 3.5.1 Amplification of STIM1, ORAI1 and VacA domain DNA sequences by nested-PCR

In the first step towards the Gateway<sup>®</sup> cloning, different domains of STIM1, ORAI1 and VacA were amplified by “nested-PCR” in two steps. In the first step, each domain was amplified by using gene specific forward and reverse primers containing partial attB sites. In the second step, a PCR was performed using complete attB (common to all genes) primers in order to insert full-length attB sites to the specific genes pre-amplified in the first PCR. The PCR products were

separated in agarose gels and the predetermined sizes of the genes was verified. Finally, PCR products containing complete *attB* sites were compatible for Gateway<sup>®</sup> cloning. The domains of STIM1, ORAI1 and VacA were summarised in table 3-1.

**Table 3-1 The domains of STIM1, ORAI1 and VacA and their amino acid positions**

Protein	Protein domain	Region (amino acid position)
STIM1	EF-SAM	58-200
STIM1	cEF	58-96
STIM1	hEF	97-128
STIM1	SAM	131-200
STIM1	CAD	342-448
ORAI1	N-terminal	48-91
ORAI1	C-terminal	255-301
VacA	p33 and p55	821

### 3.5.2 Cloning of the Gateway<sup>®</sup> compatible nested-PCR amplified products in pDonr207 vector

After the PCR amplification, all gene sequences described in table 3.1 were cloned into the Gateway<sup>®</sup> compatible pDONR207 vector by recombination (BP reaction). *E. coli* DH5 $\alpha$  were transformed with the BP reaction mixture and plated out on LB plates containing gentamicin. Plasmids were isolated from the clones and verified by sequencing. Positive clones were termed entry clones.

### 3.5.3 Sequence analysis of the genes cloned in pDONR207 vector

In order to analyze the sequence of entry clones, software Dnaman was used. Plasmid maps were constructed using the software CLC DNA workbench 6.

### 3.5.4 Recombination cloning of entry clones into yeast two-hybrid prey and bait vectors

The entry clones for the domains described in table 3-1 of STIM1, ORAI1 and VacA were cloned into prey (pGADT7) and bait (pGBKT7) vectors by recombination (LR reaction). Recombination occurs between the *attL* sites of the entry clone and *attR* sites of the prey/bait vectors (Figure 3-27 A&B). The LR reaction mixture was transformed into *E. coli* DH5 $\alpha$  and selected on LB plates containing ampicillin and kanamycin. Positive clones were screened by isolating plasmids from *E. coli* DH5 $\alpha$  and analyzed by restriction digestion and DNA sequencing.

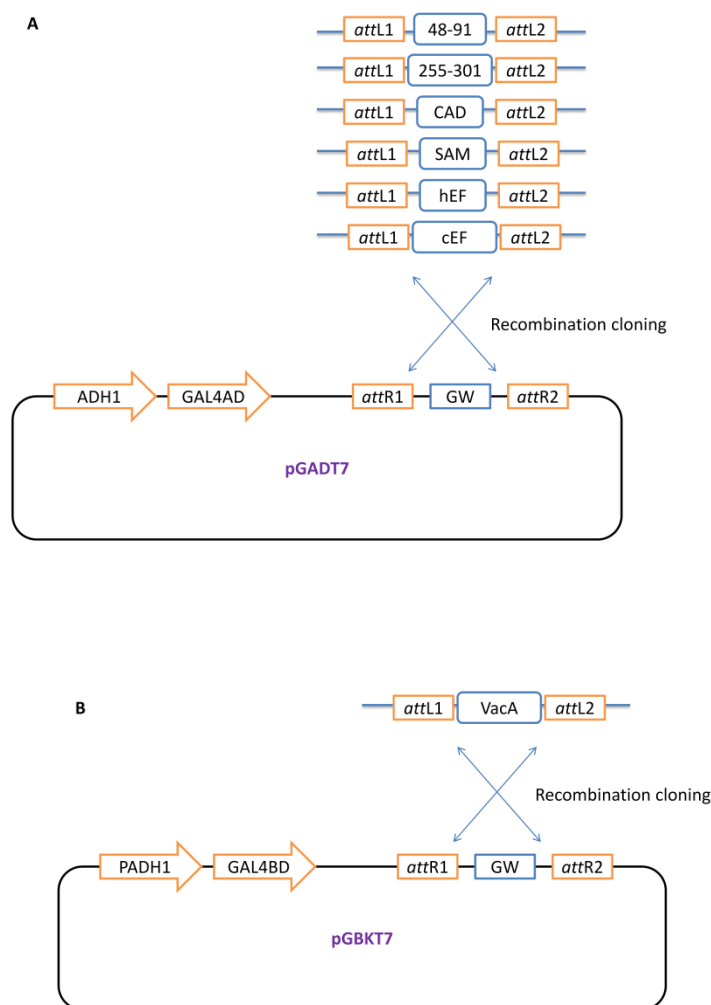


**Figure 3-27** Recombination cloning of domains of STIM1, ORAI1 and VacA into prey (pGADT7) and bait (pGBKT7) vectors.

(A) The entry clone of the domains of STIM1 and ORAI1 were cloned into prey vector (pGADT7) by recombination (LR reaction). (B) Entry clone of VacA was cloned into bait vector (pGBKT7) by recombination (LR reaction). The recombination occurred between the *attL* sites of the entry clone and *attR* sites of prey or bait vector.

### 3.5.5 Transformation of prey/bait vectors into *Saccharomyces cerevisiae*

After Gateway<sup>®</sup> cloning, positive prey/bait vectors were transformed into the *Saccharomyces cerevisiae* yeast strains. The prey vector was transformed into the CG1945 yeast strain and the bait vector in Y187 strain by LiAc transformation method to generate haploid yeast (see 2.2.2.4). The competent yeast cells were prepared in a 0.1 ml TE/LiAc solution with the prey/bait vectors to be transformed and then 0.6 ml of sterile polyethylene glycol (PEG)/LiAc solution was added to the mixture and was incubated at 30°C. After the incubation, 10% DMSO was added and the cells were heat shocked in 42°C water bath for 15 min, allowing the DNA to enter the cells. The cells were then resuspended into 0.5 ml TE buffer plated on the synthetic dropout (SD) medium with a selection marker corresponding to the yeast strain, tryptophan (pGBKT7; bait) and leucine (pGADT7; prey) were used.

### 3.5.6 Generation of diploid yeast by mating

In order to determine the interactions between STIM1 and VacA, diploid yeast cells were generated by mating with combinations of bait and prey vectors and assayed for growth on triple selective dropout medium (SD Leu/Trp/His). But first, the two haploid yeasts were mixed in a ratio at 1:1 and incubated for 24 h at 30°C. After successful mating the diploid yeasts were tested on double selective dropout medium (SD-Leu/Trp) and to confirm the mating.

Figure 3-28 shows that the haploid yeast strains were successfully mated to generate diploid yeast. In all cases, the growth of diploid yeast could be seen.

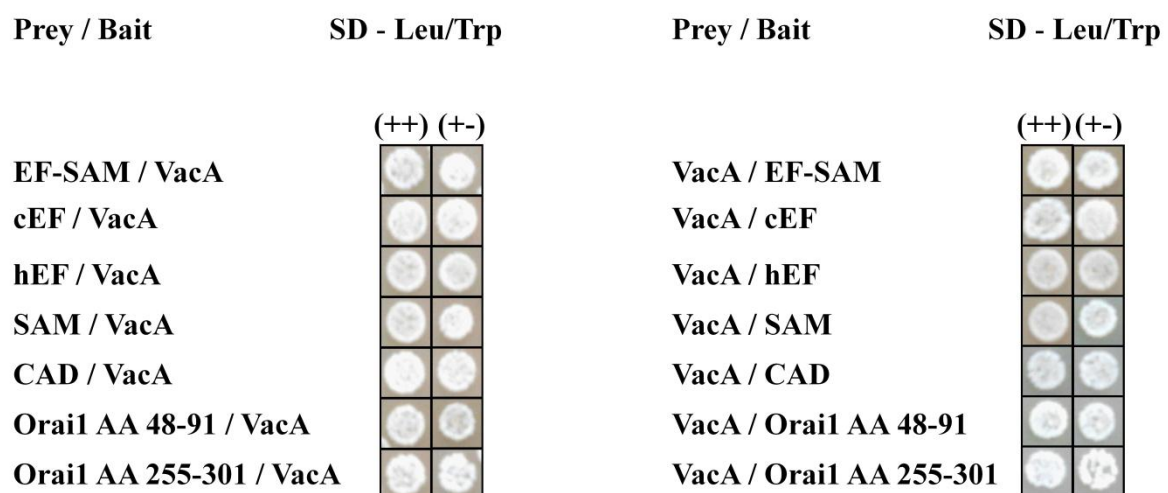


Figure 3-28 Generation of diploid yeast strains and selection on double selective dropout SD medium.

Diploid yeast strains were generated by mating of haploid prey/bait vector transformed strains. Plating on the double selective dropout medium (SD-Leu/Trp) plates confirmed that diploid yeast strains had both prey/bait vectors. Diploid yeast strains were then used for further experiments. (++) indicates both prey and bait with fragments. (+-) indicates prey with insert and empty bait.

### 3.5.7 Yeast two-hybrid growth assay to study the interaction of STIM1 with VacA

The diploid yeast strains grown on the double selective dropout medium (SD-Leu/Trp) plates were used to test the interaction between prey and bait proteins in yeast cells. Growth on double selective dropout medium (SD-Leu/Trp) indicated the ability of diploid yeast cells to synthesize tryptophan and leucine. A growth test on triple selective dropout medium (SD-Leu/Trp/His) showed the ability of diploid yeast to synthesize histidine, which is only possible if there is interaction between prey and bait proteins. Strong interactions led to growth at higher dilutions.

To analyze the possible interaction of STIM1 with VacA, various domains of STIM1 were tested. The protein fragments were fused either to the DNA binding or the activation domain of the transcription factor Gal4, which is involved in histidine biosynthesis. In the case of an interaction, the gene is transcribed, allowing yeast growth on selective media lacking histidine. In some cases, a single domain of transcription factor is sufficient to start the transcription of DNA, which is known as autoactivation. An autoactivation potential of STIM1 could be excluded in performed yeast two-hybrid assays, however autoactivation domains were further tested with empty plasmids.

#### 3.5.7.1 cEF-hand of STIM1 shows positive interaction with VacA

The performed yeast two-hybrid assay indicated that the ER luminal N-terminal Ca<sup>2+</sup>-binding canonical EF-hand domain interacts with VacA with cEF as a prey and VacA as a bait vector. No further positive interactions were found. cEF-hand domain appears to have a weak interaction (Figure 3-29), however supporting that the whole EF-hand motif may have substantial interaction with VacA. The cEF-hand domain was further tested in the other direction with VacA as prey and cEF as bait vector. Significant growth even upto a dilution of 10<sup>4</sup> was observed in VacA/cEF on triple selective dropout medium (SD- Leu/Trp/His), confirming the interaction of cEF and VacA (Figure 3-30).

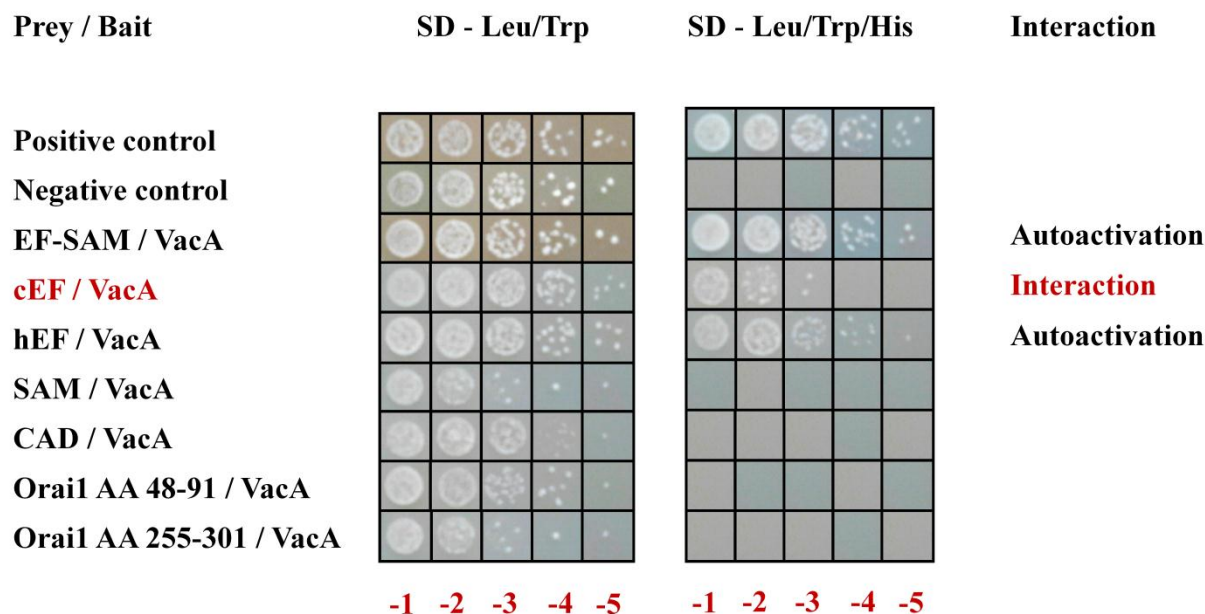


**Figure 3-29 Determination of interaction between STIM1 and ORAI1 with VacA by yeast two-hybrid growth test.**

The diploid yeast strains are plated upto dilutions  $10^5$  on double selective dropout medium (SD-Leu/Trp) and triple selective dropout medium (SD-Leu/Trp/His). The positive control shows the expression of the histidine biosynthesis and growth on triple selective dropout medium (SD-Leu/Trp/His), however the negative control does not grow. Possible interactions between EF-SAM/VacA, cEF/VacA and hEF/VacA were seen. A significant interaction was seen in cEF/VacA. No interactions were observed in ORAI1 48-91 and ORAI1 255-301.

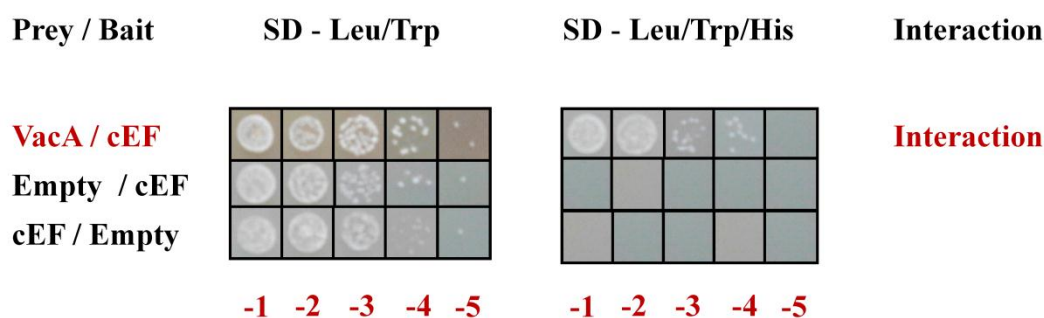


**Figure 3-30 Determination of interaction between the cEF-hand motif and VacA.**

The diploid yeast strains containing either empty prey or bait vectors with the cEF domain of STIM1 were tested on double selective dropout medium (SD-Leu/Trp) and triple selective dropout medium (SD- Leu/Trp/His). No growth was observed on triple selective dropout medium (SD-Leu/Trp/His) with either empty prey or bait vectors. Although, the significant growth at higher dilutions (upto  $10^4$ ) was observed in VacA/cEF on triple selective dropout medium (SD-Leu/Trp/His).

## 4. Discussion

*Helicobacter pylori* colonizes the stomach of more than 50% of the world's population. This colonization leads to development of chronic inflammation, gastric ulcers or adenocarcinoma (Dunn, Cohen, & Blaser, 1997). The immune response of the human host cannot eliminate *H. pylori* infections, because this bacterial pathogen developed various strategies to evade these immune responses.

Due to its chronic infection life style, *H. pylori* has evolved a number of innate immune evasion mechanisms. Thus, *H. pylori* modulates LPS by phase variable expression of fucosyl transferases to generate Lewis (Le) antigens, epitopes also found on human epithelial cells. Le expression patterns result from the on/off status of three fucosyltransferases (e.g., FutB), which are regulated via slipped-strand mispairing in intragenic poly-A or poly-C tracts (Appelmelk *et al.*, 2000). Furthermore, several typical pathogen-associated molecular patterns (PAMPS) of *H. pylori* do avoid recognition by the corresponding Toll-like receptors (TLRs). *H. pylori* LPS avoids interaction with TLR4 (Smith *et al.*, 2003; Yokota *et al.*, 2007). The bacteria possess a bundle of polar flagella, but *H. pylori* flagellin is posttranslationally modified by glycosylation involving pseudaminic acid (Pse5Ac7Ac) and is not recognized by TLR5 due to a divergent sequence in the TLR5 recognition region (Lee *et al.*, 2003). Furthermore, *H. pylori* avoids killing by delayed phagocytosis, dependent on the Cag-T4SS and VacA-dependent inhibition of phagosome acidification and formation of megasomes (Schwartz & Allen, 2006; Zheng & Jones, 2003). NADPH oxidase is directed to the plasma membrane to avoid bacterial killing in the phagosome and *H. pylori* induces iNOS expression by phagocytes through urease, but avoids NO damage by producing L-arginase (RocF), which depletes the iNOS substrate L-arginine. L-arginine depletion also blocks translation of iNOS mRNA. Finally, *H. pylori* is able to extract cholesterol from host cell plasma membranes and glucosylates it by the bacterial cholesterol- $\alpha$ -glucosyltransferase (HP0421), a process that abrogates phagocytosis of *H. pylori* and subsequent T-cell activation (Wunder *et al.*, 2006).

### 4.1 Effects of *H. pylori* VacA in epithelial and immune cells

In the last few years, there has been great progress in the understanding of the cellular effects caused by *H. pylori* VacA. These effects have been investigated intensively both *in vivo* and *in vitro*. A schematic diagram of various effects of VacA in epithelial cells and immune cells is

shown in figure 4-1 A & B. In the process of intoxication, VacA first interacts with the plasma membrane of gastric epithelial cells. The ability of VacA to cause multiple effects *in vitro* on epithelial cells has been demonstrated. Various cell surface receptors for VacA on epithelial cells have been identified. VacA targets RPTP-alpha (Yahiro *et al.*, 2003), RPTP-beta (Fujikawa *et al.*, 2003), Heparin sulphate (Utt, Danielsson, & Wadstrom, 2001), sphingomyelin (Gupta *et al.*, 2008), lipid bilayers and vesicles (Czajkowsky, Iwamoto, Cover, & Shao, 1999; Moll *et al.*, 1995), fibronectin (Hennig, Godlewski, Butruk, & Ostrowski, 2005) and epithelial growth factor receptor (EGFR) (Seto, Hayashi-Kuwabara, Yoneta, Suda, & Tamaki, 1998). Following cell binding, VacA is internalized by clathrin independent pinocytosis. (Gauthier *et al.*, 2005; Ricci *et al.*, 2000). After internalization of VacA, this toxin causes vacuolation. The formation of vacuoles is the most distinct effect of VacA. Vacuolation is attributed to the formation of anion-selective channels in membranes by VacA, causing accumulation of internal membranous vesicles in late and early endosomes (Papini *et al.*, 1994). Besides vacuole formation, VacA has been shown to exert multiple effects. VacA is localized to mitochondria (Kimura *et al.*, 1999), where it is responsible for the release of cytochrome c, thereby initiating an apoptotic cascade (Galmiche *et al.*, 2000). Prolonged exposure of VacA to the epithelial cells causes autophagy (Raju *et al.*, 2012). VacA further intoxicates immune cells, targeting T-lymphocytes by binding the beta-2 integrin subunit of lymphocyte function-associated antigen 1 (LFA-1), CD18, as a cell surface receptor (Sewald *et al.*, 2008). VacA interferes with the T-cell receptor/IL-2 signalling pathway at the level of the Ca<sup>2+</sup>-calmodulin-dependent phosphatase calcineurin resulting in abrogated translocation of Nuclear factor of activated T-cells (NFAT), which in turn causes downregulation of interleukin-2 (IL-2) transcription (Gebert, Fischer, Weiss, Hoffmann, & Haas, 2003) and surface expression of IL2 receptor- $\alpha$  (Boncristiano *et al.*, 2003).

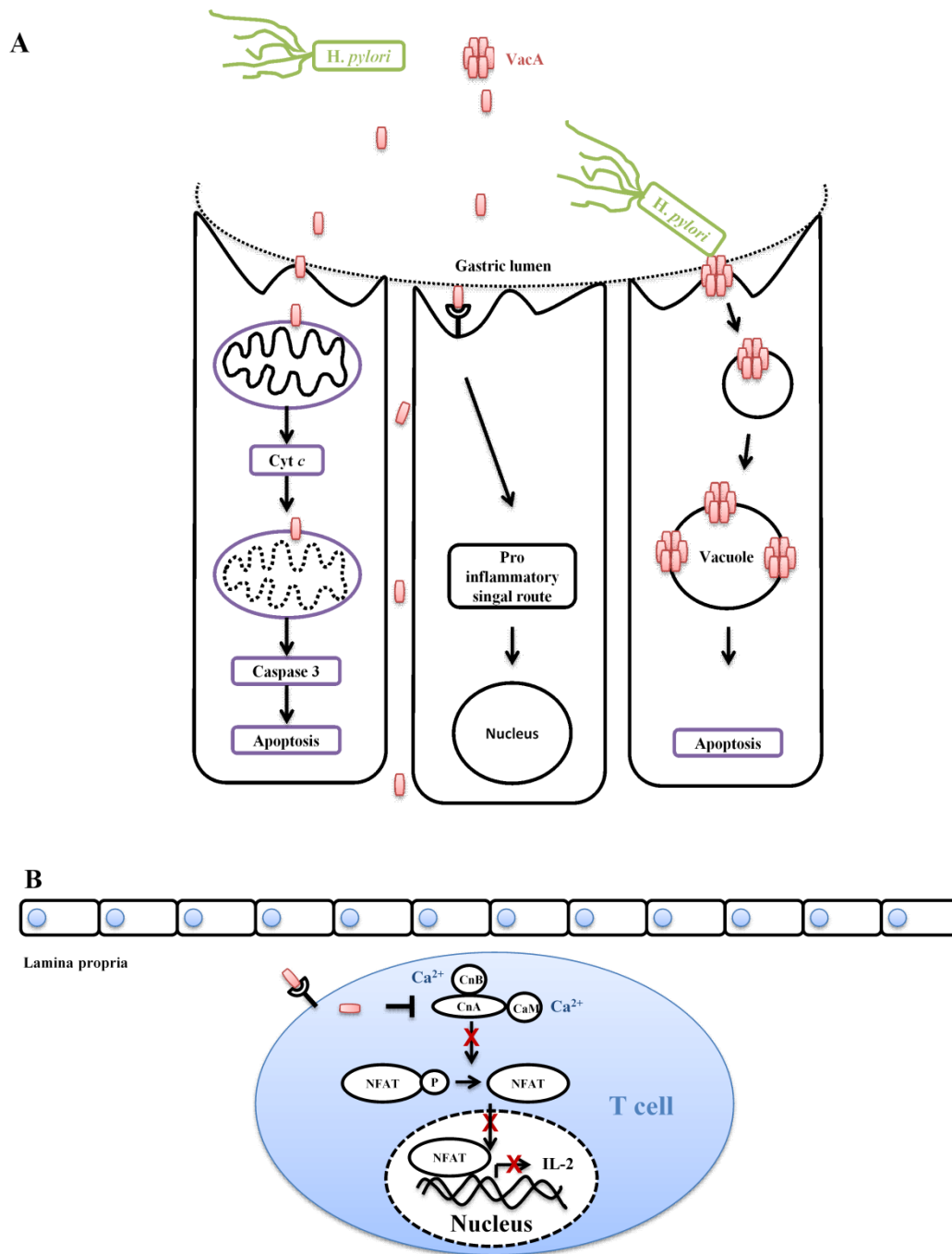


**Figure 4-1 Schematic diagram of *H. pylori* VacA effects on epithelial and immune cells.**

A. *H. pylori* VacA binds to various receptors on epithelial cells and is internalized. Once inside the cells, VacA exerts multiple effects including vacuoles formation, release of cytochrome c from mitochondria and release of proinflammatory cytokines. These effects cause apoptosis of epithelial cells. B. In the lamina propria, VacA may come into contact with T-cells to interfere with NFAT translocation to the nucleus at the level of  $\text{Ca}^{2+}$ -calmodulin-dependent phosphatase calcineurin in T-cells resulting in down regulation of interleukin-2 (IL-2) transcription.

## 4.2 *H. pylori* VacA effects on calcium influx in T-cells

As part of the physiological function of immune cells, calcium regulates a variety of processes including attachment, cell-cycle progression, electrochemical responses, enzyme activities, gene expression, motility, morphology, metabolic processes, replication and signal transduction. These functions are tightly controlled by the level of intracellular calcium concentration in cells. The concentration of extracellular calcium is typically  $10^4$  times higher than the intracellular calcium level (Uematsu, Greenberg, Reivich, Kobayashi, & Karp, 1988). To trigger intracellular  $\text{Ca}^{2+}$  elevation, at first, phospholipase C (PLC) is activated as a result of T-cell receptor or chemokine receptor activation and generates inositol 1,4,5-triphosphate (IP3) from the hydrolysis of phosphatidylinositol 4,5-bisphosphate. The increased IP3 in the cytoplasm binds to IP3R to release  $\text{Ca}^{2+}$  from the ER. This decrease of  $\text{Ca}^{2+}$  in the ER induces the opening of calcium channels in the plasma membrane and activates a calcium influx resulting in a temporary increase in intracellular calcium concentration (Lewis, 2001). The elevation of intracellular calcium levels may lead to apoptosis.

It has previously been described that VacA inhibits NFAT activation by blocking the activity of  $\text{Ca}^{2+}$ -calmodulin-dependent phosphatase calcineurin in T-cells (Gebert, Fischer, Weiss, Hoffmann, & Haas, 2003). Since the increase in intracellular calcium concentration activates the regulatory protein calmodulin, it was assumed that the inhibition of NFAT activation by VacA may occur by blocking calcium influx. For this reason, it was essential to evaluate the effect of VacA on calcium influx in T-cells.

## 4.3 *H. pylori* VacA inhibits calcium influx induced by ionomycin and thapsigargin

In order to find out which kind of calcium signalling mechanism is affected by VacA in T-cells, a calcium assay was performed. The intracellular level of  $\text{Ca}^{2+}$  was raised by two different mechanisms. In one mechanism, an ionophore ionomycin was used to induce calcium influx from the extracellular milieu. In another mechanism, the cytoplasmic level of  $\text{Ca}^{2+}$  was raised by thapsigargin. This tumor promoter is a specific inhibitor of the sarco-endoplasmic reticulum  $\text{Ca}^{2+}$ -ATPase (SERCA) pump located in the endoplasmic reticulum. Once the SERCA pump is blocked, calcium release activated calcium channels (CRAC) are opened, thereby causing an increase in level of cytoplasmic  $\text{Ca}^{2+}$ . This mechanism is called store operated calcium entry (SOCE).

We could confirm that VacA inhibited the increase of cytosolic free  $\text{Ca}^{2+}$  after stimulation by both ionomycin and thapsigargin in Jurkat E6.1 and primary  $\text{CD}^{4+}$  T-cells. In the case of thapsigargin, the effect of VacA was much more significant causing us to look more closely at VacA's effect on SOCE and its most central proteins STIM1 and ORAI1.

#### 4.4 VacA targets SOCE to inhibit calcium influx induced by thapsigargin

Putney (Putney, 1990) suggested a major  $\text{Ca}^{2+}$  entry pathway in which the activation of calcium channels is a direct consequence of intracellular  $\text{Ca}^{2+}$  store depletion. This process is now called as store operated calcium entry (SOCE). Putney also suggested a specialized region where endoplasmic reticulum and plasma membrane are closely associated. Further studies showed that  $\text{Ca}^{2+}$  store depletion activates  $\text{Ca}^{2+}$  entry into the cytosol (Muallem, Khademazad, & Sachs, 1990; Takemura & Putney, 1989). Store operated calcium entry is essential for maintaining intracellular  $\text{Ca}^{2+}$  levels and the generation of  $\text{Ca}^{2+}$  signals. These  $\text{Ca}^{2+}$  signals are controlled by a combination of both  $\text{Ca}^{2+}$  entry across the plasma membrane and  $\text{Ca}^{2+}$  release from intracellular stores such as the ER. This combination occurs by sensing of ER  $\text{Ca}^{2+}$  stores and activation of specific channels resulting in a direct conformational coupling between ER and plasma membrane proteins (Berridge, 1995). An interaction between ER and plasma membranes is important for this coupling (Patterson, van Rossum, & Gill, 1999). Supporting this idea, using an RNA interference (RNAi)-based screening to identify genes that alter thapsigargin-dependent  $\text{Ca}^{2+}$  entry in *Drosophila* S2 cells (Roos, *et al.*, 2005) and in human-derived HeLa cells (Liou, *et al.*, 2005), the STIM1 protein localized in the ER was identified to play a major role in store operated calcium entry. In further studies, ORAI1 channels were identified on the plasma membrane (Feske *et al.*, 2006), (Vig *et al.*, 2006), (Zhang *et al.*, 2006).

In order to assess the effect of VacA on this direct conformational coupling between ER and plasma membrane proteins STIM1 and ORAI1, a co-localization study was carried out by live cell imaging. After store depletion by thapsigargin, STIM1 is redistributed and oligomerizes (Figure 3-18). This redistribution of STIM1 triggers relocation towards ORAI1.

#### 4.5 VacA binds to STIM1 and not to ORAI1 in order to prevent their conformational coupling

The interaction between oligomerized STIM1 and ORAI1 can itself trigger  $\text{Ca}^{2+}$  entry from the extracellular space across the plasma membrane into the cytosol after opening of CRAC channels.

The accumulation of STIM1 protein in the discrete subregions of plasma membrane (PM) to interact with ORAI1 triggers formation of “Puncta”. The STIM1 Puncta formation is localized at ER-PM junctions. It was interesting to study how VacA may interfere with this process. Since thapsigargin causes store depletion and triggers the redistribution and movement of STIM1 in ER regions closely associated with plasma membrane thereby forming puncta with ORAI1 (Wu *et al.*, 2006), firstly, it was important to test the effect of VacA on STIM1. VacA co-localizes with STIM1 before and after stimulation by thapsigargin. After incubation with VacA, the changes of STIM1 still occurred after stimulation and store depletion by thapsigargin, however the degree of co-localization between VacA and STIM1 was increased after thapsigargin treatment. This suggested that VacA could have an effect by direct binding to STIM1 even before thapsigargin treatment. After thapsigargin administration and clustering of STIM1, VacA was seen to co-localize intensively with STIM1. In addition, co-localization of VacA with STIM1 was increased after two times thapsigargin treatment. The co-localization of VacA with ORAI1 was as well tested, but no co-localization was observed. Based on these results, it was assumed that VacA enters the endoplasmic reticulum (ER) to directly binds to STIM1 before stimulation by thapsigargin. VacA then affects the redistribution of STIM1, thereby preventing movement of STIM1 towards ORAI1. This effect of VacA was tested in the cells expressing both STIM1 and ORAI1 proteins using live cell imaging. As assumed, after thapsigargin treatment, the movement of STIM1 towards ORAI1 was not seen in areas with strong co-localization of VacA with STIM1, although a substantial co-localization occurred between STIM1 and ORAI1 where there was no co-localization of VacA with STIM1. Co-localization of VacA with STIM1 was also confirmed by expressing the ER marker Sec61, and VacA co-localized with STIM1 in close proximity with Sec61, indicating that VacA is indeed located in the ER.

The live cell imaging results presented here suggested that VacA inhibits the increase of cytosolic free  $\text{Ca}^{2+}$  by interfering with ER protein STIM1 and not with ORAI1 before and after stimulation by thapsigargin. The interference of VacA with STIM1 may cause a defective redistribution of STIM1 after thapsigargin treatment, preventing the formation of puncta and thereby inhibiting  $\text{Ca}^{2+}$  entry into the cytosol.

#### 4.6 cEF-hand domain of STIM1 is target of VacA

The next question was whether VacA interferes with SOCE via direct binding with STIM1. Taking into consideration the importance of various domains of STIM1 in SOCE, it was necessary to define which of the domains of STIM1 may interact with VacA. STIM1 has an ER luminal region, a single transmembrane segment, and a cytoplasmic region (Figure 3-26). The ER-luminal domain of STIM1 is responsible for  $\text{Ca}^{2+}$  sensing and shows a paired arrangement of two EF-hands (cEF and hEF) followed by a sterile  $\alpha$  motif (SAM) domain (Stathopoulos, Zheng, Li, Plevin, & Ikura, 2008). Only the cEF binds  $\text{Ca}^{2+}$  and senses  $\text{Ca}^{2+}$  store depletion (Stathopoulos, Li, Plevin, Ames, & Ikura, 2006). The cytosolic carboxy-terminal domain contains an Ezrin-Radixin-Moesin like domain (ERM) consisting of two coiled-coil regions called CC1 and CC2, a serin/prolin rich (S/P) domain and a polybasic lysine-rich (K) domain. The cytoplasmic region contains a CRAC activation domain (CAD) that binds directly to the N and C termini of ORAI1 to open the CRAC channel (Park *et al.*, 2009).

In search for the domain of STIM1 that binds to VacA, a yeast two-hybrid (YTH) assay was performed. Therefore, various domains of STIM1 and ORAI1 were cloned into the yeast prey and bait vectors and probed for their capacity to interact with VacA. Interestingly from the STIM1 domains only the cEF-hand domain showed a positive interaction with VacA. However, no interaction of the C-terminal and N-terminal domains of ORAI1 with VacA was observed. Knowing that the cEF hand domain of STIM1 is the  $\text{Ca}^{2+}$  binding domain and decreased luminal  $\text{Ca}^{2+}$  levels cause  $\text{Ca}^{2+}$  to dissociate from the cEF-hand domain, VacA binding could disrupt redistribution of STIM1 and thereafter prevent conformational coupling of STIM1-ORAI1 (Figure 4-2). However, the finding that the cEF-hand domain of STIM1 is the target of VacA to inhibit calcium influx needs to be further confirmed by biochemical assays (e.g. pull down assays).

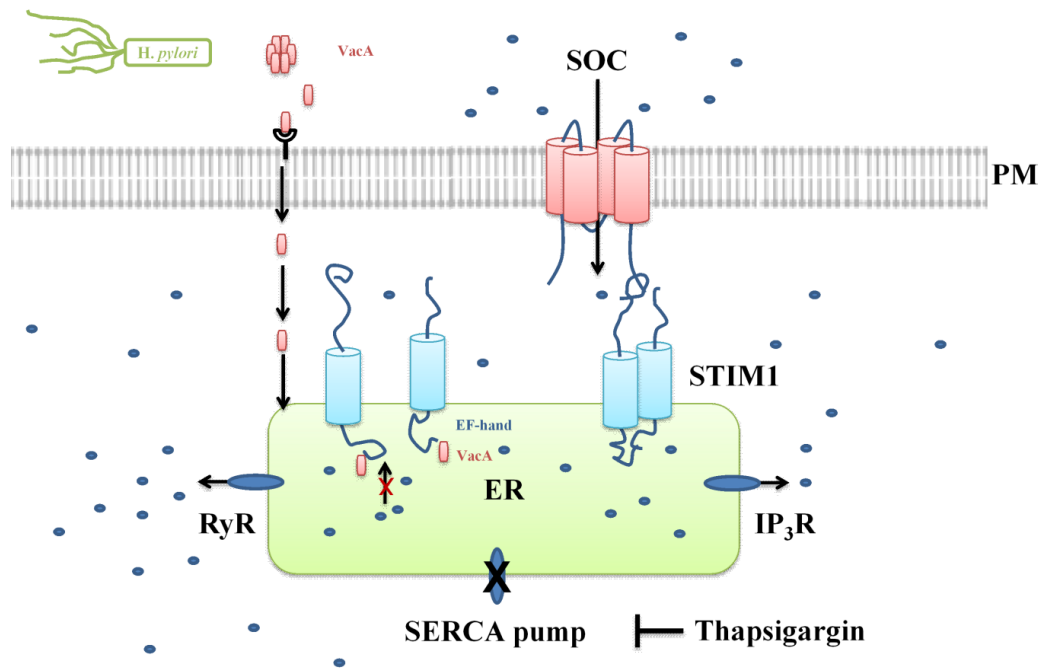


**Figure 4-2 cEF-hand domain of STIM1 is target of VacA.**

In T-cells, VacA is internalized and trafficks to the ER. Once inside the ER, VacA binds to the cEF-hand domain of STIM1. After store depletion by thapsigargin, bound EF-hand is no longer able to sense the decrease of  $\text{Ca}^{2+}$  levels in the ER. Possibly, this might prevent redistribution of STIM1 resulting in a defect in conformational coupling of STIM1 with ORAI1. This could in turn inhibit the increase of cytoplasmic free  $\text{Ca}^{2+}$  in T-cells.

#### 4.7 Effects of inhibition of calcium influx by VacA on T-cell activation and proliferation

VacA substantially inhibits the increase of cytoplasmic free  $\text{Ca}^{2+}$  in T-cells. This inhibitory effect of VacA may influence various  $\text{Ca}^{2+}$  dependent T-cell functions. Previous reports indicated that VacA interferes with the proliferation of T-cells via multiple mechanisms. VacA suppresses nuclear translocation of nuclear factor of activated T-cells (NFAT) resulting in downregulation of interleukin-2 (IL2) gene transcription to efficiently block proliferation of T-cells (Gebert, Fischer, Weiss, Hoffmann, & Haas, 2003). However, another study investigated the effect of VacA on primary human  $\text{CD}^{4+}$  T-cells and suggested that VacA inhibits T-cell proliferation through an NFAT-independent mechanism through the T-cell receptor (TCR) and CD28 (Sundrud, Torres, Unutmaz, & Cover, 2004). Whether T-cell proliferation inhibition is NFAT-dependent or -independent, it is possible that it happens via calcium signalling. Since SOCE is a major  $\text{Ca}^{2+}$  signalling pathway in primary human  $\text{CD}^{4+}$  T-cells and VacA has a substantial inhibitory effect on SOCE, this reduction of  $\text{Ca}^{2+}$  influx into the cytosol could be consequently associated with T-

cell proliferation. A schematic representation of these effects of VacA in T-cells is shown in figure 4-3.

STIM1 and ORAI1 are recruited towards the immunological synapse between primary human T-cells and dendritic cells (Lioudyno *et al.*, 2008). ORAI1 is known to be distributed throughout the plasma membrane surface and after treating cells with thapsigargin, the redistribution and movement of STIM1 towards ORAI1 to form puncta occurs. Puncta formation is exclusively localized to the T-cell/dendritic cell interface. However, Ca<sup>2+</sup> influx through CRAC channels does not require the relocalization of ORAI1 and STIM1 to the interface. On the other hand, this Ca<sup>2+</sup> influx through CRAC channels is significantly increased in activated T-cells at the T-cell/dendritic cell interface.

Because VacA prevents the movement of STIM1 towards ORAI1, thereby preventing formation of puncta, this localized calcium influx at the T-cell/dendritic cell interface could be diminished. However, the process by which VacA interferes with the relocalization of ORAI1 and STIM1 to the interface in T-cells has yet to be studied in detail.

Another mechanism by which VacA inhibits NFAT activation is by blocking the activity of the Ca<sup>2+</sup>-calmodulin-dependent phosphatase calcineurin in T-cells. Since activation of the regulatory protein calmodulin is a Ca<sup>2+</sup>-mediated event where the increased Ca<sup>2+</sup> binds to calmodulin to activate calcineurin, VacA may interfere with this mechanism by blocking Ca<sup>2+</sup> influx. Thus, VacA may act indirectly on this Ca<sup>2+</sup>-binding protein by inhibiting SOCE.

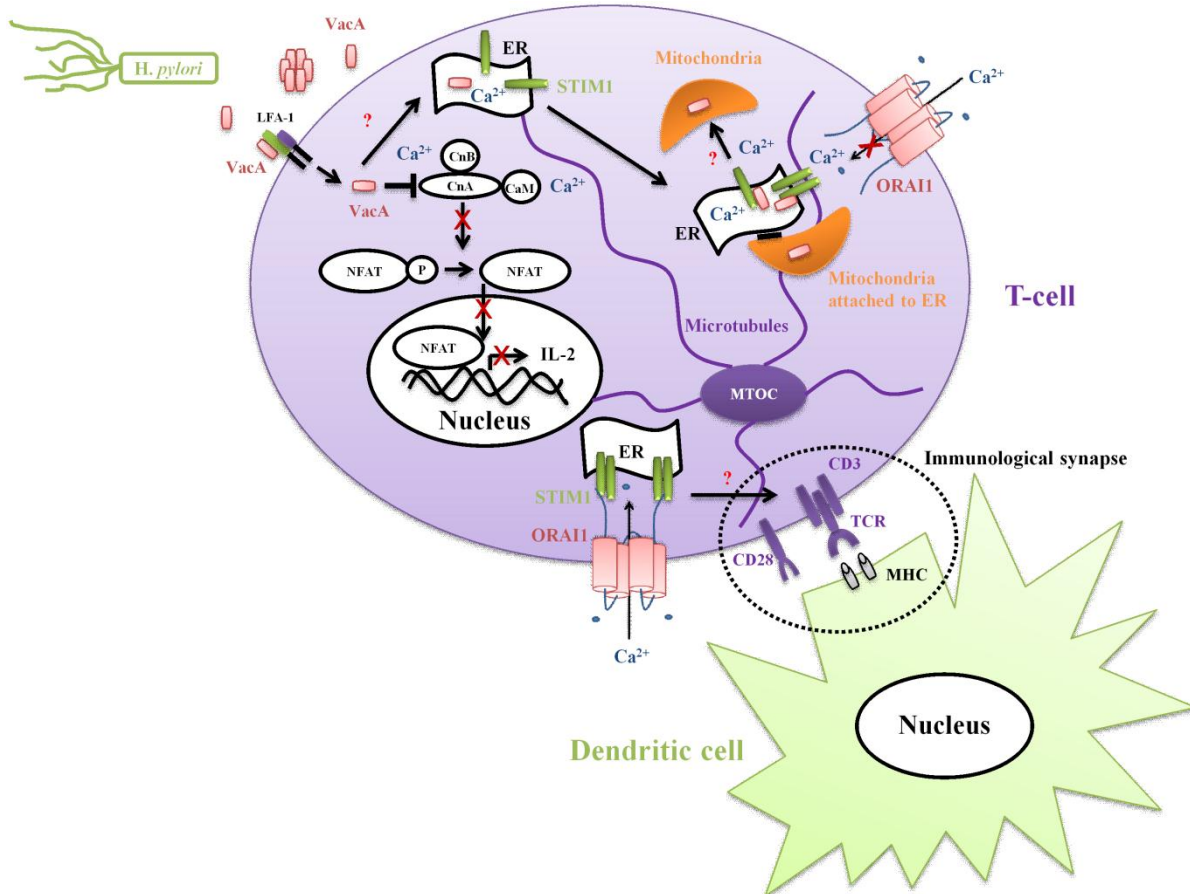


**Figure 4-3 Possible *H. pylori* VacA effects on calcium signalling in T-cells.**

*H. pylori* VacA binds to the cell surface integrin receptor LFA-1 in T-cells and is internalized. Inside T-cells, VacA is trafficked to the endoplasmic reticulum (ER) where it binds the EF-hand domain of STIM1, thereby inhibiting the  $\text{Ca}^{2+}$  sensing ability and formation of puncta with plasma membrane protein ORAI1. VacA consequently blocks store operated calcium entry (SOCE) and therefore the increase of cytosolic free  $\text{Ca}^{2+}$  in the cells. After localizing to STIM1 in the ER, VacA could be transferred to other cell organelles such as mitochondria during  $\text{Ca}^{2+}$  exchange between ER and mitochondria. After blocking the  $\text{Ca}^{2+}$  influx of SOCE, in result, VacA further blocks nuclear translocation of NFAT, resulting in downregulation of interleukin-2 (IL2) gene transcription and proliferation of T-cells. Since VacA localizes to STIM1 and inhibits conformational coupling with ORAI1, it causes inhibition of relocation of STIM1-ORAI1 towards the T-cell-dendritic cell interface, thereby inhibiting a localized calcium influx at the immunological synapse.

#### 4.8 Effects of VacA on localized calcium uptake in mitochondria

In addition to energy supply, mitochondria are important for other cellular functions including calcium signalling and buffering. In T-cells, mitochondria are preferentially localized in close vicinity of the immunological synapse (IS) (Quintana *et al.*, 2007). Since immunological synapse formation also induces accumulation of STIM1/ORAI1 and mitochondria are involved in the regulation of SOCE (Nunez *et al.*, 2006), such a large agglomeration of Ca<sup>2+</sup> binding proteins and organelles shows the importance of IS in T-cell activation. Besides, mitochondrial Ca<sup>2+</sup> uptake is stimulated after adding thapsigargin (Takekawa, Furuno, Hirashima, & Nakanishi, 2012), thereby releasing Ca<sup>2+</sup> from the ER and by STIM1 mediated SOCE.

With the results of VacA localization and interference with STIM1 in the ER, the possibility of VacA translocation to the mitochondria from the ER during calcium buffering needs to be examined. A previous study suggested that SOCE and STIM1 are involved in the regulation of shape and bioenergetics of mitochondria (Henke *et al.*, 2012). After store depletion, mitochondria appeared more susceptible to Ca<sup>2+</sup> uptake, smaller and more densely packed (Csordas *et al.*, 2006). These susceptible mitochondria buffer increased cytoplasmic Ca<sup>2+</sup> in the region close to the ER where they sense local Ca<sup>2+</sup> release. It is possible that after store depletion the aggregation of VacA-STIM1 is in close vicinity of the mitochondrial surface in contact with the ER (Figure 4-3). The effect of VacA on this localized calcium signalling after the activation of T-cells with APC in the presence of VacA and the formation of the immunological synapse need to be investigated in future experiments.

#### 4.9 Role of cytoplasmic free Ca<sup>2+</sup> in regulating the effects of bacterial toxins

Protein toxins provide bacteria an advantage to interact, colonize and cause infections to the host cells. During host-pathogen interaction, bacterial toxins alter multiple effects on various cell lines. One of the key strategies of bacterial toxins is to modulate calcium metabolism by either increase or decrease of cytosolic Ca<sup>2+</sup> concentrations in host cells. For instance, in this study of *H. pylori* VacA on calcium signalling, VacA inhibits an increase of cytosolic free Ca<sup>2+</sup> concentrations in T-cells. In other instances, bacterial toxins can also induce an increase in the cytosolic free Ca<sup>2+</sup> concentrations in host cells. The Rtx A1 toxin of *Vibrio vulnificus* causes cell death by Ca<sup>2+</sup>-dependent mitochondrial pathway in HeLa cells. Rtx A1-mediated cell death occurs by an increase in cytoplasmic Ca<sup>2+</sup> influx causing Ca<sup>2+</sup> sequestration in mitochondria (Kim *et al.*, 2013). Cholera toxin B subunit (Ctx B) of *Vibrio cholera* stimulates Ca<sup>2+</sup> influx by

interacting with GM1 ganglioside in N18 and NG 108-15 neuroblastoma cells causing neuritogenesis (Fang, Xie, Ledeen, & Wu, 2002). *Clostridium difficile* toxin B, a protein toxin associated with *Clostridium difficile* colitis infection causes sequential dissociation of actin microfilaments in NIH-3T3 fibroblasts. This response of *C. difficile* toxin B on actin cytoskeleton is triggered by an elevation of intracellular  $\text{Ca}^{2+}$  concentration. This rise in intracellular calcium is attributed to  $\text{Ca}^{2+}$  influx from the extracellular space (Gilbert, Pothoulakis, LaMont, & Yakubovich, 1995).

Thus to study the mode of action of bacterial toxins on calcium homeostasis is important. In the case of *H. pylori* VacA, a major interest of effects of VacA on calcium signalling is to show how VacA traffics into the ER to inhibit store operated calcium entry. Furthermore, it would be also interesting to understand in more detail the subsequent effects of VacA on SOCE in target cells. Understanding the diversity of *H. pylori* VacA effects on target hosts is a major challenge and continued studies on VacA will extend our knowledge of *H. pylori* pathogenesis.

---

## References

- Achtman, M., & Suerbaum, S. (2000). Sequence variation in *Helicobacter pylori*. *Trends Microbiol*, **8**, 57-58.
- Ackerman, M. J., & Clapham, D. E. (1997). Ion channels-basic science and clinical disease. *N Engl J Med*, **336**, 1575-1586.
- al-Moagel, M. A., Evans, D. G., Abdulghani, M. E., Adam, E., Evans, D. J., Jr., Malaty, H. M., & Graham, D. Y. (1990). Prevalence of *Helicobacter* (formerly *Campylobacter*) *pylori* infection in Saudia Arabia, and comparison of those with and without upper gastrointestinal symptoms. *Am J Gastroenterol*, **85**, 944-948.
- Alm, R. A., & Trust, T. J. (1999). Analysis of the genetic diversity of *Helicobacter pylori*: the tale of two genomes. *J Mol Med (Berl)*, **77**, 834-846.
- Amieva, M. R., & El-Omar, E. M. (2008). Host-bacterial interactions in *Helicobacter pylori* infection. *Gastroenterology*, **134**, 306-323.
- Amieva, M. R., Vogelmann, R., Covacci, A., Tompkins, L. S., Nelson, W. J., & Falkow, S. (2003). Disruption of the epithelial apical-junctional complex by *Helicobacter pylori* CagA. *Science*, **300**, 1430-1434.
- Appelmek, B. J., Martin, S. L., Monteiro, M. A., Clayton, C. A., McColm, A. A., Zheng, P., Kusters, J. G. (1999). Phase variation in *Helicobacter pylori* lipopolysaccharide due to changes in the lengths of poly(C) tracts in alpha3-fucosyltransferase genes. *Infect Immun*, **67**, 5361-5366.
- Appelmek, B. J., Martino, M. C., Veenhof, E., Monteiro, M. A., Maaskant, J. J., Negrini, R., Vandenbroucke-Grauls, C. M. (2000). Phase variation in H type I and Lewis a epitopes of *Helicobacter pylori* lipopolysaccharide. *Infect Immun*, **68**, 5928-5932.
- Atherton, J. C., Cao, P., Peek, R. M., Jr., Tummuru, M. K., Blaser, M. J., & Cover, T. L. (1995). Mosaicism in vacuolating cytotoxin alleles of *Helicobacter pylori*. Association of specific VacA types with cytotoxin production and peptic ulceration. *J Biol Chem*, **270**, 17771-17777.
- Backert, S., Moese, S., Selbach, M., Brinkmann, V., & Meyer, T. F. (2001). Phosphorylation of tyrosine 972 of the *Helicobacter pylori* CagA protein is essential for induction of a scattering phenotype in gastric epithelial cells. *Mol Microbiol*, **42**, 631-644.

- Backert, S., & Selbach, M. (2008). Role of type IV secretion in *Helicobacter pylori* pathogenesis. *Cell Microbiol*, **10**, 1573-1581.
- Berridge, M. J. (1995). Capacitative calcium entry. *Biochem J*, **312**, 1-11.
- Berridge, M. J., Bootman, M. D., & Roderick, H. L. (2003). Calcium signalling: dynamics, homeostasis and remodelling. *Nat Rev Mol Cell Biol*, **4**, 517-529.
- Bik, E. M., Eckburg, P. B., Gill, S. R., Nelson, K. E., Purdom, E. A., Francois, F., Relman, D. A. (2006). Molecular analysis of the bacterial microbiota in the human stomach. *Proc Natl Acad Sci U S A*, **103**, 732-737.
- Boncrisiano, M., Paccani, S. R., Barone, S., Ulivieri, C., Patrussi, L., Ilver, D., Baldari, C. T. (2003). The *Helicobacter pylori* vacuolating toxin inhibits T cell activation by two independent mechanisms. *J Exp Med*, **198**, 1887-1897.
- Bradford, M. M. (1976). A rapid and sensitive method for the quantitation of microgram quantities of protein utilizing the principle of protein-dye binding. *Anal Biochem*, **72**, 248-254.
- Brenner, H., Rothenbacher, D., Bode, G., Dieudonne, P., & Adler, G. (1999). Active infection with *Helicobacter pylori* in healthy couples. *Epidemiol Infect*, **122**, 91-95.
- Brown, L. M. (2000). *Helicobacter pylori*: epidemiology and routes of transmission. *Epidemiol Rev*, **22**, 283-297.
- Busler, V. J., V. J. Torres, M. S. McClain, O. Tirado, D. B. Friedman, and T. L. Cover. 2006. Protein-protein interactions among *Helicobacter pylori* Cag proteins. *J. Bacteriol*, **188**, 4787-4800.
- Chan, K. L., Zhou, H., Ng, D. K., & Tam, P. K. (2001). A prospective study of a one-week nonbismuth quadruple therapy for childhood *Helicobacter pylori* infection. *J Pediatr Surg*, **36**, 1008-1011.
- Chatila, T., Silverman, L., Miller, R., & Geha, R. (1989). Mechanisms of T cell activation by the calcium ionophore ionomycin. *J Immunol*, **143**, 1283-1289.
- Chung, C., Olivares, A., Torres, E., Yilmaz, O., Cohen, H., & Perez-Perez, G. (2010). Diversity of VacA intermediate region among *Helicobacter pylori* strains from several regions of the world. *J Clin Microbiol*, **48**, 690-696.
- Clapham, D. E. (2003). TRP channels as cellular sensors. *Nature*, **426**, 517-524.

- Cover, T. L., & Blaser, M. J. (1992). Purification and characterization of the vacuolating toxin from *Helicobacter pylori*. *J Biol Chem*, **267**, 10570-10575.
- Cover, T. L., Hanson, P. I., & Heuser, J. E. (1997). Acid-induced dissociation of VacA, the *Helicobacter pylori* vacuolating cytotoxin, reveals its pattern of assembly. *J Cell Biol*, **138**, 759-769.
- Cover, T. L., Tummuru, M. K., Cao, P., Thompson, S. A., & Blaser, M. J. (1994). Divergence of genetic sequences for the vacuolating cytotoxin among *Helicobacter pylori* strains. *J Biol Chem*, **269**, 10566-10573.
- Crew, K. D., & Neugut, A. I. (2006). Epidemiology of gastric cancer. *World J Gastroenterol*, **12**, 354-362.
- Csordas, G., Renken, C., Varnai, P., Walter, L., Weaver, D., Buttle, K. F., Hajnoczky, G. (2006). Structural and functional features and significance of the physical linkage between ER and mitochondria. *J Cell Biol*, **174**, 915-921.
- Czajkowsky, D. M., Iwamoto, H., Cover, T. L., & Shao, Z. (1999). The vacuolating toxin from *Helicobacter pylori* forms hexameric pores in lipid bilayers at low pH. *Proc Natl Acad Sci U S A*, **96**, 2001-2006.
- de Bernard, M., Cappon, A., Pancotto, L., Ruggiero, P., Rivera, J., Del Giudice, G., & Montecucco, C. (2005). The *Helicobacter pylori* VacA cytotoxin activates RBL-2H3 cells by inducing cytosolic calcium oscillations. *Cell Microbiol*, **7**, 191-198.
- de Bernard, M., Papini, E., de Filippis, V., Gottardi, E., Telford, J., Manetti, R., Montecucco, C. (1995). Low pH activates the vacuolating toxin of *Helicobacter pylori*, which becomes acid and pepsin resistant. *J Biol Chem*, **270**, 23937-23940.
- de Jonge, R., Pot, R. G., Loffeld, R. J., van Vliet, A. H., Kuipers, E. J., & Kusters, J. G. (2004). The functional status of the *Helicobacter pylori* sabB adhesin gene as a putative marker for disease outcome. *Helicobacter*, **9**, 158-164.
- Dossumbekova, A., Prinz, C., Mages, J., Lang, R., Kusters, J. G., Van Vliet, A. H., Rad, R. (2006). *Helicobacter pylori* HopH (OipA) and bacterial pathogenicity: genetic and functional genomic analysis of hopH gene polymorphisms. *J Infect Dis*, **194**, 1346-1355.
- Dunn, B. E., Cohen, H., & Blaser, M. J. (1997). *Helicobacter pylori*. *Clin Microbiol Rev*, **10**, 720-741.

- Falush, D., Kraft, C., Taylor, N. S., Correa, P., Fox, J. G., Achtman, M., & Suerbaum, S. (2001). Recombination and mutation during long-term gastric colonization by *Helicobacter pylori*: estimates of clock rates, recombination size, and minimal age. *Proc Natl Acad Sci U S A*, **98**, 15056-15061.
- Fang, Y., Xie, X., Ledeen, R. W., & Wu, G. (2002). Characterization of cholera toxin B subunit-induced Ca(2+) influx in neuroblastoma cells: evidence for a voltage-independent GM1 ganglioside-associated Ca(2+) channel. *J Neurosci Res*, **69**, 669-680.
- Feldman, R. A., Eccersley, A. J., & Hardie, J. M. (1998). Epidemiology of *Helicobacter pylori*: acquisition, transmission, population prevalence and disease-to-infection ratio. *Br Med Bull*, **54**, 39-53.
- Ferguson, D. A., Jr., Li, C., Patel, N. R., Mayberry, W. R., Chi, D. S., & Thomas, E. (1993). Isolation of *Helicobacter pylori* from saliva. *J Clin Microbiol*, **31**, 2802-2804.
- Feske, S., Gwack, Y., Prakriya, M., Srikanth, S., Puppel, S. H., Tanasa, B., Rao, A. (2006). A mutation in Orai1 causes immune deficiency by abrogating CRAC channel function. *Nature*, **441**, 179-185.
- Fox, J. G. (2002). The non-*H pylori* helicobacters: their expanding role in gastrointestinal and systemic diseases. *Gut*, **50**, 273-283.
- Fujikawa, A., Shirasaka, D., Yamamoto, S., Ota, H., Yahiro, K., Fukada, M., Noda, M. (2003). Mice deficient in protein tyrosine phosphatase receptor type Z are resistant to gastric ulcer induction by VacA of *Helicobacter pylori*. *Nat Genet*, **33**, 375-381.
- Galmiche, A., Rassow, J., Doye, A., Cagnol, S., Chambard, J. C., Contamin, S., Boquet, P. (2000). The N-terminal 34 kDa fragment of *Helicobacter pylori* vacuolating cytotoxin targets mitochondria and induces cytochrome c release. *EMBO J*, **19**, 6361-6370.
- Gangwer, K. A., Mushrush, D. J., Stauff, D. L., Spiller, B., McClain, M. S., Cover, T. L., & Lacy, D. B. (2007). Crystal structure of the *Helicobacter pylori* vacuolating toxin p55 domain. *Proc Natl Acad Sci U S A*, **104**, 16293-16298.
- Gauthier, N. C., Monzo, P., Kaddai, V., Doye, A., Ricci, V., & Boquet, P. (2005). *Helicobacter pylori* VacA cytotoxin: a probe for a clathrin-independent and Cdc42-dependent pinocytic pathway routed to late endosomes. *Mol Biol Cell*, **16**, 4852-4866.

- Gebert, B., Fischer, W., Weiss, E., Hoffmann, R., & Haas, R. (2003). *Helicobacter pylori* vacuolating cytotoxin inhibits T lymphocyte activation. *Science*, **301**, 1099-1102.
- Gerhard, M., Lehn, N., Neumayer, N., Boren, T., Rad, R., Schepp, W., Prinz, C. (1999). Clinical relevance of the *Helicobacter pylori* gene for blood-group antigen-binding adhesin. *Proc Natl Acad Sci U S A*, **96**, 12778-12783.
- Gilbert, R. J., Pothoulakis, C., LaMont, J. T., & Yakubovich, M. (1995). *Clostridium difficile* toxin B activates calcium influx required for actin disassembly during cytotoxicity. *Am J Physiol*, **268**, G487-495.
- Go, M. F. (2002). Review article: natural history and epidemiology of *Helicobacter pylori* infection. *Aliment Pharmacol Ther*, **16 Suppl 1**, 3-15.
- Graham, D. Y., Malaty, H. M., Evans, D. G., Evans, D. J., Jr., Klein, P. D., & Adam, E. (1991). Epidemiology of *Helicobacter pylori* in an asymptomatic population in the United States. Effect of age, race, and socioeconomic status. *Gastroenterology*, **100**, 1495-1501.
- Gupta, V. R., Patel, H. K., Kostolansky, S. S., Ballivian, R. A., Eichberg, J., & Blanke, S. R. (2008). Sphingomyelin functions as a novel receptor for *Helicobacter pylori* VacA. *PLoS Pathog*, **4**, e1000073.
- Hakii, H., Fujiki, H., Suganuma, M., Nakayasu, M., Tahira, T., Sugimura, T., Christensen, S. B. (1986). Thapsigargin, a histamine secretagogue, is a non-12-O-tetradecanoylphorbol-13-acetate (TPA) type tumor promoter in two-stage mouse skin carcinogenesis. *J Cancer Res Clin Oncol*, **111**, 177-181.
- Hanahan, D. (1983). Studies on transformation of *Escherichia coli* with plasmids. *J Mol Biol*, **166**, 557-580.
- Henke, N., Albrecht, P., Pfeiffer, A., Toutzaris, D., Zanger, K., & Methner, A. (2012). Stromal interaction molecule 1 (STIM1) is involved in the regulation of mitochondrial shape and bioenergetics and plays a role in oxidative stress. *J Biol Chem*, **287**, 42042-42052.
- Hennig, E. E., Godlewski, M. M., Butruk, E., & Ostrowski, J. (2005). *Helicobacter pylori* VacA cytotoxin interacts with fibronectin and alters HeLa cell adhesion and cytoskeletal organization *in vitro*. *FEMS Immunol Med Microbiol*, **44**, 143-150.

- Hewavitharana, T., Deng, X., Wang, Y., Ritchie, M. F., Girish, G. V., Soboloff, J., & Gill, D. L. (2008). Location and function of STIM1 in the activation of Ca<sup>2+</sup> entry signals. *J Biol Chem*, **283**, 26252-26262.
- Higashi, H., Tsutsumi, R., Muto, S., Sugiyama, T., Azuma, T., Asaka, M., & Hatakeyama, M. (2002). SHP-2 tyrosine phosphatase as an intracellular target of *Helicobacter pylori* CagA protein. *Science*, **295**, 683-686.
- Hopkins, R. J., Vial, P. A., Ferreccio, C., Ovalle, J., Prado, P., Sotomayor, V., Morris, J. G., Jr. (1993). Seroprevalence of *Helicobacter pylori* in Chile: vegetables may serve as one route of transmission. *J Infect Dis*, **168**, 222-226.
- Hyams, K. C., Taylor, D. N., Gray, G. C., Knowles, J. B., Hawkins, R., & Malone, J. D. (1995). The risk of *Helicobacter pylori* infection among U.S. military personnel deployed outside the United States. *Am J Trop Med Hyg*, **52**, 109-112.
- Ito, Y., Azuma, T., Ito, S., Suto, H., Miyaji, H., Yamazaki, Y., Kuriyama, M. (1998). Full-length sequence analysis of the VacA gene from cytotoxic and noncytotoxic *Helicobacter pylori*. *J Infect Dis*, **178**, 1391-1398.
- Ji, X., Fernandez, T., Burroni, D., Pagliaccia, C., Atherton, J. C., Reyrat, J. M., Telford, J. L. (2000). Cell specificity of *Helicobacter pylori* cytotoxin is determined by a short region in the polymorphic midregion. *Infect Immun*, **68**, 3754-3757.
- Jimenez-Soto, L. F., Kutter, S., Sewald, X., Ertl, C., Weiss, E., Kapp, U., Haas, R. (2009). *Helicobacter pylori* type IV secretion apparatus exploits beta1 integrin in a novel RGD-independent manner. *PLoS Pathog*, **5**, e1000684.
- Jimenez-Soto, L. F., Rohrer, S., Jain, U., Ertl, C., Sewald, X., & Haas, R. (2012). Effects of cholesterol on *Helicobacter pylori* growth and virulence properties *in vitro*. *Helicobacter*, **17**, 133-139.
- Kim, Y. R., Lee, S. E., Kang, I. C., Nam, K. I., Choy, H. E., & Rhee, J. H. (2013). A bacterial RTX toxin causes programmed necrotic cell death through calcium-mediated mitochondrial dysfunction. *J Infect Dis*, **207**, 1406-1415.
- Kimura, M., Goto, S., Wada, A., Yahiro, K., Niidome, T., Hatakeyama, T., Kondo, T. (1999). Vacuolating cytotoxin purified from *Helicobacter pylori* causes mitochondrial damage in human gastric cells. *Microb Pathog*, **26**, 45-52.

- Konturek, J. W., Gillessen, A., Konturek, S. J., & Domschke, W. (1995). Eradication of *Helicobacter pylori* restores the inhibitory effect of cholecystokinin on postprandial gastrin release in duodenal ulcer patients. *Gut*, **37**, 482-487.
- Konturek, J. W., Stoll, R., Menzel, J., Konturek, M., Konturek, S. J., & Domschke, W. (2001). Eradication of *Helicobacter pylori* restores the inhibitory effect of cholecystokinin on gastric motility in duodenal ulcer patients. *Scand J Gastroenterol*, **36**, 241-246.
- Kuipers, E. J., Israel, D. A., Kusters, J. G., Gerrits, M. M., Weel, J., van Der Ende, A., Blaser, M. J. (2000). Quasispecies development of *Helicobacter pylori* observed in paired isolates obtained years apart from the same host. *J Infect Dis*, **181**, 273-282.
- Kusters, J. G., Gerrits, M. M., Van Strijp, J. A., & Vandenbroucke-Grauls, C. M. (1997). Coccoid forms of *Helicobacter pylori* are the morphologic manifestation of cell death. *Infect Immun*, **65**, 3672-3679.
- Kwok, T., Zabler, D., Urman, S., Rohde, M., Hartig, R., Wessler, S., Backert, S. (2007). *Helicobacter* exploits integrin for type IV secretion and kinase activation. *Nature*, **449**, 862-866.
- Lang, S., Erdmann, F., Jung, M., Wagner, R., Cavalie, A., & Zimmermann, R. (2011). Sec61 complexes form ubiquitous ER Ca<sup>2+</sup> leak channels. *Channels (Austin)*, **5**, 228-235.
- Lee, S. K., Stack, A., Katzowitsch, E., Aizawa, S. I., Suerbaum, S., & Josenhans, C. (2003). *Helicobacter pylori* flagellins have very low intrinsic activity to stimulate human gastric epithelial cells via TLR5. *Microbes Infect*, **5**, 1345-1356.
- Leunk, R. D., Johnson, P. T., David, B. C., Kraft, W. G., & Morgan, D. R. (1988). Cytotoxic activity in broth-culture filtrates of *Campylobacter pylori*. *J Med Microbiol*, **26**, 93-99.
- Lewis, R. S. (2001). Calcium signaling mechanisms in T lymphocytes. *Annu Rev Immunol*, **19**, 497-521.
- Liou, J., Kim, M. L., Heo, W. D., Jones, J. T., Myers, J. W., Ferrell, J. E., Jr., & Meyer, T. (2005). STIM is a Ca<sup>2+</sup> sensor essential for Ca<sup>2+</sup>-store-depletion-triggered Ca<sup>2+</sup> influx. *Curr Biol*, **15**, 1235-1241.
- Lioudyno, M. I., Kozak, J. A., Penna, A., Safrina, O., Zhang, S. L., Sen, D., Cahalan, M. D. (2008). Orai1 and STIM1 move to the immunological synapse and are up-regulated during T cell activation. *Proc Natl Acad Sci U S A*, **105**, 2011-2016.

- Liu, C., & Hermann, T. E. (1978). Characterization of ionomycin as a calcium ionophore. *J Biol Chem*, **253**, 5892-5894.
- Lobo, F. M., Zanjani, R., Ho, N., Chatila, T. A., & Fuleihan, R. L. (1999). Calcium-dependent activation of TNF family gene expression by Ca<sup>2+</sup>/calmodulin kinase type IV/Gr and calcineurin. *J Immunol*, **162**, 2057-2063.
- Louw, J. A., Kidd, M. S., Kummer, A. F., Taylor, K., Kotze, U., & Hanslo, D. (2001). The relationship between *Helicobacter pylori* infection, the virulence genotypes of the infecting strain and gastric cancer in the African setting. *Helicobacter*, **6**, 268-273.
- Lu, H., Wu, J. Y., Beswick, E. J., Ohno, T., Odenbreit, S., Haas, R., Yamaoka, Y. (2007). Functional and intracellular signaling differences associated with the *Helicobacter pylori* AlpAB adhesin from Western and East Asian strains. *J Biol Chem*, **282**, 6242-6254.
- Lupetti, P., Heuser, J. E., Manetti, R., Massari, P., Lanzavecchia, S., Bellon, P. L., Telford, J. L. (1996). Oligomeric and subunit structure of the *Helicobacter pylori* vacuolating cytotoxin. *J Cell Biol*, **133**, 801-807.
- Lytton, J., Westlin, M., & Hanley, M. R. (1991). Thapsigargin inhibits the sarcoplasmic or endoplasmic reticulum Ca-ATPase family of calcium pumps. *J Biol Chem*, **266**, 17067-17071.
- Mahdavi, J., Sonden, B., Hurtig, M., Olfat, F. O., Forsberg, L., Roche, N., Boren, T. (2002). *Helicobacter pylori* SabA adhesin in persistent infection and chronic inflammation. *Science*, **297**, 573-578.
- Malaty, H. M. (2007). Epidemiology of *Helicobacter pylori* infection. *Best Pract Res Clin Gastroenterol*, **21**, 205-214.
- Malaty, H. M., Evans, D. G., Evans, D. J., Jr., & Graham, D. Y. (1992). *Helicobacter pylori* in Hispanics: comparison with blacks and whites of similar age and socioeconomic class. *Gastroenterology*, **103**, 813-816.
- Manji, S. S., Parker, N. J., Williams, R. T., van Stekelenburg, L., Pearson, R. B., Dziadek, M., & Smith, P. J. (2000). STIM1: a novel phosphoprotein located at the cell surface. *Biochim Biophys Acta*, **1481**, 147-155.
- McClain, M. S., Cao, P., Iwamoto, H., Vinion-Dubiel, A. D., Szabo, G., Shao, Z., & Cover, T. L. (2001). A 12-amino-acid segment, present in type s2 but not type s1 *Helicobacter pylori* VacA

- proteins, abolishes cytotoxin activity and alters membrane channel formation. *J Bacteriol*, **183**, 6499-6508.
- McClain, M. S., Iwamoto, H., Cao, P., Vinion-Dubiel, A. D., Li, Y., Szabo, G., Cover, T. L. (2003). Essential role of a GXXXG motif for membrane channel formation by *Helicobacter pylori* vacuolating toxin. *J Biol Chem*, **278**, 12101-12108.
- Mendz, G. L., Shepley, A. J., Hazell, S. L., & Smith, M. A. (1997). Purine metabolism and the microaerophily of *Helicobacter pylori*. *Arch Microbiol*, **168**, 448-456.
- Mimuro, H., Suzuki, T., Nagai, S., Rieder, G., Suzuki, M., Nagai, T., Sasakawa, C. (2007). *Helicobacter pylori* dampens gut epithelial self-renewal by inhibiting apoptosis, a bacterial strategy to enhance colonization of the stomach. *Cell Host Microbe*, **2**, 250-263.
- Mitchell, H. M., Li, Y. Y., Hu, P. J., Liu, Q., Chen, M., Du, G. G., Hazell, S. L. (1992). Epidemiology of *Helicobacter pylori* in southern China: identification of early childhood as the critical period for acquisition. *J Infect Dis*, **166**, 149-153.
- Moll, G., Papini, E., Colonna, R., Burrioni, D., Telford, J., Rappuoli, R., & Montecucco, C. (1995). Lipid interaction of the 37-kDa and 58-kDa fragments of the *Helicobacter pylori* cytotoxin. *Eur J Biochem*, **234**, 947-952.
- Morgan, A. J., & Jacob, R. (1994). Ionomycin enhances  $\text{Ca}^{2+}$  influx by stimulating store-regulated cation entry and not by a direct action at the plasma membrane. *Biochem J*, **300 ( Pt 3)**, 665-672.
- Muallem, S., Khademazad, M., & Sachs, G. (1990). The route of  $\text{Ca}^{2+}$  entry during reloading of the intracellular  $\text{Ca}^{2+}$  pool in pancreatic acini. *J Biol Chem*, **265**, 2011-2016.
- Mullis, K., Faloona, F., Scharf, S., Saiki, R., Horn, G., & Erlich, H. (1986). Specific enzymatic amplification of DNA *in vitro*: the polymerase chain reaction. *Cold Spring Harb Symp Quant Biol*, **51 Pt 1**, 263-273.
- Murata-Kamiya, N., Kurashima, Y., Teishikata, Y., Yamahashi, Y., Saito, Y., Higashi, H., Hatakeyama, M. (2007). *Helicobacter pylori* CagA interacts with E-cadherin and deregulates the beta-catenin signal that promotes intestinal transdifferentiation in gastric epithelial cells. *Oncogene*, **26**, 4617-4626.

- Nunez, L., Valero, R. A., Senovilla, L., Sanz-Blasco, S., Garcia-Sancho, J., & Villalobos, C. (2006). Cell proliferation depends on mitochondrial  $\text{Ca}^{2+}$  uptake: inhibition by salicylate. *J Physiol*, **571**, 57-73.
- O'Toole, P. W., Lane, M. C., & Porwollik, S. (2000). *Helicobacter pylori* motility. *Microbes Infect*, **2**, 1207-1214.
- Odenbreit, S., Puls, J., Sedlmaier, B., Gerland, E., Fischer, W., & Haas, R. (2000). Translocation of *Helicobacter pylori* CagA into gastric epithelial cells by type IV secretion. *Science*, **287**, 1497-1500.
- Papini, E., de Bernard, M., Milia, E., Bugnoli, M., Zerial, M., Rappuoli, R., & Montecucco, C. (1994). Cellular vacuoles induced by *Helicobacter pylori* originate from late endosomal compartments. *Proc Natl Acad Sci U S A*, **91**, 9720-9724.
- Park, C. Y., Hoover, P. J., Mullins, F. M., Bachhawat, P., Covington, E. D., Raunser, S., Lewis, R. S. (2009). STIM1 clusters and activates CRAC channels via direct binding of a cytosolic domain to Orai1. *Cell*, **136**, 876-890.
- Patterson, R. L., van Rossum, D. B., & Gill, D. L. (1999). Store-operated  $\text{Ca}^{2+}$  entry: evidence for a secretion-like coupling model. *Cell*, **98**, 487-499.
- Peek, R. M., Jr., & Blaser, M. J. (2002). *Helicobacter pylori* and gastrointestinal tract adenocarcinomas. *Nat Rev Cancer*, **2**, 28-37.
- Phadnis, S. H., Ilver, D., Janson, L., Normark, S., & Westblom, T. U. (1994). Pathological significance and molecular characterization of the vacuolating toxin gene of *Helicobacter pylori*. *Infect Immun*, **62**, 1557-1565.
- Pounder, R. E., & Ng, D. (1995). The prevalence of *Helicobacter pylori* infection in different countries. *Aliment Pharmacol Ther*, **9 Suppl 2**, 33-39.
- Putney, J. W., Jr. (1990). Capacitative calcium entry revisited. *Cell Calcium*, **11**, 611-624.
- Quintana, A., Schwindling, C., Wenning, A. S., Becherer, U., Rettig, J., Schwarz, E. C., & Hoth, M. (2007). T cell activation requires mitochondrial translocation to the immunological synapse. *Proc Natl Acad Sci U S A*, **104**, 14418-14423.
- Raju, D., Hussey, S., Ang, M., Terebiznik, M. R., Sibony, M., Galindo-Mata, E., Jones, N. L. (2012). Vacuolating cytotoxin and variants in Atg16L1 that disrupt autophagy promote *Helicobacter pylori* infection in humans. *Gastroenterology*, **142**, 1160-1171.

- Replogle, M. L., Glaser, S. L., Hiatt, R. A., & Parsonnet, J. (1995). Biologic sex as a risk factor for *Helicobacter pylori* infection in healthy young adults. *Am J Epidemiol*, **142**, 856-863.
- Ricci, V., Galmiche, A., Doye, A., Necchi, V., Solcia, E., & Boquet, P. (2000). High cell sensitivity to *Helicobacter pylori* VacA toxin depends on a GPI-anchored protein and is not blocked by inhibition of the clathrin-mediated pathway of endocytosis. *Mol Biol Cell*, **11**, 3897-3909.
- Ricci, V., Sommi, P., Fiocca, R., Romano, M., Solcia, E., & Ventura, U. (1997). *Helicobacter pylori* vacuolating toxin accumulates within the endosomal-vacuolar compartment of cultured gastric cells and potentiates the vacuolating activity of ammonia. *J Pathol*, **183**, 453-459.
- Rogers, T. B., Inesi, G., Wade, R., & Lederer, W. J. (1995). Use of thapsigargin to study Ca<sup>2+</sup> homeostasis in cardiac cells. *Biosci Rep*, **15**, 341-349.
- Roos, J., DiGregorio, P. J., Yeromin, A. V., Ohlsen, K., Liudyno, M., Zhang, S., Stauderman, K. A. (2005). STIM1, an essential and conserved component of store-operated Ca<sup>2+</sup> channel function. *J Cell Biol*, **169**, 435-445.
- Sabbioni, S., Barbanti-Brodano, G., Croce, C. M., & Negrini, M. (1997). GOK: a gene at 11p15 involved in rhabdomyosarcoma and rhabdoid tumor development. *Cancer Res*, **57**, 4493-4497.
- Schmitt, W., & Haas, R. (1994). Genetic analysis of the *Helicobacter pylori* vacuolating cytotoxin: structural similarities with the IgA protease type of exported protein. *Mol Microbiol*, **12**, 307-319.
- Schwartz, J. T., & Allen, L. A. (2006). Role of urease in megasome formation and *Helicobacter pylori* survival in macrophages. *J Leukoc Biol*, **79**, 1214-1225.
- Selbach, M., Moese, S., Hauck, C. R., Meyer, T. F., & Backert, S. (2002). Src is the kinase of the *Helicobacter pylori* CagA protein *in vitro* and *in vivo*. *J Biol Chem*, **277**, 6775-6778.
- Seto, K., Hayashi-Kuwabara, Y., Yoneta, T., Suda, H., & Tamaki, H. (1998). Vacuolation induced by cytotoxin from *Helicobacter pylori* is mediated by the EGF receptor in HeLa cells. *FEBS Lett*, **431**, 347-350.
- Sewald, X., Gebert-Vogl, B., Prassl, S., Barwig, I., Weiss, E., Fabbri, M., Haas, R. (2008). Integrin subunit CD18 Is the T-lymphocyte receptor for the *Helicobacter pylori* vacuolating cytotoxin. *Cell Host Microbe*, **3**, 20-29.

- Smith-Garvin, J. E., Koretzky, G. A., & Jordan, M. S. (2009). T cell activation. *Annu Rev Immunol*, **27**, 591-619.
- Smith, M. F., Jr., Mitchell, A., Li, G., Ding, S., Fitzmaurice, A. M., Ryan, K., Goldberg, J. B. (2003). Toll-like receptor (TLR) 2 and TLR5, but not TLR4, are required for *Helicobacter pylori*-induced NF-kappa B activation and chemokine expression by epithelial cells. *J Biol Chem*, **278**, 32552-32560.
- Smoak, B. L., Kelley, P. W., & Taylor, D. N. (1994). Seroprevalence of *Helicobacter pylori* infections in a cohort of US Army recruits. *Am J Epidemiol*, **139**, 513-519.
- Solnick, J. V., Hansen, L. M., Salama, N. R., Boonjakuakul, J. K., & Syvanen, M. (2004). Modification of *Helicobacter pylori* outer membrane protein expression during experimental infection of rhesus macaques. *Proc Natl Acad Sci U S A*, **101**, 2106-2111.
- Spassova, M. A., Soboloff, J., He, L. P., Hewavitharana, T., Xu, W., Venkatachalam, K., Gill, D. L. (2004). Calcium entry mediated by SOCs and TRP channels: variations and enigma. *Biochim Biophys Acta*, **1742**, 9-20.
- Stathopoulos, P. B., Li, G. Y., Plevin, M. J., Ames, J. B., & Ikura, M. (2006). Stored Ca<sup>2+</sup> depletion-induced oligomerization of stromal interaction molecule 1 (STIM1) via the EF-SAM region: An initiation mechanism for capacitive Ca<sup>2+</sup> entry. *J Biol Chem*, **281**, 35855-35862.
- Stathopoulos, P. B., Zheng, L., Li, G. Y., Plevin, M. J., & Ikura, M. (2008). Structural and mechanistic insights into STIM1-mediated initiation of store-operated calcium entry. *Cell*, **135**, 110-122.
- Stein, M., Bagnoli, F., Halenbeck, R., Rappuoli, R., Fantl, W. J., & Covacci, A. (2002). c-Src/Lyn kinases activate *Helicobacter pylori* CagA through tyrosine phosphorylation of the EPIYA motifs. *Mol Microbiol*, **43**, 971-980.
- Sundrud, M. S., Torres, V. J., Unutmaz, D., & Cover, T. L. (2004). Inhibition of primary human T cell proliferation by *Helicobacter pylori* vacuolating toxin (VacA) is independent of VacA effects on IL-2 secretion. *Proc Natl Acad Sci U S A*, **101**, 7727-7732.
- Takekawa, M., Furuno, T., Hirashima, N., & Nakanishi, M. (2012). Mitochondria take up Ca<sup>2+</sup> in two steps dependently on store-operated Ca<sup>2+</sup> entry in mast cells. *Biol Pharm Bull*, **35**, 1354-1360.

- Takemura, H., Hughes, A. R., Thastrup, O., & Putney, J. W., Jr. (1989). Activation of calcium entry by the tumor promoter thapsigargin in parotid acinar cells. Evidence that an intracellular calcium pool and not an inositol phosphate regulates calcium fluxes at the plasma membrane. *J Biol Chem*, **264**, 12266-12271.
- Takemura, H., & Putney, J. W., Jr. (1989). Capacitative calcium entry in parotid acinar cells. *Biochem J*, **258**, 409-412.
- Taylor, D. N., & Blaser, M. J. (1991). The epidemiology of *Helicobacter pylori* infection. *Epidemiol Rev*, **13**, 42-59.
- Tombola, F., Carlesso, C., Szabo, I., de Bernard, M., Reyrat, J. M., Telford, J. L., Zoratti, M. (1999). *Helicobacter pylori* vacuolating toxin forms anion-selective channels in planar lipid bilayers: possible implications for the mechanism of cellular vacuolation. *Biophys J*, **76**, 1401-1409.
- Uematsu, D., Greenberg, J. H., Reivich, M., Kobayashi, S., & Karp, A. (1988). *In vivo* fluorometric measurement of changes in cytosolic free calcium from the cat cortex during anoxia. *J Cereb Blood Flow Metab*, **8**, 367-374.
- Uetz, P., Dong, Y. A., Zeretzke, C., Atzler, C., Baiker, A., Berger, B., Haas, J. (2006). Herpesviral protein networks and their interaction with the human proteome. *Science*, **311**, 239-242.
- Utt, M., Danielsson, B., & Wadstrom, T. (2001). *Helicobacter pylori* vacuolating cytotoxin binding to a putative cell surface receptor, heparan sulfate, studied by surface plasmon resonance. *FEMS Immunol Med Microbiol*, **30**, 109-113.
- Vig, M., Peinelt, C., Beck, A., Koomoa, D. L., Rabah, D., Koblan-Huberson, M., Kinet, J. P. (2006). CRACM1 is a plasma membrane protein essential for store-operated Ca<sup>2+</sup> entry. *Science*, **312**, 1220-1223.
- Vinion-Dubiel, A. D., McClain, M. S., Czajkowsky, D. M., Iwamoto, H., Ye, D., Cao, P., Cover, T. L. (1999). A dominant negative mutant of *Helicobacter pylori* vacuolating toxin (VacA) inhibits VacA-induced cell vacuolation. *J Biol Chem*, **274**, 37736-37742.
- Weiss, A., Imboden, J., Shoback, D., & Stobo, J. (1984). Role of T3 surface molecules in human T-cell activation: T3-dependent activation results in an increase in cytoplasmic free calcium. *Proc Natl Acad Sci U S A*, **81**, 4169-4173.

- Wu, M. M., Buchanan, J., Luik, R. M., & Lewis, R. S. (2006).  $\text{Ca}^{2+}$  store depletion causes STIM1 to accumulate in ER regions closely associated with the plasma membrane. *J Cell Biol*, **174**, 803-813.
- Wunder, C., Churin, Y., Winau, F., Warnecke, D., Vieth, M., Lindner, B., Meyer, T. F. (2006). Cholesterol glucosylation promotes immune evasion by *Helicobacter pylori*. *Nat Med*, **12**, 1030-1038.
- Yahiro, K., Wada, A., Nakayama, M., Kimura, T., Ogushi, K., Niidome, T., Hirayama, T. (2003). Protein-tyrosine phosphatase alpha, RPTP alpha, is a *Helicobacter pylori* VacA receptor. *J Biol Chem*, **278**, 19183-19189.
- Yamaoka, Y., Kikuchi, S., el-Zimaity, H. M., Gutierrez, O., Osato, M. S., & Graham, D. Y. (2002). Importance of *Helicobacter pylori* oipA in clinical presentation, gastric inflammation, and mucosal interleukin 8 production. *Gastroenterology*, **123**, 414-424.
- Yokosuka, T., & Saito, T. (2010). The immunological synapse, TCR microclusters, and T cell activation. *Curr Top Microbiol Immunol*, **340**, 81-107.
- Yokota, S., Ohnishi, T., Muroi, M., Tanamoto, K., Fujii, N., & Amano, K. (2007). Highly-purified *Helicobacter pylori* LPS preparations induce weak inflammatory reactions and utilize Toll-like receptor 2 complex but not Toll-like receptor 4 complex. *FEMS Immunol Med Microbiol*, **51**, 140-148.
- Zhang, S. L., Yeromin, A. V., Zhang, X. H., Yu, Y., Safrina, O., Penna, A., Cahalan, M. D. (2006). Genome-wide RNAi screen of  $\text{Ca}^{2+}$  influx identifies genes that regulate  $\text{Ca}^{2+}$  release-activated  $\text{Ca}^{2+}$  channel activity. *Proc Natl Acad Sci U S A*, **103**, 9357-9362.
- Zheng, P. Y., & Jones, N. L. (2003). *Helicobacter pylori* strains expressing the vacuolating cytotoxin interrupt phagosome maturation in macrophages by recruiting and retaining TACO (coronin 1) protein. *Cell Microbiol*, **5**, 25-40.

---

## Abbreviations

%	A percentage
(v/v)	Volume-to-Volume concentration
(w/v)	Mass to volume concentration
°C	Degree celsius
μl	Microlitre
μM	Micromolar
aa	Amino acid
AM	Acetoxymethyl
APC	Antigen presenting cell
BAPTA	1, 2-bis(o-aminophenoxy)ethane-N,N,N',N'-tetraacetic acid
BCIP	5-Bromo-4-chloro-3-indolylphosphate
BSA	Bovine serum albumin
CAD	CRAC activation domain
CagA	Cytotoxin-associated gene A
CLSM	Confocal laser scanning microscopy
cm	Centimetre
CRAC	Calcium release-activated calcium channel
DMEM	Dulbecco's modified eagle medium
DMSO	Dimethylsulfoxide
dNTP	Deoxyribonucleotide triphosphate
EDTA	Ethylenediaminetetraacetic acid
EGTA	Ethylene glycol tetraacetic acid
ER	Endoplasmic reticulum
FBS	Fetal bovine serum

---

FCS	Fetal Calf Serum
GFP	Green fluorescent protein
HCl	Hydrochloric acid
HEPES	4-(2-hydroxyethyl)-1- piperazineethanesulfonic acid
His	Histidine
IS	Immunological synapse
Leu	Leucine
LGICs	Ligand gated ion channels
LPS	Lipopolysaccharide
MACS	Magnetic cell sorting
mg/ml	Milligram per millilitre
ml	Millilitre
NaOH	Sodium hydroxide
NFAT	Nuclear factor of activated T-cells
nm	Nanometer
NRU	Neutral red uptake
OD	Optical density
OMPs	Outer membrane proteins
PAGE	Polyacrylamide gel electrophoresis
PBLC	Peripheral blood lymphocytes
PBS	Phosphate buffered saline
PCR	Polymerase chain reaction
PEG	Polyethylene glycol
PLC- $\gamma$	Phospholipase c-gamma
PM	Plasma membrane
PMA	Phorbol myristate acetate

---

PMSF	Phenylmethylsulfonyl fluoride
PVDF	Polyvinylidene fluoride
ROI	Reactive oxygen intermediates
rpm	Revolutions per min
RPMI	Roswell park memorial institute
s	seconds
SDS	Sodium dodecyl sulphate
SERCA	Sarcoplasmic/endoplasmic reticulum calcium ATPase
SOCE	Store-operated calcium entry
STIM1	Stromal interaction molecule 1
TCR	T-cell receptor
Tg	Thapsigargin
TLRs	Toll-like receptors
TM	Transmembrane
TMD	Transmembrane domain
Trp	Tryptophan
TRPC	Transient receptor potential channel
VacA M	Vacuolating cytotoxin A produced by mutant strain
VacA WT	Vacuolating cytotoxin A produced by wild type strain
VDCC	Voltage-dependent calcium channels
YTH	Yeast two-hybrid

## Acknowledgements

I am highly grateful to give my expression by my heart to my supervisor Prof. Dr. Rainer Haas for taking interest in my research, giving constant encouragement and valuable suggestions that helped me to go ahead for my steps towards my doctoral thesis. I feel very much obliged for his kind support during my tenure in the lab. I am extremely thankful for his belief towards me and consider me as his Ph.D student.

I specially would like to thank my co-supervisor Dr. Jimenez Soto Luisa Fernanda for her continuous support and encouragement to shape my project in right direction. Her valuable advices during my difficult times for my experiments helped me a lot. More than co-supervisor, she has been one of my best friends and will remain.

I would like to give my very special thanks to Bea for her tremendous efforts for reviewing my thesis time to time. I could not imagine writing my thesis without her support. She motivated me a lot for my time during lab work as a best colleague and a true friend. I am lucky to have such a lab mate.

Benjamin, I could not imagine my microscopy stuff to be finished without your help. I am thankful for it. More importantly, you had been a moral support to deal with bunch of girls in the lab.

Evelyn, I have no words to say for you, because words are very small to describe your personality. Your genuine helping nature in our lab as well as in my life in Germany made my heart full of regards towards you, which I will never ever forget. Thanks for all, what you have done for me so far.

Caro, I always liked having short talks with you, for sure these chit chats made us cheerful. Thanks for your motive to bring liveliness during work.

Friederike & Wolfgang, I always imagine you guys quite senior people in our lab. I am thankful that I have learnt a lot from you. I always enjoyed nice discussions with Friederike about various topics. I never felt that I was out of India, as it was like a family relations with both of you.

I want to thank all my lab mates Lea, Verena, Thuy and Qing. I will miss you people wherever I will be.

## Declaration

I hereby declare and undersign that this dissertation entitled “Effects of *Helicobacter pylori* Vacuolating Cytotoxin A on intracellular calcium signalling in T-lymphocytes,” is entirely my own work, and that all the sources I have used or quoted have been indicated or acknowledged by means of completed references.

Place, Date

Utkarsh Jain

## Curriculum Vitae

### Utkarsh Jain

---

Max von Pettenkofer-Institute

Pettenkoferstr.9a

80336, Munich, Germany

Email: utkarshmicromvp@gmail.com



### ACADEMIC PROFILE

---

#### Ph.D (2008 -2013)

Max von Pettenkofer-Institute, Ludwig-Maximilians Universität (LMU), Munich, Germany

- Submitting thesis entitled “Effects of *Helicobacter pylori* Vacuolating Cytotoxin A on intracellular calcium signalling in T-lymphocytes.”

#### M.Sc. Microbiology (2004 -2006)

Seedling Academy of Design Technology and Management, University of Rajasthan, Jaipur, India

- Thesis entitled: “Studies on Growth and control of *E.coli* and *salmonella* in Mango juice Processing.”

#### B.Sc. Microbiology (1998 -2001)

MVM College, Barkatullah University, Bhopal

- Major Subjects: Microbiology, Chemistry and Zoology

## PROFESSIONAL EXPERIENCE

---

### Lecturer, Microbiology (Apr 2007–Aug 2008)

Teerthanker Mahaveer Dental College and Research Centre, Moradabad, India

### Q.C. Microbiologist (Jul 2006 – Mar 2007)

Mapaex Remedies Pvt. Ltd, Baddi, India

## PUBLICATIONS

---

- Luisa F. Jiménez-Soto, Stefanie Rohrer, **Utkarsh Jain**, Claudia Ertl, Xaver Sewald, and Rainer Haas (2012), Effects of Cholesterol on *Helicobacter pylori* Growth and Virulence Properties *In Vitro*. ***Helicobacter* 17(2):** 133-139.
- Pandit Nitin Prakash, **Utkarsh Jain** and Maheshwari Sanjiv Kumar, (2008). Development of cloning and expression system for L- Asparaginase II for *E. coli*. ***J. Plant agriculture resource* 24:1.**

## CONFERENCES ATTENDED & POSTER PRESENTATION

---

- 3rd Joint congress of the German society of Hygiene and Microbiology (DGHM) and the Association of General and Applied Microbiology (VAAM), 28th – 3rd March 2010, Hannover, Germany. Presented poster entitled “**Receptor mediated endocytosis of VacA into human T lymphocytes**”.
- “8<sup>th</sup> International *Helicobacter pylori* workshop from DGHM (Deutsche Gesellschaft für Hygiene und Mikrobiologie), 18<sup>th</sup>-20<sup>th</sup> November, 2011, Ammersea, Germany.
- Medizinische Infektionsgenomik Seminar, 21<sup>st</sup>-22<sup>nd</sup> September, 2011, Göttingen, Germany
- “7<sup>th</sup> International *Helicobacter pylori* workshop from DGHM (Deutsche Gesellschaft für Hygiene und Mikrobiologie), 4<sup>th</sup>-6<sup>th</sup> December, 2009, Gosler, Germany.
- Short-term training on ‘Functional Genomics and Evolutionary Biology’ sponsored by

Department of Biotechnology, (DBT), Govt. of India, ILS, Bhubneshwar, India.

- CME, 2008 organised by TMDC&RC, Moradabad, India.

## PERSONAL INFORMATION

---

Name: Utkarsh Jain  
Nationality: Indian  
Date of birth: 13.03.1980  
E-mail: utkarshmicromvp@gmail.com  
jain@mvp.uni-muenchen.de

## REFERENCES

---

**Prof. Dr. Rainer Haas**, Max von Pettenkofer-Institute, Ludwig-Maximilian-University, Munich,  
Telephone: +49 (0)89/2180-72855, Fax: +49(0)89/2180-9972855  
E-mail: [haas@mvp.uni-muenchen.de](mailto:haas@mvp.uni-muenchen.de)

**Dr. Wolfgang Fischer**, Max von Pettenkofer-Institute, Ludwig-Maximilian-University, Munich,  
Telephone: +49 (0)89/2180-72877, Fax: +49(0)89/2180-9972855  
E-mail: [fischer@mvp.uni-muenchen.de](mailto:fischer@mvp.uni-muenchen.de)

**Dr. Jimenez Soto Luisa Fernanda**, Max von Pettenkofer-Institute, Ludwig-Maximilian-University Munich, Telephone: +49(0)89/2180-72877, Fax: +49(0)89/2180-9972855  
E-mail: [jimenez@mvp.uni-muenchen.de](mailto:jimenez@mvp.uni-muenchen.de)

I here by declare that the details provided here are true to best of my knowledge.

**UTKARSH JAIN**